

In vivo insights into the pathogenesis of demyelination in multiple sclerosis and its animal model

Dissertation
der Fakultät für Biologie
der Ludwig-Maximilians-Universität München



Angefertigt am Institut für Klinische Neuroimmunologie, LMU München

Eingereicht von

Elisa Romanelli

München, 2015

ERKLÄRUNG

Hiermit versichere ich ehrenwörtlich, dass meine Dissertation selbständig und ohne unerlaubte Hilfsmittel angefertigt worden ist. Die vorliegende Dissertation wurde weder ganz, noch teilweise bei einer anderen Prüfungskommission vorgelegt. Ich habe noch zu keinem früheren Zeitpunkt versucht, eine Dissertation einzureichen oder an einer Doktorprüfung teilzunehmen.

München, den 08.07.2015

Dissertation eingereicht am: 08.07.2015

1. Gutachter: Prof. Dr. Hans Straka

2. Gutachter: Prof. Dr. Anja Horn – Bochtler

Tag der mündlichen Prüfung: 08.12.2015

*“..è questo l’aspetto più appassionante della ricerca in generale
e di quella biologica in particolare:
Ogni scoperta, piccola o grande, è come una porta che si apre
Su un mondo ignorato e affascinante”*

Rita Levi-Montalcini

From “Cronologia di una scoperta,,

TABLE OF CONTENTS

LIST OF ABBREVIATIONS	I
ABSTRACT.....	IV
ZUSAMMENFASSUNG	VI
CHAPTER I – INTRODUCTION	1
1. MULTIPLE SCLEROSIS	1
<i>Introduction and history of the disease</i>	<i>1</i>
<i>Clinical course and diagnosis of MS.....</i>	<i>2</i>
<i>Epidemiology.....</i>	<i>4</i>
<i>Pathology of MS.....</i>	<i>5</i>
<i>Animal models of demyelination and inflammation</i>	<i>12</i>
<i>Treatment of MS.....</i>	<i>16</i>
2. OLIGODENDROCYTES PHYSIOLOGY AND PATHOLOGY	21
<i>Oligodendrocytes physiology</i>	<i>21</i>
<i>Oligodendrocytes damage in MS and EAE</i>	<i>26</i>
<i>Oligodendrocyte repair and remyelination</i>	<i>30</i>
3. IN VIVO IMAGING	34
<i>Principles of two-photon excitation microscopy</i>	<i>34</i>
<i>Imaging the healthy and diseased central nervous system.....</i>	<i>35</i>
CHAPTER II - AIM OF THE STUDY	39
CHAPTER III – MATERIALS & METHODS	41
1. MATERIALS.....	41
<i>Surgery procedures.....</i>	<i>41</i>
<i>Perfusion and immunohistochemistry</i>	<i>43</i>
<i>Imaging.....</i>	<i>46</i>
<i>EAE induction.....</i>	<i>47</i>
<i>Electron Microscopy.....</i>	<i>47</i>
<i>Software.....</i>	<i>48</i>
2. METHODS	49
<i>Experimental animals.....</i>	<i>49</i>
<i>Induction of experimental autoimmune encephalomyelitis (EAE)</i>	<i>50</i>
<i>Immunohistochemistry.....</i>	<i>51</i>
<i>Confocal microscopy.....</i>	<i>51</i>
<i>In vivo imaging</i>	<i>52</i>
<i>Tissue fixation and processing for electron microscopy</i>	<i>53</i>
<i>Near infrared branding (NIRB) and correlated serial electron microscopic reconstruction.....</i>	<i>54</i>
<i>Histopathological analysis</i>	<i>55</i>
<i>Single cell labelling and quantification.....</i>	<i>56</i>
<i>Antibody transfer experiment</i>	<i>56</i>
<i>B cells depletion protocol.....</i>	<i>57</i>
<i>Fixed tissue quantification.....</i>	<i>57</i>

<i>Statistics</i>	58
CHAPTER IV – RESULTS	60
1. <i>IN VIVO</i> IMAGING OF THE SPINAL CORD USING VITAL DYES	60
<i>Surgical procedure and imaging setup</i>	60
<i>Concentration dependence and reliability of vital dyes</i>	63
<i>Structural dyes</i>	68
<i>Functional dyes</i>	70
<i>Use of vital dyes to assess disease models in the spinal cord</i>	72
2. <i>IN VIVO</i> ANALYSIS OF MYELIN IN MULTIPLE SCLEROSIS AND ITS ANIMAL MODEL	73
<i>Characterization of the animal model</i>	73
<i>Cellular sequence of demyelination in acute EAE</i>	77
<i>Imaging myelin loss in vivo</i>	81
<i>Correlated light and electron microscopy of myelinosomes</i>	83
<i>Insight into the mechanism of myelinosome formation</i>	85
<i>Relevance for the human pathology</i>	91
CHAPTER V – DISCUSSION.....	94
1. KEY FINDINGS	94
2. VITAL DYES: A NEW TOOL <i>FOR IN VIVO</i> IMAGING STUDIES	97
3. OLIGODENDROCYTE DAMAGE AND DEMYELINATION IN MICE	98
<i>Demyelination as an outside-inside process</i>	98
<i>Time lapse in vivo imaging reveals myelin abnormalities</i>	100
<i>Ultrastructural analysis of myelinosomes</i>	102
4. INVOLVEMENT OF THE IMMUNE SYSTEM	104
<i>Macrophages interaction</i>	104
<i>Antibodies and myelinosomes formation</i>	105
<i>Myelinosome formation as an antibody-complement mediated mechanism</i>	107
5. RELEVANCE FOR MS.....	108
<i>Demyelination in MS lesions</i>	108
ACKNOWLEDGEMENTS	113
BIBLIOGRAPHY	114

LIST OF ABBREVIATIONS

Ab	Antibody
aCSF	artificial Cerebrospinal Fluid
APC	Antigen Presenting Cell
BBB	Blood Brain Barrier
BCR	B Cell Receptor
Caspr1	Contactin-Associated Protein 1
CIS	Clinically Isolated Syndrome
CNP	2',3'-Cyclic Nucleotide 3'-Phosphodiesterase
CNS	Central Nervous System
CSF	Cerebrospinal Fluid
CVF	Cobra Venom Factor
DTA	Diphtheria Toxin A fragment
DTR	Diphtheria Toxin Receptor
EAE	Experimental Autoimmune Encephalomyelitis
EBV	Epstein Barr Virus
EM	Electron Microscopy
FAD	Focal Axon Degeneration
FcR	Fc Receptor
FDA	Food and Drug Administration
GA	Glatiramer Acetate
GFAP	Glial Fibrillary Acidic Protein
GFP	Green Fluorescent Protein
HCA₂	Hydroxycarboxylic Acid Receptor 2
HLA	Human Leukocyte Antigen
iCP9	Inducible Caspase 9
IFN-β	Interferon-β
IFN-γ	Interferon-γ
Ig	Immunoglobulin
JC	John Cunningham virus
Kv	Potassium voltage gated channel

MAC	Membrane Attack Complex
MAG	Myelin Associated Glycoprotein
MBP	Myelin Basic Protein
MCT	Monocarboxylate Transporter
MDMs	Monocyte Derived Macrophages
MHCII	Major Histocompatibility Complex II
MiDMs	Microglia Derived Macrophages
MOG	Myelin Oligodendrocyte Glycoprotein
MRF	Myelin gene Regulatory Factor
MRI	Magnetic Resonance Imaging
MS	Multiple Sclerosis
Nav	Sodium voltage gated channel
NAWM	Normal Appearing White Matter
NF155	Neurofascin 155
NF186	Neurofascin 186
NIRB	Near-infrared Braining
NK	Natural Killer
NMO	Neuromyelitis Optica
NMSS	National Multiple Sclerosis Society
OL	Oligodendrocyte
OPCs	Oligodendrocyte Precursors Cells
PFA	Paraformaldehyde
PLP	myelin Proteolipid Protein
PML	Progressive Multifocal Leukoencephalopathy
PPMS	Primary Progressive MS
PRMS	Progressive Relapsing MS
RIS	Radiologically Isolated Syndrome
RRMS	Relapsing Remitting MS
RXR-γ	Retinoid X Receptor- γ
SFB-SEM	Serial Block-Face Scanning Electron Microscopy
SPMS	Secondary Progressive MS
SVZ	Subventricular Zone
T reg	lymphocyte T regulatory
Th	lymphocyte T helper

TNF- α

Tumor Necrosis Factor- α

VCAM-1

Vascular Cell Adhesion Molecule-1

ZFp191

Zinc Finger protein 191

ABSTRACT

Multiple sclerosis (MS) is an immune-mediated demyelinating disease of the human central nervous system (CNS). Although demyelination represents the major histopathological hallmark of the disease, currently the mechanism that mediates myelin loss is not fully understood. My PhD study aimed to understand how myelin is damaged in experimental autoimmune encephalomyelitis (EAE), the most commonly used animal model of MS, by combining two photon *in vivo* imaging with confocal microscopy and ultrastructural analysis.

For my experiments I used the chronic EAE model that is induced in BiozziABH mice by immunization with myelin oligodendrocytes glycoprotein (MOG). The clinical course of in this model resembles the human disease multiple sclerosis as mice initially develop a chronic relapsing-remitting form of EAE, which later evolves into a steady progression of the disease. In this model, I investigated the process of demyelination and the sequence that leads to myelin damage. My findings suggest that oligodendrocyte (OL) damage in EAE follows an outside-to-inside pattern, affecting myelin first and only later leading to OLs loss.

Once I identified myelin as the primary target of the immune attack, I used time-lapse *in vivo* imaging to observe how myelin damage is initiated in acute EAE lesions. To efficiently label this subcellular compartment *in vivo*, I established a novel strategy based on the application of a specific vital dye (MitoTracker Red) which, at a given concentration, stains the myelin sheath, to the exposed spinal cord. *In vivo* imaging of fluorescently labelled axons and their myelin sheath revealed that in active demyelinating lesions, myelin is detached from axons in bulb-like structures that we called “myelinosomes”. Such myelinosomes are detectable in

acute and in chronic stages of the MS model, with the highest frequency being present at the peak of inflammatory activity.

I then correlated light and electron microscopy as described previously (*Bishop et al., 2011*) to visualize the ultrastructure of myelinosomes and their cellular context. This technique confirmed the presence of myelinosomes in acute lesions and showed that in some cases they encompass the entire myelin sheath, while in others they consist of single or few myelin leaflets.

From the ultrastructural analysis, I also gained some information regarding the formation of these myelin outfoldings. I noticed that myelinosomes are usually in direct contact with phagocytic cells, which completely engulf them. Thus, I hypothesized that these cells drive the formation of myelin bulbs and the subsequent demyelination. I therefore investigated the mechanisms that mediate the development of myelinosomes. I could show that the transfer of anti-MOG antibodies not only enhanced demyelination, but also increased the frequency of myelinosomes suggesting that antibodies mediate the adhesive interaction between myelin and phagocyte.

In the last part of my project, I studied the relevance of my findings for MS. Here, I could confirm key findings of my *in vivo* analysis in human brain biopsies from MS patients. For example, I observed a similar outside-inside pattern of oligodendrocyte damage in actively demyelinating MS lesions where extensive demyelination was present in the absence of OLs cell loss. Moreover, I could detect myelinosomes-like structures in MS biopsies, which further supports the idea that in demyelinating pathologies the formation of myelinosomes might underlie myelin removal.

ZUSAMMENFASSUNG

Die Multiple Sklerose (MS) ist eine immunvermittelte demyelinisierende Erkrankung des zentralen Nervensystems (ZNS). Obwohl die Demyelinisierung das zentrale histopathologische Korrelat dieser Erkrankung ist, ist der Mechanismus, der zum Myelinverlust führt, nicht gut verstanden. In meiner Doktorarbeit habe ich deswegen untersucht, wie Myelin in dem am häufigsten verwendeten Tiermodell der MS, der experimentellen autoimmunen Enzephalomyelitis (EAE), geschädigt wird. Für diese Untersuchungen habe ich 2-Photon *in vivo* Mikroskopie mit konfokaler Mikroskopie und ultrastrukturellen Analyse kombiniert.

Für die Experimente wurde ein chronisches EAE Modell, das in BiozziABH Mäusen durch die Immunisierung mit Myelin Oligodendrozyten Glykoprotein (MOG) induziert wird, verwendet. Dieses Modell zeigt einen der menschlichen Erkrankung ähnlichen Krankheitsverlauf mit einer frühen schubförmig-remittierenden Phase, auf welche ein chronisch-progredienter Krankheitsprozess folgt. In diesem Modell untersuchte ich zunächst, in welchen zellulären Kompartiment die Oligodendrozytenschädigung initiiert wird. Meine Ergebnisse zeigen, dass Oligodendrozyten in der EAE von außen nach innen geschädigt werden. Zuerst ist Myelin betroffen und erst in einem späteren Stadium kommt es zu einem Oligodendrozytenverlust.

Nachdem diese Untersuchungen das Myelin als das Primärziel des entzündlichen Angriffs identifiziert hatten, studierte ich mit Hilfe der *time lapse in vivo* Mikroskopie, wie die Myelinschädigung in akuten entzündlichen Läsionen induziert wird. Zu diesem Zweck habe ich zunächst eine neuartige Strategie etabliert, um effizient Myelin *in vivo* zu färben. Diese Strategie basiert auf der Applikation eines spezifischen Vitalfarbstoffes (MitoTracker Red)

auf das Rückenmark, welcher in einem bestimmten Konzentrationsbereich spezifisch die Myelinhülle färbt. Die *In vivo* Mikroskopie von fluoreszenz-markierten Axone und ihrer Myelinschicht zeigte dann, dass sich in aktiv demyelinisierenden Läsionen das Myelin von den Axonen in „ballartigen“ Strukturen ablöst, die wir „Myelinosomen“ benannt haben. Solche Myelinosomen finden sich in akuten und chronischen Stadien der EAE, wobei die höchste Dichte , während der Zeit der maximalen Entzündungsaktivität beobachtet wird.

Um mehr über die Ultrastruktur und den zellulären Kontext der Myelinosomen zu erfahren, haben wir einen korrelativen Licht- und Elektronenmikroskopie-Ansatz verwendet, der bereits in Bishop et al. (2011) beschrieben wurde. Diese Methode bestätigt die Anwesenheit von Myelinosomen in akuten EAE Läsionen und zeigt, dass diese in einigen Fällen die gesamte Myelinhülle umfassen, während in anderen diese nur aus einzelnen oder wenigen Myelinschichten bestehen.

Die ultrastrukturelle Analyse lieferte auch wichtige Hinweise zur Pathogenese der Myelinosomenbildung. So konnten wir zeigen, dass Myelinosomen häufig von Phagozyten kontaktiert werden, welche vollständig die Myelinosomen umhüllen und einschließen. Daher folgerte ich, dass diese Zellen verantwortlich für die Bildung der Myelinosomen und die nachfolgende Demyelinisierung sind. Als nächstes untersuchte ich den Mechanismus der Myelinosombildung genauer. Ich konnte zeigen, dass der Transfer von anti-MOG Antikörpern nicht nur die Demyelinisierung verstärkt, sondern auch die Häufigkeit der Myelinosomen erhöht. Dies legt nahe, dass myelin-reaktive Antikörper die Adhäsion zwischen Myelinsom und Phagozyten vermitteln.

Im letzten Teil meines Projekts untersuchte ich dann die Bedeutung meiner Ergebnisse für MS. Interessanterweise konnte ich zeigen, dass wichtige im Tiermodell erhobene Befunde auch auf die menschliche Erkrankung übertragen werden können. So fand ich bei der

Untersuchung von Hirnbiopsien, dass auch in aktiven MS Läsionen die Oligodendrozytenschädigung mit dem Verlust von Myelin beginnt. Darüberhinaus konnte ich auch Myelinosom-ähnliche Strukturen in MS Biopsien entdecken. Diese Beobachtungen unterstützen die Hypothese, dass Myelin in demyelinisierenden Pathologien über die Bildung von Myelinosomen entfernt wird.

CHAPTER I – Introduction

1. Multiple Sclerosis

Introduction and history of the disease

Multiple sclerosis (MS) is an inflammatory disease of the central nervous system (CNS), in which a complex activation of the immune system leads to myelin damage and axonal pathology.

One of the first recognised medical reports was published in 1840 by McKenzie who described a 23 years-old man with progressive “*palsy of his limbs and confusion of vision*”, also displaying incontinence and asymmetric arms weakness. These symptoms disappeared after two months and his motor function and eyesight were restored (McKenzie, 1840). Few years earlier, two independent reports by Sir Robert Carswell and Jean Cruveilhier, described and illustrated MS-like clinical manifestations and CNS lesions; however, neither of them categorized such disease as a newly discovered pathology. Carswell’s atlas was published in 1837 and the legends to his illustrations describe “*a peculiar diseased state of the cord and pons to the grey substance*” and “*patches on the spinal cord occupying the medullary substance which was hard, semitransparent and atrophie*” (Pearce, 2005). Similar to his colleague, Cruveilhier reported CNS lesions as “*reddish grey islets*” and referred to their appearance as “*a grey degeneration of the columns of the spinal cord (...)*” and “*grey degeneration in the cord, brainstem and cerebellum*” (Flamm, 1973).

Although a lot of pathologists and physicians were interested in diseases of the brain, Jean-Martin Charcot was the first who successfully described the clinical and pathological hallmarks of MS, which was known as “Charcot disease” until 1921. He caught interest in the

disease after observing the early symptoms and the progressive disability of his housemaid, whose autopsy showed scattered plaques in her brain and spinal cord. In 1866, Charcot and his colleague Vulpian referred to this disease as “*Sclerose en plaques disseminee*”, and a couple of years later he gave a very accurate description of the main neurological and pathological findings: clinically, the disorder is characterized by different symptoms, among which tremor, nystagmus and scanning speech; pathologically, he showed that loss of myelin, thickening of blood vessels, fatty macrophages, gliosis scar, and damaged axons were evident in the CNS of the patients (*Clanet, 2008*).

Nowadays we are aware of many historical figures who lived before Charcot and that suffered a MS-like disease. Among those is Sir Augustus D’Este, grandson of King George III. He kept a diary where he carefully documented the progression of his disorder, from weakness, numbness, difficulty in walking, spasms, to depression. His diary with its meticulous notes is widely accepted as possibly the first known patient’s description of MS (*Pearce, 2005; Firth, 1948*).

Clinical course and diagnosis of MS

MS is a heterogeneous disease that can manifest through at least four different clinical subtypes (*Lublin et al., 2014*): i) relapsing-remitting MS (RRMS), characterized by an alternation of periods, in which the patient shows neurologic symptoms followed by full or partial recovery, this type occurs in 80-85% of cases; ii) primary progressive MS (PPMS), in which no recovery periods can be observed (10-15% of cases); iii) secondary progressive MS (SPMS), developed by most of the RRMS patients and characterized by a steady progression of the symptoms; iiiii) progressive relapsing (PRMS), characterized by a continuous progression of the disease from the onset with defined attacks, with or without recovery. This

description of MS subtypes was presented in 1996 by the US National Multiple Sclerosis Society (NMSS) Advisory Committee on Clinical Trials in Multiple Sclerosis, when the Committee also provided a definition of benign MS, in which the patient does not show neurological deficits 15 years after the onset of the disease, and malignant MS, which is characterized by a rapid course of the disease with strong disability and eventually death (*Lublin et al., 2014; Milo and Miller, 2014*) (**Figure 1**).

In 2012 the same Committee gathered to review the old clinical course descriptions, and two new clinical courses were added to the pre-existing list: i) clinically isolated syndrome (CIS), described as the first clinical presentation of the disease (suggesting that it may be MS), and ii) radiologically isolated syndrome (RIS), where the patient fails to show any clinical signs although MS-like plaques can be identified by MRI imaging (*Lublin et al., 2014*).

As MS lesions are typically disseminated both in time and space, diagnosis is mainly based on clinical symptom manifestations, which can be referred to white matter lesions. Among those clinical symptoms, the most common are numbness, motor weakness, visual deficit, diplopia, gait disturbances, but also incontinence, sensory loss, ataxia, as well as depression and cognitive dysfunction. Besides clinical observations, specific tests can help to diagnose MS: cerebrospinal fluid (CSF) analysis, electrophysiological studies, and MRI. The majority of MS patients present oligoclonal IgG bands in their CSF; the presence of 2 or more bands indicates CNS-specific antibody production and it is a fundamental step in defining the pathological scenario as MS. Electrophysiological studies can be used to assess whether there are demyelinating lesions, as those normally lead to delayed latencies of visual, somatosensory and auditory evoked potentials. Finally, MRI has become the most sensitive technique to reveal MS lesions, and a crucial tool to monitor disease progression, measure brain atrophy and axonal loss, estimate lesion density, both in grey and white matter (*Milo and Miller, 2014; Compston and Coles, 2008*).

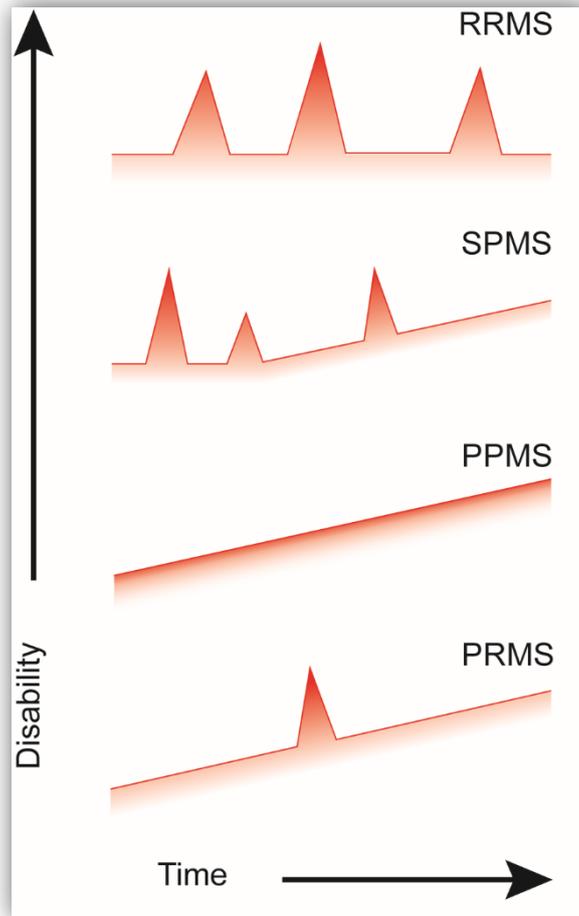


Figure 1 - Multiple sclerosis clinical subtypes: Progressive Relapsing MS (PRMS), Primary Progressive MS (PPMS), Secondary Progressive MS (SPMS), Relapsing Remitting MS (RRMS). Inspire by *Coles, 2009*.

Epidemiology

MS affects primarily young adults, with the first symptoms usually appearing in the late 20s/early 30s; the incidence of the disease decreases with age, and it becomes rare in people in their 50s or above. The risk is higher among white non-Hispanic individuals, and it appears to be lower in black, Hispanic and Asian populations (*Ascherio et al., 2012*).

The susceptibility to MS is influenced by different determinants, including genetic components as well as environmental factors. Studies on twins and siblings have shown that the strongest genetic risk is associated with the HLA-DRB1 gene on chromosome 6p21,

specifically the HLA-DRB1*1501 allele. HLA (Human Leukocyte Antigen) molecules are involved in immune responses and antigen binding and presentation. This might explain why the DRB1 gene is associated with higher susceptibility to MS; however, the exact mechanisms are still unknown (*Hauser et al., 2006*).

As mentioned above, the environment also plays an important role in the development of MS: viral and bacterial infections, dietary habits, pollution, exposure to minerals or animals, and many other factors have been investigated. A prominent candidate is infection with the Epstein Barr virus (EBV), a double-stranded DNA virus, which is transmitted mainly by saliva. Its infection is asymptomatic in the first years of life, but it can lead to acute fever (known as infectious mononucleosis) when it affects adults. The risk of developing MS appears to be lower in EBV-negative individuals, while individuals infected with virus are more susceptible to the disease.

Additional studies have revealed high vitamin D levels as a possible protective factor in MS, and have shown how cigarette smoking increases the risk of developing MS. Therefore, vitamin D supplementation and smoking cessation are likely to decrease the risk of MS and improve life of individuals with MS (*Ascherio et al., 2012; Schmidt et al., 2007*).

Pathology of MS

MS is characterized by demyelinating plaques scattered throughout the CNS, mostly in white matter areas but also found in gray matter. Hallmarks of the lesions are the presence of inflammatory cells, damaged axons, myelin debris, and gliosis. According to a study published in 2000 by Lucchinetti et al., we can identify 4 types of active demyelinating lesions depending on their demyelination pattern: I) *Pattern I*, “macrophage-associated demyelination”, characterized by T cells infiltration and macrophages activation, the latter seemingly responsible for the myelin damage; II) *Pattern II*, “antibody-mediated

demyelination”, in which immune infiltrates are composed of T cells and macrophages as in pattern I, and demyelination seems induced by antibodies and activated complement; III) Pattern III, “distal oligodendroglipathy and apoptosis”, in which inflammation is less prominent and again driven by T cells and macrophages, but it is mainly characterized by distal degeneration of oligodendrocytes processes and diffuse apoptosis; IV) Pattern IV, “primary oligodendroglia degeneration”, this is the least common pattern of demyelination in MS and oligodendrocytes degeneration is the most prominent feature (*Lucchinetti et al., 2000; Lassman et al., 2001*). The lesion patterns described above are all characterized by the infiltration of T cells and macrophages. In fact, although the CNS is considered an immune-privileged site as the blood brain barrier (BBB) protects the brain from the entry of blood-borne molecules and circulating leukocytes, in MS disruption of the BBB is an early event that allows leukocytes to enter the CNS parenchyma (*Prat et al., 2002*). For a long time MS was believed to be mediated only by autoreactive myelin-specific CD4⁺ T cells, but it has become more and more clear that instead it involves different immune cell types from both adaptive and innate immune system, as well as glial cells (*Duffy et al., 2014*). Below I will briefly review the different cellular subsets involved in the pathogenesis of MS and discuss their contribution to the disease (**Figure 2**).

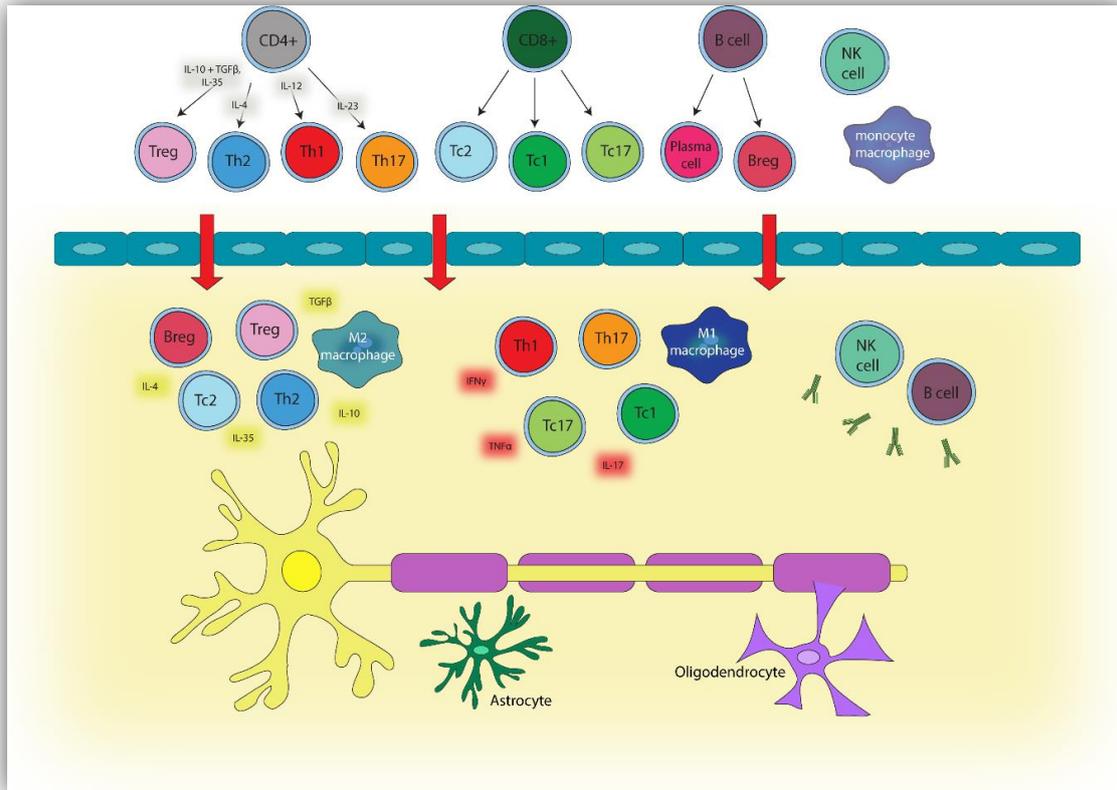


Figure 2 - schematic representation of the contribution of different immune and glial cells to the pathogenesis of MS.

T lymphocytes

Thymus-derived T cells are part of the adaptive immune system and can be classified into 3 main categories: T helper (Th/CD4+), cytotoxic (CD8+), and regulatory T (T reg) cells.

T helper type 1 (Th1) cells differentiate in response to IL-12 and, once activated, release proinflammatory cytokines such as interferon- γ (IFN- γ) and tumour necrosis factor- α (TNF- α) (Dittel *et al.*, 2008). TNF- α has been found in MS lesions and elevated TNF- α levels in serum and CSF of MS patients correlated in some cases with disease progression. Therefore, it was proposed as a possible target in the therapy of the disease and a TNF- α receptor-immunoglobulin G (IgG) 1 fusion protein called Lenercept was tested: while it appeared to have positive results in the animal model of MS, its administration in human didn't show any

improvement (*The Lenercept Multiple Sclerosis Study Group and The University of British Columbia MS/MRI Analysis Group, 1999*). IFN- γ has also been investigated: one of the first studies that described the use of an antibody to IFN- γ , reported how the blockade of this cytokine can ameliorate the disease course in MS patients (*Skurkovich et al., 2001*).

Conversely, a different subtype of T helper named T helper type 2 (Th2) cells are known to play a beneficial role, and release cytokines such as IL-4, IL-5, IL-10 and IL-13 (*Bitain et al., 2010*).

Another subtype of T helper lymphocytes are type 17 (Th17) cells, which differentiate in response to IL-23. These cells are described as pro-inflammatory cells and their signature cytokine is IL-17; recent studies have described that IL-17 receptor is expressed on human endothelial cells that form the brain blood barrier (BBB) (*Kebir et al., 2007*), and therefore it may be crucial in inducing a breach in the barrier with consequently trafficking of autoreactive T cells from the systemic compartment into the CNS parenchyma.

Cytotoxic CD8⁺ T cells can also be subdivided in pro-inflammatory and anti-inflammatory, depending on the cytokines they produce: Tc1 and Tc17 belong to the pro-inflammatory family, releasing respectively IFN- γ and IL-17; Tc2 have an anti-inflammatory role and produce IL-4, IL-5, IL-10. Cytotoxic T cells have been reported in actively demyelinating lesions in MS, in close proximity to demyelinated axons, and with a higher density than CD4⁺; these findings suggest a role in the induction of tissue damage (*Babbe et al., 2000*; *Skulina et al., 2004*).

The last category of T cells are the regulatory T cells (Treg). These cells act as immunomodulators of the adaptive immune system and are characterized by the expression of CD4, CD25, CD39 and the transcription factor FoxP3. Whether those cells play a big role in the modulation of disease initiation and progression, is not yet clear. However, a number of studies showed that Treg cells can be found in MS lesions as well as in CSF of MS patients,

and their density appears to be less frequent in the lesions compared to the CSF compartment, where they express an apoptotic phenotype (*Fritzsching et al., 2011*). Interestingly, it was also shown that CD39⁺ Treg cells can cope with a Th17 expansion during the remitting phase of MS, but not during relapse (*Peelen et al., 2011*).

B lymphocytes

B cells lymphocytes are part of the adaptive immune system and appear both as positive and negative modulators of immunity: in fact, not only are they responsible for the production of antibodies, but they also act as antigen presenting cells (APCs) and release soluble factors (*Pistoia, 1997*). Antibodies have already been described in the past as contributors to lesion formation, with IgG found in demyelinating lesions and on myelin sheaths (*Lucchinetti et al., 1996; Barnett et al., 2009*). A more recent study confirmed IgG and IgM presence in both acute and chronic active and inactive lesions, independently of disease duration and clinical course (*Sadaba et al., 2012*), and it has been suggested that B cells are able to secrete additional factors toxic to the oligodendrocytes, thus contributing through different mechanisms to demyelination in MS (*Lisak et al., 2012*). The clear pathogenic role of B cells has been demonstrated by the positive results obtained by the administration of the B-cell depleting antibody Rituximab in RRMS patients (*Carrithers, 2014*).

As mentioned before, B cells also have an immunoregulatory function: regulatory B cells (Breg) secrete the immunoregulatory cytokine IL-10, and a crosstalk between Bregs and Tregs has been shown. Bregs were proposed to have a role in autoimmune disorders (*Fillantreau et al., 2002*) as they inhibit Th1 differentiation and ameliorate arthritis in mice (*Mauri et al., 2003; Brimnes et al., 2014*).

Natural killer

Natural killer (NK) cells are components of the innate immune system which fight pathogens directly by cell contact or indirectly by promoting an adaptive inflammatory response through T cells activation. NK cells express different levels of CD56, accordingly to their role: CD56^{dim} cells are highly cytotoxic and represent the majority of the circulating NK, while CD56^{bright} are immature NK with immunomodulatory functions. The latter have also been implicated in the beneficial effect of a drug used in the therapy of MS -daclizumab- (*Bielekova et al., 2006*). IFN- β , one of the earliest and most common treatments for MS, was also shown to induce the expansion of CD56^{bright} cell, which correlates to a positive clinical response (*Martinez-Rodriguez et al., 2011; Hamann et al., 2013*). However, while there are data suggesting a regulatory role of NK cells in MS, the mechanisms by which this is mediated are still unclear and further studies will be necessary to better understand the role of these cells in MS pathology.

Macrophages/microglia

MS lesions are characterized by different cells crossing the BBB and infiltrating the CNS. Among those cells infiltrating monocyte derived macrophages together with resident microglia play a crucial role in the initiation and progression of the disease (*Lucchinetti et al., 2000*). The developmental origins of macrophages and microglia are distinct: macrophages derive from hematopoietic stem cells in the bone marrow, and subsequently become monocytes and differentiate into macrophages when they enter the tissue in response to inflammation; microglia come from hematopoietic cells in the yolk sac and migrate to the CNS during prenatal development before the BBB is formed (*Prinz et al., 2014*). Resident microglia make up for 5-15% of the total brain cell population, and take part to the initiation

and the progression of CNS inflammatory responses; they are also involved in the clearance of apoptotic cells, and in elimination and maintenance of synapses (*Aguzzi et al., 2013*). Microglia cells are considered poor antigen presenting cells as they normally express low levels of MHC class II. However, when activated microglia can participate in antigen presentation as evidenced by their increased expression of B7.2 and CD40 in the presence of IFN- γ and TNF- α (*Carson, 2002; Kreutzberg, 1996; Becher and Antel, 1996*).

Macrophages can acquire different pro-inflammatory and anti-inflammatory phenotypes, which are respectively termed M1 and M2 macrophages. The distinction is based on different cytokine production, distinct inducing factors and on differences in phagocytic capability. M1 macrophages classically express iNOS, CD16/32, and T-cell stimulating IL-12, while M2 macrophages are characterized by expression of Arg1, CD206 and IL-10 (*Liu et al., 2013*).

The polarization of macrophages into M1 or M2 phenotype depends on different environmental cues: IFN- γ and Toll-like receptor stimulating bacterial components promote differentiation into M1 macrophages, while IL-4, IL-13 and IL-10 polarize M2 cells (*Deng et al., 2012*). Interestingly, macrophages are very plastic cells, which can sequentially show pro- and anti-inflammatory properties; their ability to switch between one phenotype and the other is rapid and reversible, and it can be modulated by removal and/or replacement of a cytokine (*Porcheray et al., 2005*). It was shown that in the animal model of MS, M1 and M2 cells play a key role in the inflammation severity; in fact, M1 are predominantly present during relapses while administration of M2 macrophages attenuates the progression of the disease and increases the expression of immunomodulatory factors that promote recovery (*Mikita et al., 2011*).

Animal models of demyelination and inflammation

The most extensively characterized animal model for autoimmune CNS inflammation is Experimental Autoimmune Encephalomyelitis (EAE), which was described for the first time in 1933 by Rivers and colleagues (*Rivers et al., 1933*). EAE shares a lot of similarities with human demyelinating diseases, such as multiple sclerosis: the damage of myelin sheaths; the development of scattered lesions throughout the CNS and their perivascular location; the presence of immune cell infiltration and antibodies in the CNS and cerebrospinal fluid (*Baxter et al., 2007*). EAE pathology and its clinical features depend on the animal species, in which it is induced; to date, EAE has been successfully reproduced in guinea pigs, rabbits, goats, hamsters, dogs, sheeps, marmosets, chickens, rats and mice (*Freund et al., 1947; Olitsky and Yager, 1949; Tal et al., 1958; Thomas et al., 1950; Innes et al., 1951; Genain et al., 1995; Ranshoff, 2012*).

EAE is induced by immunisation with different myelin proteins, such as myelin basic protein (MBP), myelin oligodendrocytes glycoprotein (MOG) or proteolipoprotein (PLP), depending on the immunogenicity of such antigens in the different animals/strains (active EAE). Also, the model can be induced by adoptive transfer of T cells isolated from animals previously injected with myelin antigens (passive EAE). In active EAE, proteins are first emulsified in complete Freund's adjuvant (containing *Mycobacterium tuberculosis*) and then animals receive one or two intraperitoneal injections with pertussis toxin e.g. at the day of immunization and 2 days after (*Stromnes and Goverman, 2006a*). Although both of models are known to be T cell mediated, passive EAE allows more manipulations to study the role of T lymphocytes; for instance, it is possible to label T cells before their transfer and therefore follow their localization and activity in the recipient mouse; another option is to manipulate T cells *in vitro* before transfer, allowing the study of specific T cells functions in the pathogenesis of EAE (*Stromnes and Goverman, 2006b*).

The EAE model has also proven to be useful to study the *in vivo* mechanisms of demyelination, axon damage, and especially CNS inflammation, thus allowing to define therapeutic targets for MS. More specifically, three major compounds used in the treatment of MS have been developed based on EAE studies: glatiramer acetate, mitoxantrone and natalizumab (*Steinman and Zamvil, 2006*).

Nonetheless, despite its indisputable advantages, EAE has some important limitations. First, although few spontaneous EAE models do exist (*Krishnamoorthy et al., 2006; Krishnamoorthy and Wekerle, 2009*), in most cases it is an inducible disease, which makes it difficult to use it to shed light on MS etiology. Second, the multifactorial and complex pathogenesis of MS cannot be replicated in a single animal model, even though use of different animal strains or protocols can better model the numerous aspects of MS.

In the classical EAE model, CD4⁺ T cells play a crucial role in the development of the pathology. C57/Bl6 mice are commonly used and are susceptible to immunization with a peptide from the myelin oligodendrocytes glycoprotein (MOG₃₅₋₅₅). After induction of EAE, the mice manifest an ascending clinical paralysis, which progressively extends to hindlimbs and forelimbs. In such a disease paradigm, and in contrast to most MS cases, inflammatory lesions form predominantly in the spinal cord. This model is for example useful to study the contribution of specific CD4⁺ T cell subtypes to disease initiation and tissue damage. The finding that not only Th1 clones, but also Th17 cells can induce EAE (*Cua et al., 2003*), also led to insights in disease mechanisms, showing that inflammation dominated by Th1 or Th17 lymphocytes substantially differ, with Th17-induced EAE showing not only limbs paralysis, but also ataxia, rolling, and proprioception defects (*Jäger et al., 2009*).

EAE lesions are usually populated by a high number of phagocytes, which can derive from differentiated circulating monocytes or from activated microglia. This dichotomy was better elucidated by Ransohoff and his group who used a transgenic mouse model, which allows the

differentiation of monocyte-derived macrophages (MDMs) and microglia-derived macrophages (MiDMs). In these mice, MiDMs (Ly6C^{lo} monocytes expressing high levels of CX₃CR1) express GFP, while MDMs (Ly6C^{hi} monocytes expressing high levels of chemokine receptor 2) are RFP positive (*Saederup et al., 2010*). This model allowed to describe density and recruitment dynamics of MDMs and MiDMs in the lesion area: while MDMs appear to be responsible for the detrimental demyelination process, which seems to start preferentially at the nodal and paranodal regions, MiDMs are involved in the removal of myelin debris (*Yamasaki et al., 2014*).

As reviewed before in this thesis, B cells are also involved in the pathology of MS and their role has also been extensively studied in the EAE model. However their specific contribution to the disease process remains controversial as results substantially vary depending on the used EAE model. To study their contribution to EAE, both B cell deficient animals (μ MT^{-/-}) and anti-CD20 antibody mediated depletion have been used. After induction of EAE with recombinant MOG (known to activate B cells through their B cell receptor (BCR) and lead to their differentiation in plasma cells capable of producing antibodies against MOG), B cell depletion ameliorated the clinical symptoms of EAE, reduced anti-MOG antibody titers, and decreased the density of encephalitogenic Th1 and Th17. These findings would support a major proinflammatory role for B cells in the development of the disease. However, upon induction of EAE with MOG₃₅₋₅₅ peptide (a model that doesn't involve B cells activation), B cell depletion worsened the clinical course of the disease, possibly indicating that depletion of naive B cells is not beneficial (*Weber et al., 2010; Simmons et al., 2013*).

EAE can also develop spontaneously in several mouse lines. These include a model of spontaneous opticospinal EAE which is characterized by demyelinating lesions in the spinal cord and in the optic nerve, resembling neuromyelitis optica (NMO) (*Krishnamoorthy et al., 2006*), or SJL/J animals which recapitulate the major features of RRMS. The disease appears

spontaneously and usually takes a relapsing-remitting course, showing lesions not only in the spinal cord but also in cerebellum, brainstem and optic nerve (*Pöllinger et al., 2009*). These lesions are composed of T cells, macrophages/microglia, B cells, activated complement and antibodies (*Berer et al., 2011*).

Relapsing-remitting EAE can also be induced in C57/B16 mice by immunization with low dose of MOG₃₅₋₅₅ (*Berard et al., 2010*), or when the saponin extract Quil A is used as adjuvant (*Peiris et al., 2007*).

Secondary progressive MS can for example be studied in BiozziABH animals. This strain was described for the first time in 1972 by Guido Biozzi, who reported that these mice had high antibody titers in response to specific antigens (*Biozzi et al., 1972*). Following immunization with myelin antigens, these mice initially develop a relapsing-remitting EAE which evolves into a steady clinical progression. Demyelination is particularly strong during the relapses, and the lesions are associated with the presence of macrophages, CD4+ T cells and immunoglobulin deposition (*Baker et al., 1990; Amor et al., 2005*).

Histopathologically, the pattern of CNS damage of the models described above resemble lesion pattern I and II of MS, in which infiltrates are mainly composed by T cells and macrophages, and with a strong involvement of antibodies and complement deposition (*Lucchinetti et al., 2000*). To model pattern III and IV, characterized primarily by oligodendrocytes degeneration and apoptosis, administration of toxins or solvents such as the copper chelator cuprizone or lysophosphatidylcholine respectively, have been used. Furthermore, these models are particularly interesting for remyelination studies (*Lucchinetti et al., 2000; Ransohoff, 2012; Simmons et al., 2013*).

Lastly, it is important to remember that while the EAE models described till now mainly elicit CD4+ T cells response, it is known that CD8+ have an important role in the pathogenesis of the human disease, being the majority of the T lymphocytes present in the

MS lesions (*Babbe et al., 2000*). Adoptive transfer of MBP-specific CD8⁺ clones resulted in the development of EAE; however, the disease induced by CD8⁺ T cells seems different from the CD4⁺ induced EAE, with the majority of the lesions located in the brain and not in the spinal cord. Further they show extensive demyelination and significant oligodendrocytes death, resembling more pattern III and IV (*Huseby et al., 2001*).

Treatment of MS

As reviewed in paragraph 1.4 of this thesis, the pathogenesis of MS involves the infiltration and local activation of different immune cell types, which are the main targets for the treatment of the disease. To date, there are 12 drugs available in the majority of the countries (approved e.g. by the U.S. Food and Drug administration -FDA-) to treat MS, and those are aimed at managing the symptoms, preventing relapses and slowing disease progression: interferon β -1a and β -1b (Avonex, Plegridy, Rebif, Betaseron, Extavia), glatiramer acetate (Copaxone), mitoxantrone (Novantrone), natalizumab (Tysabri), alemtuzamab (Lemtrada), fingolimod (Gilenya), teriflunomide (Aubagio), dimethyl fumarate (Tecfidera) (<http://www.nationalmssociety.org/>) (Figure 3).

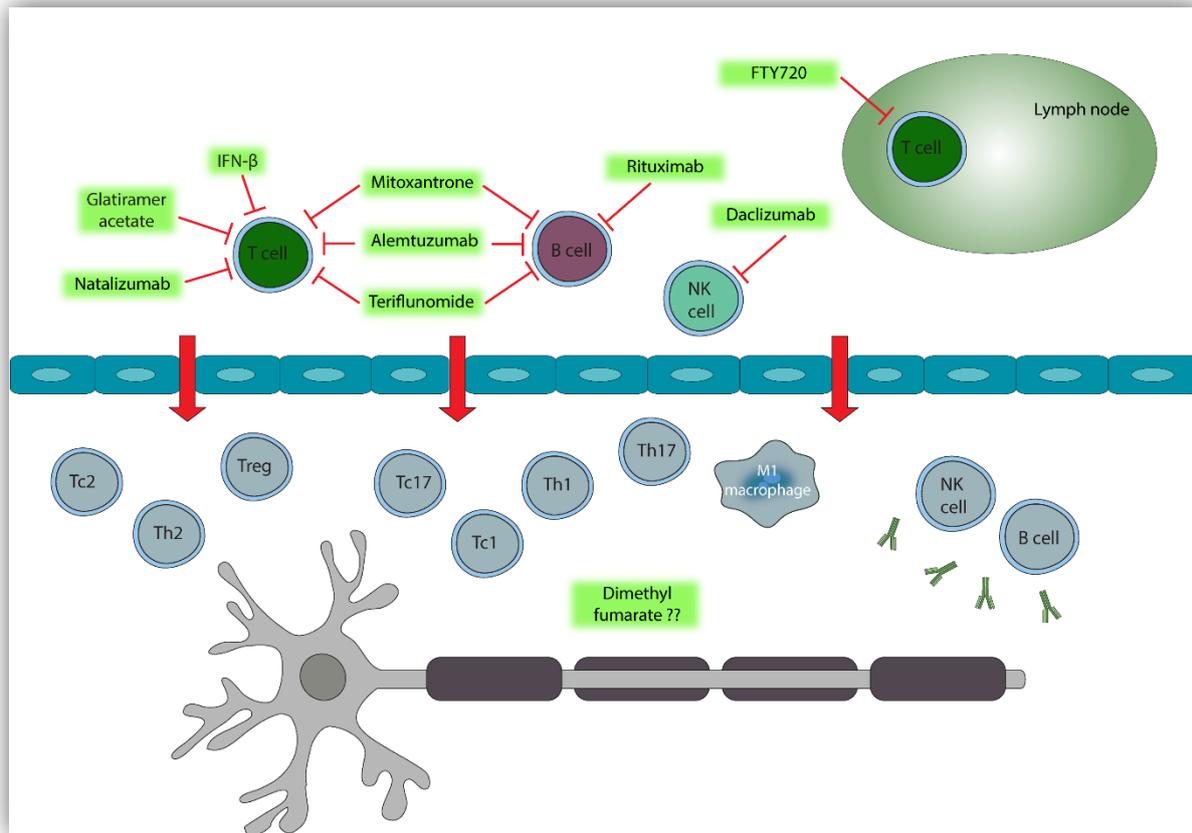


Figure 3 - MS treatments. The figure illustrates the targets of action of the drugs used in the therapy of MS. Some of these drugs act on both T lymphocytes and B cells, including mitoxantrone, alemtuzumab and teriflunomide. Others are specific for T cells, such as IFN-β, glatiramer acetate and natalizumab, while rituximab works only on B cells. Daclizumab and FTY720 specifically exert their function respectively on NK cells and T lymphocytes in the LN.

The first widely used treatments for MS were interferon β (IFN-β) and glatiramer acetate. The mechanisms of action are not fully clear, but most likely they act on T cells, decreasing their number and interfering with their activation, as well as stimulating Treg and IL-10 response (*Bashir and Whitaker, 1998*). Interferons (IFNs) are proteins secreted in response to pathogens, and their job is to modulate the immune response. The type I IFNs include IFN-α and IFN-β, and they have anti-inflammatory properties. On the other hand, type II IFNs include IFN-γ, which has pro-inflammatory activity. In therapy IFN-β1a and IFN-β1b are used, which have similar biological effects and similar side effects. The former involve i) modulation of T cell activation by inhibition of upregulation of MHC II molecules induced

by IFN- γ (Panitch *et al.*, 1987), ii) enhanced secretion of IL-10 and reduced IL-12 (Wang *et al.*, 2000), iii) inhibition of metalloproteinase 9 (which digests matrix membrane and favours entrance of cells into the CNS through the BBB) production by T cells, and therefore decreased openings of the BBB (Stuve *et al.*, 1996). The latter are injection site reactions, anaemia, flu-like symptoms, fever and depression. Glatiramer acetate (GA) is a synthetic polypeptide composed of 4 aminoacids that shares some crossreactivity with the structure of the possible MS autoantigen myelin basic protein (MBP). It is able to inhibit MBP-reactive T cells and to preferentially induce Th2 activation (Dhib-Jailbut, 2002). Both GA and IFNs are used in the treatment of RRMS and are self-injectable drugs, which need to be administered either subcutaneously or intramuscular very frequently (every other day for IFN- β 1b, weekly for IFN- β 1a, and daily for GA) (Wingerchuk and Carter, 2014).

Another drug used in RRMS is mitoxantrone that also shows some effect in the treatment for SPMS. Mitoxantrone was originally developed as an anti cancer agent; it inhibits proliferation of dividing cells including lymphocytes and its mechanisms of action include its ability to intercalate in the DNA causing strand breakage (Marriott and Miyasaki, 2010). Due to its strong side effect, in particular the higher risk of cardiomyopathy, the use of this treatment is restricted to a maximum of 2 years (Wingerchuk and Carter, 2014).

Natalizumab was approved for the first time as treatment for RRMS in 2004. It is a monoclonal antibody against the α -4 chain of the α 4 β 1 integrin on leukocytes surface and prevents the interaction with vascular cell adhesion molecule-1 (VCAM-1), therefore blocking T cells trafficking across the BBB (Barten *et al.*, 2010). It has been shown that in patients that received 24-36 months of intravenous natalizumab, there is a higher risk of developing progressive multifocal leukoencephalopathy (PML); this is a rare neurological disorder caused by the John Cunningham virus (JC) which leads to irreversible disability and often to death (Kleinschmidt-DeMasters *et al.*, 2005).

Alemtuzumab is a humanized monoclonal antibody against CD52, a protein expressed on monocytes and lymphocytes. Its effects are rapid and induce a broad lymphocytes depletion: while B cells repopulate in 5-6 months, T cells -in particular CD4+ T cells- remain depleted up to 1 year (*Cosburn et al., 2011; Wingerchuk and Carter, 2014*). It is injected intravenously for 5 consecutive day cycles in a month, and later 3 consecutive days at 12 and 24 months. In a study aimed to compare the benefits of alemtuzumab versus IFN- β 1a, alemtuzumab was more effective with substantial reduction of disability and fewer relapses compared to the patients treated with IFN- β 1a (*The CAMMS223 Trial Investigators, 2008*). However, it is associated with strong side effects: at least 20% of patients developed antibody-mediated autoimmune diseases, and roughly 3% immune thrombocytopenic purpura, as well as hyper or hypothyroidism (*Cosburn et al., 2011*).

The medications described above are all administered intravenously, subcutaneously or intramuscularly, therefore causing injection site reactions. In the past years the FDA approved three oral treatments for relapsing MS: fingolimod, teriflunomide, and dimethyl fumarate.

Fingolimod (FTY720) modulates the S1P1 receptor. This receptor is expressed on lymphocytes and it is responsible for the exiting of lymphocytes from the lymph node. As a result, lymphocytes are trapped in the lymph nodes and cannot enter the CNS and form lesions (*Barten et al., 2010*). Fingolimod is a daily treatment and it seems to be more efficient compared to IFN- β 1a (*Cohen et al., 2010*). It is not free of adverse effects too, which are mainly related to lymphopenia, such as an elevated risk of viral infections. It is also important to keep in mind that the S1P1 receptor can be expressed by other cell types, thus leading to a broader spectrum of potential side effects including bradycardia, macular edema, or hypertension (*Wingerchuk and Carter, 2014*).

Teriflunomide is an inhibitor of dihydroorotate dehydrogenase, an enzyme responsible for the synthesis of the pyrimidines in proliferating cells. The final effect is the inhibition of T and B cell activation, thereby reducing the inflammation. Teriflunomide is also able to block protein tyrosine-kinases and modulate the production of cytokines and expression of cell surface molecules. It is an oral drug that needs to be taken once a day; it is well tolerated by patients, who usually refer to its side effects as mild or moderate. The higher risk is represented by its teratogenicity, which makes it an unsuitable medication for pregnant women; it also has a long half-life, and it takes up to 2 years to fully clear this drug (*Barten et al., 2010; Oh and O'Connor, 2013*).

The latest commercially available oral treatment for multiple sclerosis is dimethyl fumarate. Its mechanism of action is still not fully described, but it is believed to reduce oxidative stress and protect axons (*Albrecht et al., 2012*). It was recently suggested that dimethyl fumarate active metabolite (monomethyl fumarate) acts as agonist of the hydroxycarboxylic acid receptor 2 (HCA₂), a G protein coupled membrane receptor expressed by immune cells and especially by neutrophils (*Chen et al., 2014*). The administration of dimethyl fumarate is two times per day; it is used in RRMS patients, which show a significant reduction in the frequency of relapses and in the size lesions. It is quite well tolerated, with the main adverse effect being flushing and gastrointestinal symptoms (*Barten et al., 2010*).

Other treatments are under investigation. Among those, the monoclonal antibodies rituximab and daclizumab. The rituximab antibody targets the CD20 protein expressed on B cells and leads to their depletion; while it seemed to reduce the relapse rate in RRMS patients, it did not give positive results on PPMS. Rituximab is not yet approved as a treatment for MS; however, there is an increasing interest in developing new drugs that target B cells, especially in secondary progressive MS (*Carrithers, 2014*). Ocrelizumab, for example, is another anti-CD20 antibody structurally similar to rituximab that is currently studied in advanced clinical

trials. A different, and novel, target are natural killer cells: in fact, daclizumab is an antibody against CD25 that stimulates CD56^{bright} cells; first studies show its efficacy in improving clinical symptoms and reducing lesions (*Barten et al., 2010*).

2. Oligodendrocytes physiology and pathology

Oligodendrocytes physiology

Oligodendrocytes are glial cells of the CNS; their main role is to form myelin around the axons and therefore allow a fast transmission of the nerve impulse. However, this is not their only function in the CNS; as I will briefly review in this paragraph, they play multiple important roles in supporting axon integrity and function.

The origins of oligodendrocytes in the spinal cord are different from those in the brain. The oligodendrocyte precursor cells (OPCs) in the spinal cord arise from the ventral neuroepithelium; the first wave of OPCs production starts at embryonic day 12.5 (E12.5), which is then followed by a second wave at E15.5 and a third one after birth. On the contrary, the first wave of OPCs in the brain starts ventrally at E12.5, but it is soon replaced by more dorsally generated precursors; second and third waves are generated from the lateral and caudal ganglionic eminences (*Mitew et al., 2014*).

OPC differentiation comprises different stages defined by sequential expression of developmental markers and changes in proliferative capacity, migratory ability, and morphology. Few genes have been recognised as necessary for a correct differentiation: *Olig2* and *Olig1*, for instance, represent important regulators of oligodendrocytes (OLs) development. *Olig2* is expressed throughout the entire differentiation, while *Olig1* is predominantly present during the transition between preOLs and OLs (*Rowitch, 2004*;

Silbereis et al., 2010). Other signaling pathways are involved in OLs development, such as bone morphogenetic protein (BMP), Wnt, Notch, and sonic hedgehog (*Fancy et al., 2010*).

OPCs are characterized by the expression of platelet-derived growth factor- α receptor (PDGF α R) and chondroitin sulfate proteoglycan NG2, and other markers; these proteins are down-regulated when the progenitors reach their final destination in the spinal cord or in the brain. At this point, the OPCs differentiate into mature oligodendrocytes (also called premyelinating oligodendrocytes, preOLs) and later into myelinating oligodendrocytes (OLs); the later ones express high level of myelin proteins, such as PLP, MBP, and also APC-CC1. When the OL is capable of myelinating axons, its morphology changes showing more elaborated processes. (**Figure 4**).

As mentioned already, a key function of OLs is to myelinate axons. The study of myelin biology started in 1717 when Leeuwenhoek, who was interested in the observation of plants and animal tissue using self-made microscopes, reported: “*Sometimes I observe nervule to be completely surrounded by fatty parts*”. According to Cajal, the credit for myelin discovery goes to Ehrenberg in 1833, who described nerve fibers consisting of cylindrical tubes. After him, a lot of scientists took interest in nerve fibers, but Ranvier was the first one, in 1871, to realize that myelin sheaths are periodically interrupted and discontinuous. The development of electron microscopy finally allowed to characterize the “*fatty parts*” described 200 years before, as concentric membranes belonging to OLs, and not secreted by the axon as hypothesized by Cajal in 1909. The role of myelin in allowing saltatory signal conduction in axons was eventually revealed by Huxley and Staempfli in 1949 (*Rosenbluth, 1999*).

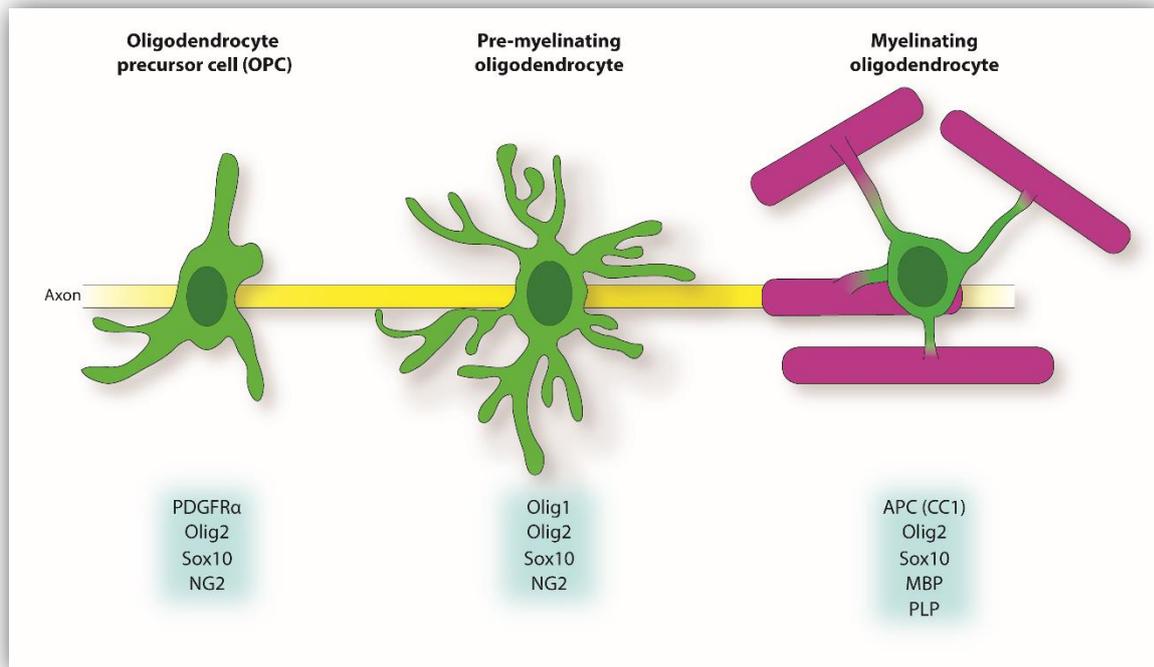


Figure 4 - Oligodendrocyte differentiation and markers expressed. The different stages in the maturation of an OL can be defined based on the expression of specific markers. Although some of them are specific for OPC or myelinating OL, some others like Olig2 or Sox10 are present throughout the entire developmental process.

It is now known that a single OL can form up to 80 internodes on different axons, a feature with regional variations that also depends on axon diameter: the bigger the diameter, the thicker the myelin will be, and the less internodes will be formed by the OL (*Snaidero and Simons, 2014*).

Myelin, named so by Virchow in 1854, is a periodic structure, in which electron-dense lines alternate with light layers, and it is the main component of CNS white matter. Its dry weight consists of 70% lipids and 30% proteins. Among these proteins, myelin basic protein (MBP) is the one of the most abundant. In mice with a deletion of MBP gene, the dense line in myelin structure is missing, thus revealing an important role of MBP in myelin compaction (*Privat et al., 1979*). Another major component of myelin, corresponding to 50% of all myelin proteins, is the proteolipid protein (PLP); it is a tetraspan membrane protein which is

an important stabilizer of the membrane junction after myelin compaction (Nave, 2010). MBP and PLP are the main components of myelin, but there are other well characterized proteins: CNP (4% of total myelin proteins) is a protein that hydrolyzes 2',3'-cyclic nucleotides into their 2'-derivates, it is localized not only on myelin but also on retina photoreceptor, and it was demonstrated that it is involved in cytoskeleton reorganization and arborization of OLs processes (Lee *et al.*, 2005); MAG (1% of the total proteins), mainly localized in the paranodal region, is not part of the compact myelin and belongs to the immunoglobulin superfamily; and MOG, whose presence correlates with the late stages of maturation, is restricted to myelinating OLs and located on the outermost layers of compact myelin. MOG is widely used to induce EAE and which can trigger both T-cell mediated and antibody-mediated responses (Baumann and Pham-Dinh, 2001) (**Figure 5**).

CNS myelination is a long process starting postnatally and reaching completion in mice around 40-60 days of age. In the human CNS, it starts during fetal life in the spinal cord and it reaches its maximum peak in the first year of life (Baumann and Pham-Dinh, 2001). However, OPCs continue to differentiate into mature OLs also during adulthood. A recent study demonstrated further that these newly formed OLs are mainly involved in myelin remodelling and plasticity rather than *de novo* myelin formation. Also, the configuration of the internodes are different, in fact late-born OLs generate more and shorter internodes than early-born OLs (Young *et al.*, 2013). Compared to rodents, the OLs in humans are less dynamic, with a 100-fold lower generation rate (0.32%/year in humans versus 36.5%-186%/year in adolescent and adult mice) (Yeung *et al.*, 2014).

Once the oligodendrocyte process has contacted the axon it progresses to myelinate in a spiralling way. This progression has been the subject of multiple studies: Bunge *et al.* proposed that the oligodendrocyte membrane extends along the entire internode and then starts to myelinate the axon, with the inner tongue rolling underneath the previously

generated layers of myelin and all the layers running parallel to the axon axis (“Carpet crawler” model) (*Bunge et al., 1961*). However, we now know that within a single internode, the number of myelin leaflets can vary. This led to the suggestion of the “serpent model”, according to which a single process contacts the axon and starts to turn around it; when it has reached the desired number of turns, the layers will start to grow laterally and slide one onto each other (*Pedraza et al., 2009*). The “liquid croissant” model (*Sobottka et al., 2011*) came a couple of years later, and it suggests that the outer layers are added in a croissant-like manner on the inner layers. Lastly, recent improvements in electron microscopy allowed to describe a new myelination model, in which the leading edge at the inner tongue continuously wraps around the axon, while the formed myelin layers expand laterally towards the nodal region (*Snaidero et al., 2014; Snaidero and Simons, 2014*).

The function of OLs in the CNS is not only restricted to myelin production; two recent publications have brought attention to their role in supporting axonal energy metabolism. Myelinated axons appear to have limited access to extracellular energy substrates; however, they require a lot of energy metabolites like glucose and lactate. The works from Lee et al. and Fünfschilling et al. suggest that OLs can produce lactate and are able to transfer it directly to the axons: OLs express MCT1 (monocarboxylate transporter-1, implicated in the transport of lactate, pyruvate and ketone bodies) and, through interaction with MCT2 on axons, are able to transfer lactate (or pyruvate) to neurons, and therefore support axonal integrity (*Lee et al., 2012; Morrison et al., 2013; Fünfschilling et al., 2012*).

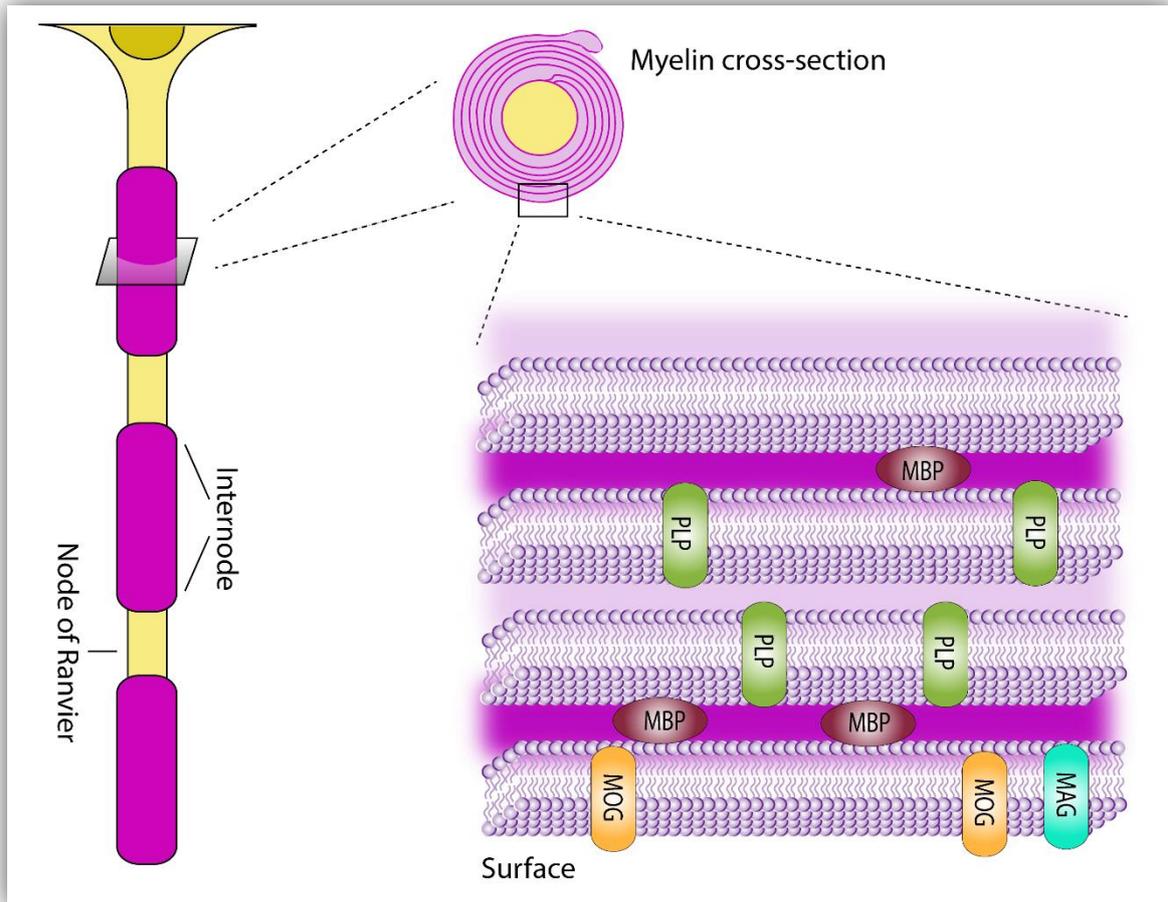


Figure 5 - Proteins of the myelin sheath. Myelin is a highly compact structure composed by lipids (70% of the total dry weight) and proteins (30%). Among those proteins, the major components are myelin basic protein (MBP), proteolipid protein (PLP), myelin oligodendrocytes glycoprotein (MOG) and myelin associated glycoprotein (MAG).

Oligodendrocytes damage in MS and EAE

MS and its animal model EAE are believed to be primarily demyelinating diseases, in which OLs and their myelin sheaths appear to be the main targets of the inflammatory reaction. Recent studies have however brought attention to axonal pathology, which can occur independently of the myelination status of the axon, thus implying that axons may also be a primary target of the immune attack (Nikić *et al.*, 2011).

Oligodendrocytes can in principle be damaged in different ways. One possibility is that OLs death can be induced by oxidative damage. OLs are particularly vulnerable to oxidative stress for several reasons: 1) they need to synthesize and maintain a large amount of myelin, and this requires energy; therefore OLs produce a lot of ATP and consequently hydrogen peroxide (a toxic byproduct of ATP synthesis), which –if not metabolized correctly- can lead to DNA degradation and OLs death (*Wosik et al., 2003*); 2) OLs store iron in large quantities because it is required for myelin production; however, iron is also very reactive and can evoke the production of free radicals and lipid peroxidation (*Todorich et al., 2009*); 3) OLs have low concentrations of the antioxidant enzyme glutathione (*Juurink et al., 1998*; *McTigue and Tripathi, 2008*). Indeed, it has been shown that reactive oxygen species can damage myelin sheaths, as well as axons (*Haider et al. 2011*; *Nikić et al., 2011*) and components of the blood-brain-barrier (*Rubanyi, 1988*), and that ROS scavenger can prevent myelin phagocytosis (*van der Goes et al., 1998*).

OLs are also susceptible to excitotoxicity that is most commonly induced by excessive glutamate. The resulting overactivation of AMPA and kainate receptors on OLs can in fact lead to OLs injury and death. Studies have shown that the treatment of EAE animals with AMPA/kainate antagonists (such as NQBX or MPQX) improves the clinical scores and increases OLs survival (*Pitt et al., 2000*; *Smith et al., 2000*; *Matute et al., 2001*).

Another pathway of excitotoxic cell death is induced by extracellular ATP, the concentration of which is significantly higher at sites of injury. Its receptor P2X₇ is expressed by oligodendrocytes and it is highly permeable to Ca²⁺. In EAE, it was therefore suggested that the sustained activation of P2X₇ receptor by ATP is lethal for OL and that the application of P2X₇ antagonist ameliorates the motor deficits and reduces demyelination (*Matute et al., 2007*).

With regards to OL damage in MS, the sequence of events that leads to demyelination remains an open question. In fact, given their morphology, OLs can be attacked at different sites. They can be targeted at the cell body, in which case the damage will spread towards the myelin sheath, or vice versa myelin can be the main target and the damage will then move towards the soma.

On the one hand, Lucchinetti et al. have suggested that in rare cases, lesions are mainly characterized by OLs damage (pattern III and IV). Particularly in pattern IV lesions, OLs are the primary target and they undergo degeneration and apoptosis, while demyelination appears to be only a secondary process (this sequence would represent an “inside-outside” gradient of demyelination) (Lucchinetti et al., 2000; Lassman et al., 2001). The hypothesis that OLs death can be a major hallmark of MS pathology is supported by another study that described the formation of new lesions. Here the authors suggest, that the first step involves apoptosis of OLs with no myelin phagocytosis, which appears only in the final stages of lesion formation (Barnett and Prineas, 2004). Experimental models of primary OLs pathology may therefore be useful to explain the role of OLs and their death in MS. Different transgenic mice have been recently generated to selectively kill OLs *in vivo* in which either diphtheria toxin receptor (DTR) or diphtheria toxin fragment A (DTA) are expressed by oligodendrocytes (i.e. MOGiCreiDTR mice, MBP-DTR mice or PLPCreER^T:ROSA26-eGFP-DTA), and the administration of diphtheria toxin or the activation of DTA triggers OLs paralysis and death. In these models, demyelination is delayed in respect to OLs death, which probably means that myelin can survive for few weeks even without the support of the connected OL (Traka et al., 2010; Locatelli et al., 2012); in the MBP-DTR mouse it appears that myelin damage is restricted only to the nodal region, with paranodal loop eversion and redistribution of nodal proteins (Oluich et al., 2012). Other models have been proposed to study the effect of OLs death, like for example the one suggested by Capriariello et al. who

created a novel mouse model in which a lentiviral construct expressing inducible caspase 9 (iCP9) under the control of a MBP promoter efficiently leads to OLs apoptosis. Interestingly, in these animals OLs apoptosis stimulated local microglia activation and rapid demyelination (*Caprariello et al., 2012*).

On the other hand, in other MS lesions subtypes (pattern I and II) described as the most common patterns (*Lucchinetti et al., 2000*), myelin itself seems to be the primary target of tissue destruction and demyelination would follow an “outside-inside” gradient. The assumption that myelin is the primary target is not surprising considering that many myelin proteins can serve as autoantigens in MS and thus lead to primary inflammatory demyelination. MOG is localized at the outermost layer of the myelin sheath; its role as a potent autoantigen in the pathogenesis of EAE has been clear for several years, and it is known that anti-MOG antibodies can induce demyelination. The conformation of the antigen also plays a role to determine its encephalitogenicity: for example, re-folded MOG seems to be more pathogenic than its non-refolded counterpart, with conformational MOG antibodies found in the serum of rats immunized with refolded MOG and strong T-cell response induction (*de Graaf et al., 2012*). Antibodies against MOG have also been reported in pediatric cases of MS, but are not commonly detected in adult patients (*Pröbstel et al., 2011*). PLP and MBP are other candidate autoantigens, considering also their pathogenic role in the development of EAE in specific laboratory mouse strains. Anti-PLP antibodies as well as autoimmune PLP-specific T cells reactive with PLP have been found in MS patients. Anti-MBP antibodies have been detected in close proximity to injured axons within a lesion, and are thought to specifically damage myelin membrane inducing therefore demyelination (*Derfuss and Meinel, 2012; Quintana et al., 2012*).

The nodal region can also be a starting point for demyelination and this possibility has raised quite some interest over the past years. The nodes of Ranvier are short unmyelinated regions

of the axons where Na^+ enters to generate action potentials. The nodal area includes the node of Ranvier itself, the paranodal segment and the juxtaparanodal region. The node of Ranvier is characterized by a high density of Na^+ channels (Nav1.1, Nav1.6) and some K^+ channels (Kv); a large number of scaffolding and adhesion proteins, such as ankyrin G and neurofascin 186 (NF186), are also clustered in this area. In MS and EAE the nodes appear longer and this might be associated with a retraction of the myelin sheath and the disruption of the paranodal area (*Fu et al., 2009*). The paranode is defined as the region where myelin loops are in contact with the axons, and it is located at both sides of the node; the proteins which dominate this area are contactin-1 and contactin associated protein-1 (Caspr1), and neurofascin 155 (NF155) on the myelin membrane. This appears to be a very vulnerable structure as it has been shown that in demyelinating diseases the myelin loops of the paranode appear loose and the proteins arrangement is disorganized. Interestingly, autoantibodies against NF155 and NF186 have been found in MS patients, and in the same study it was shown that these antibodies exacerbate the clinical course of EAE in a rat model of T-cell transfer EAE (*Mathey et al., 2007*). Lastly, the juxtaparanodal region is populated by K^+ channels (Kv1.1 and Kv1.2), adhesion molecules (contactin-2/TAG-1 and Caspr-2), and metalloprotease (ADAM22). Contactin2/TAG-1 has also been recognised as a potential autoantigen for autoantibodies and T cells activation in MS patients (*Meinl, 2011; Derfuss et al., 2009; Simons et al., 2014*).

Oligodendrocyte repair and remyelination

Remyelination is defined as the process of generating new myelin sheaths around a previously demyelinated axon. In 1979 Smith and colleagues showed for the first time that in remyelinated axons conduction is restored, which prompted subsequent studies to investigate mechanisms that can improve remyelination (*Smith et al., 1979*). Remyelination is indeed an

important recovery process; firstly because it helps axonal survival and protects them from further degeneration (*Irvine et al., 2008*), and secondly because by reorganizing the nodes and paranodes with their voltage dependent channels it restores appropriate saltatory conduction of action potentials.

One way to identify remyelination is to measure the g ratio, which is the ratio between the diameter of the axon and the myelin thickness: remyelinated axons show a thinner and shorter myelin sheath, resulting in a higher than normal g ratio. The average g ratio of a myelinated axon is between 0.6 and 0.8, while a remyelinated axon typically has a g ratio of 0.8-1 (*Olsen et al., 2014*). (**Figure 6**).

Remyelination is a multistep process triggered by demyelination. Following injury in fact OPCs become activated and respond to pro-migratory and mitogen factors that induce their migration and proliferation to the site of injury. Once they reach the demyelinated lesion, OPCs change morphology and differentiate into mature myelinating cells, which ultimately will remyelinate the area.

Remyelination is initiated by the generation of new OLs derived by a population of precursor cells; in adulthood, these cells are widespread in the white and gray matter in the CNS, and can be recognized by the expression of markers such as NG2, PDGFR α , Olig2, Olig1 and more. Few studies have shown that those OPCs are the main source of remyelinating OLs by the use of *in vitro* and transplantation approaches describing OPCs being able to differentiate into OLs and remyelinate areas of demyelination (*Groves et al., 1993; Nunes et al., 2003*). Also, demyelinated areas during remyelination display cells that express both OPCs and OLs markers (*Fancy et al., 2004*). Recently it has also been suggested that NG2⁺ precursors constantly migrate through the adult brain and can directly differentiate into mature OLs without proliferating; interestingly, it seems that these cells also participate in the glial scar

formation extending their processes toward the lesion site and surrounding the site of injury, as it was observed by time-lapse *in vivo* imaging (Hughes *et al.*, 2013).

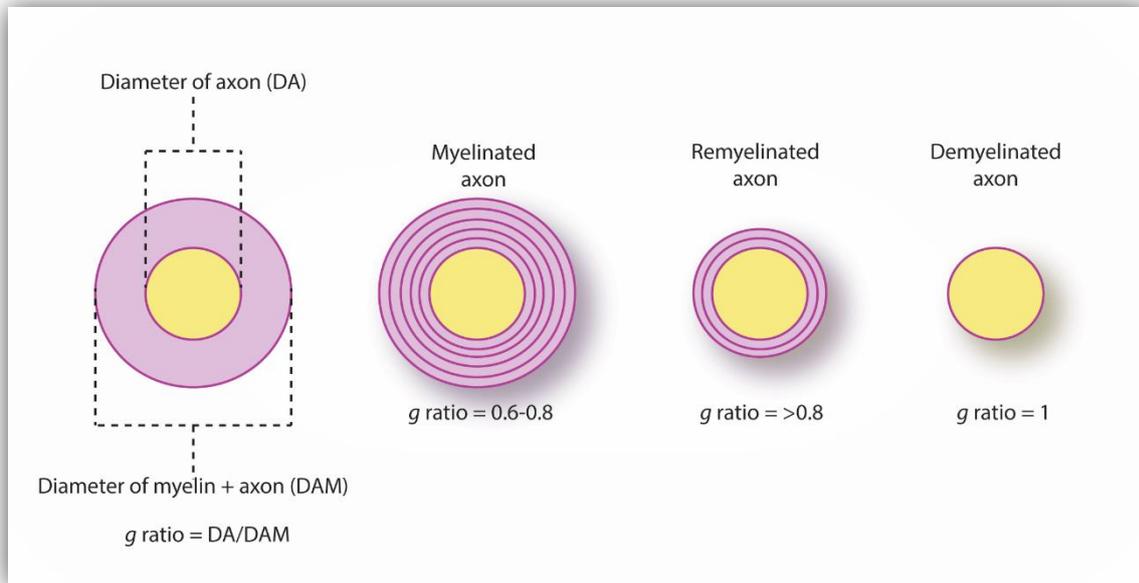


Figure 6 - g-ratio of myelin sheaths in relation to axon diameters. Inspired by Olsen *et al.*, 2014.

New OLs can also derive from cells in the subventricular zone (SVZ), either from precursor cells involved in the rostral migratory stream or from GFAP-expressing stem cells. These cells are for example the major contributors to remyelination in the corpus callosum following damage to myelin structure (Franklin and ffrench-Constant, 2008).

The regulation of OPCs differentiation from pre-myelinating cells to myelinating OLs depends on different intrinsic and extrinsic factors. Among the intrinsic factors, there are both positive and negative regulators. An example of a positive regulator is the myelin gene regulatory factor (MRF) which is essential for OPCs differentiation into MBP-positive and MOG-positive OLs (Emery, 2010). Zinc finger protein 191 (Zfp191) is also important for myelination; in mice, the mutation of Zfp191 causes hypomyelination with OLs that appear functional, but are not capable of myelinating axons (Howng *et al.*, 2009). Retinoid X receptor- γ (RXR- γ) was found to be upregulated during remyelination in a rat model of

demyelination, and its pharmacological stimulation enhanced remyelination. RXR- γ expression was also detected in MS lesions, and it was mainly localized in the nucleus or cytosol of Olig1+ precursors (*Huang et al., 2011*). Important to mention are the Notch-Jagged1 and the Wnt signalling pathways. The former has an inhibitory role on OPCs maturation and its pharmacological block in EAE enhances recovery and myelin repair (*Jurynczyk et al., 2005; Luessi et al., 2014*). The latter negatively regulates myelin formation as well, making it a good target for therapeutic studies. OPCs differentiation is also regulated by extrinsic factors, either secreted by neurons or by macrophages/microglia. Those are for example bone morphogenetic protein 4 (BMP4) or Lingo-1, both working as inhibitors of OPCs maturation. Interestingly recently an important role for macrophages/microglia during remyelination has been proposed based on the demonstration that macrophages switch from M1 to M2 phenotype at the time of remyelination. M2 macrophages then promote OLs differentiation by production of activin-A. In line with these findings M2 depletion resulted in a lower oligodendrocyte differentiation rate (*Miron et al., 2013*).

Once the OLs are differentiated into myelinating cells, they can contact axons and wrap around their processes to form a new myelin sheath. However, we know that remyelination does not work efficiently in MS. One possible explanation of why remyelination fails might be that OPCs cannot repopulate properly and are low in number; however, this idea is most likely to be excluded because it has been described that OPCs can efficiently migrate to the lesion site (*Aguirre et al., 2007; Fancy et al., 2004; Nakatani et al., 2013*). A second failure mechanism might be that OPCs are not correctly recruited and therefore do not reach and differentiate in the demyelinated area. In support of this idea it has been shown that MS patients can have autoantibodies against NG2, providing evidence that OPCs can also be a target of autoimmune attack in MS (*Niehaus et al., 2000*). The last, and probably the most accurate, hypothesis is that OPCs migrate and proliferate, but do not differentiate into

myelinating cells. One explanation might be that the demyelinated areas contain factors that inhibit their differentiation (such as Notch-Jagged1 or Wnt) (*Franklin and ffrench-Constant, 2008; Franklin and Gallo, 2014*).

3. *In vivo* imaging

Principles of two-photon excitation microscopy

Multi photon microscopy is a nonlinear optical microscopy technique suited for high resolution imaging of physiological processes, morphology and cell-cell interactions in tissue and living animals. It was theoretically described for the first time in 1931 in a doctoral thesis by Maria Goeppert-Mayer, but experimentally verified only in 1990 (*Denk et al., 1990*).

The principle of two photon microscopy lies in the excitation of a fluorescent molecule by the simultaneous absorption of two photons of equal energy, the total energy of which is the same as the one required for a single photon excitation of the fluorophore. Once the molecule reaches the excited state, the emission is the same in one photon and two photon excitation (**Figure 7a**).

Two-photon imaging has become the most popular technique for *in vivo* imaging, and it presents numerous advantages. First, while in standard one-photon microscopy the excitation process requires photons in the ultraviolet/blue/green spectral range, multiphoton absorption occurs in the near-infrared wavelength range; near-infrared light has the advantage of allowing a deeper penetration into the tissue (up to 1000um), reducing phototoxicity and minimizing photobleaching. Second, multiphoton absorption is restricted to the focal plane and there is no out-of-focus excitation, in contrast to standard single-photon excitation, where the fluorescence signals are generated above and below the focal plane (*Zipfel et al., 2003; Helmchen and Denk, 2005*) (**Figure 7b**).

The setup of a two-photon microscope is similar to a single-photon confocal laser scanning microscope; the main difference is the presence of a pulsed laser source, most typically a Titanium-sapphire (Ti:Sapphire) oscillator, which provides ultrashort (femtoseconds or picoseconds) near-infrared pulses at high repetition rate (100 MHz). The wavelength is tuneable usually in the range of 670nm-1040nm, allowing the two photon excitation of a broad spectrum of fluorophores (*Diapstro et al., 2006; Helmchen and Denk, 2005*).

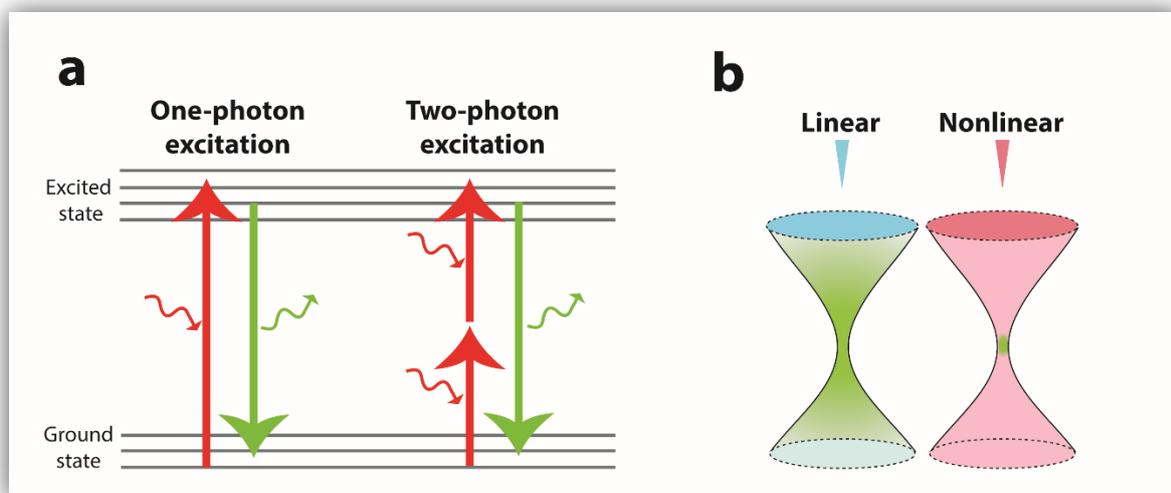


Figure 7 – Principles of one-photon excitation versus two-photon excitation. **a)** Jablonski diagram illustrating one- and two-photon excitation of a fluorophore from the ground state to the excited state; **b)** on the left, blue light is used to excite in one-photon microscopy, and the excitation generates a cone of fluorescent light; on the right, near-infrared light is used to excite in two-photon microscopy, and there is not out-of-focus signal. Inspired by *Helmchen and Denk, 2005*.

Imaging the healthy and diseased central nervous system

In vivo imaging has become a powerful tool in neuroscientific research: it allows to directly follow cell dynamics, to observe the same cell over the time and see how it changes in response to an injury, and to study how different cells interact with each other. Imaging in the CNS is performed in the brain by implanting a cranial window or by the thinned skull method (*Grutzendler et al., 2002; Zuo et al., 2005; Xu et al., 2007; Holtmaat et al., 2009; Yang et al.,*

2010); these techniques are useful to visualize the same area at different timepoints within the same experiment, allowing chronic imaging sessions. When it comes to the spinal cord, acute imaging sessions are the most common; however, repetitive imaging is also possible, and recent spinal cord windows have been developed (*Farrar et al., 2012; Fenrich et al., 2012*).

Advances in microscopy techniques go hand in hand with advances in labelling techniques. The discovery that indisputably changed labeling strategies was the introduction of the jellyfish green fluorescent protein (GFP) as a vital stain (*Chalfie et al., 1994*). The first report used GFP to label neurons (*Chalfie et al., 1994*), but in the following years GFP (and its spectral variants yellow [YFP], cyan [CFP], red [RFP] fluorescent proteins) technologies were extensively applied to generate transgenic mice that express the fluorescent proteins under different promoters in order to drive the labelling to specific cell types of interest (neurons, glial cells, immune cells,..) or organelles (mitochondria, peroxisomes, microtubules,..) (**Table 1**).

Neuroscientists have used these *in vivo* imaging approaches to study calcium dynamics (*Svoboda et al., 1997; Helmchen and Waters, 2002*), neuronal plasticity (*Svoboda et al., 1996*), as well as neurological diseases (*Misgeld and Kerschensteiner, 2006; Sorbara et al., 2012*). The use of *in vivo* imaging and transgenic mice is particularly useful to unravel the *in vivo* pathogenesis of neurological disorders such as Alzheimer's disease (*Fuhrmann et al., 2010; Kuchibhotla et al., 2008; Busche et al., 2008*), ischemia (*Nishimura et al., 2006; Sakadzic et al., 2010*), injury (*Nguyen et al., 2002; Kerschensteiner et al., 2005*) and multiple sclerosis. The latter has been the subject of a number of studies aiming at understanding on one hand recruitment, trafficking, function and activation of T cells (*Bartholomaeus et al., 2009; Siffrin et al., 2009; Mues et al., 2013*), and on the other hand mechanisms of axonal loss (*Siffrin et al., 2010; Nikić et al., 2011*); a recent publication also raised interest in the role of mitochondrial transport deficits (*Sorbara et al., 2014*).

Cell type	Promoter	Fluorescent protein	Reference
Neurons	Thy1-promoter	XFP	Feng et al., 2010
Neuronal mitochondria	Thy1-promoter, with mito targeting sequence	CFP	Misgeld et al., 2007b
Oligodendrocytes	PLP-promoter	GFP	Mallon et al., 2002
Schwann cells	S100-promoter	GFP, YFP	Zuo et al., 2004
Astrocytes	GFAP-promoter Aldh1L1-promoter	GFP	Zhuo et al., 1997 Gong et al., 2003
Microglia *	Cx ₃ CR1-locus	GFP, YFP	Jung et al., 2000
Monocyte derived macrophages *	CCR2-locus	RFP	Saederup et al., 2010
T cells	CD2-promoter	GFP	Singbartl et al., 2001
<i>*knock-in mouse strains</i>			

Table 1 - Transgenic mouse lines widely used for *in vivo* imaging.

CHAPTER II - Aim of the study

Though demyelination is an important feature in the pathogenesis of multiple sclerosis (MS), currently the mechanisms that mediate oligodendrocyte damage and myelin loss are not fully understood. The overall aim of my PhD work was to investigate how myelin is damaged in EAE, using a combined approach of *in vivo* imaging, confocal microscopy and ultrastructural analysis.

The first project was focused on establishing a new strategy to reliably label myelin *in vivo*. This approach involved the local application of vital dyes that allowed us to visualize different cell types, subcellular compartments, organelles, and the release of soluble mediators. A major advantage of this new method is that the use of vital dyes can be easily combined with transgenic labelling strategies (see Chapter I, Table 1), therefore enhancing the information gained in each experiment. It represents a reliable strategy to label cells and subcellular compartments, and provided that the right dyes are available can be a cheaper and faster alternative to the creation of new transgenic mouse lines. The aims of this project were to answer the following specific questions:

- Which vital dyes can successfully be applied *in vivo*?
- Which is the appropriate concentration and the application settings needed for an optimal imaging quality and tissue penetration?
- What are the best fixation conditions that will allow further post-fixation analysis on the samples previously imaged with the vital dye?

With the first project I established a novel, fast and reliable way to label myelin *in vivo*. This finding was useful for the second project which centered on the *in vivo* analysis of the demyelination process. Oligodendrocytes and myelin are the main targets of the inflammatory attack in MS and its animal model EAE; however, the mechanisms underlying their damage could so far not be observed *in vivo*. Here I used advanced microscopy techniques to answer the following questions:

- In the animal model EAE, how does demyelination occur? What is the primary immune attack: oligodendrocytes or myelin?
- Using *in vivo* imaging techniques, is it possible to detect changes in myelin structure and morphology which could be related to demyelination? If yes, at which timepoint of the disease do they first appear and when are they most frequently encountered?
- How do these morphological abnormalities appear at the ultrastructural level?
- What are the molecular mechanisms that induce a change in the myelin structure and lead to demyelination in neuroinflammatory lesions?
- What is the relevance of these findings for the human disease MS?

The results of the first project have been published in a peer-reviewed journal (*Romanelli et al., 2013*), while a manuscript describing the results of the second project is currently in preparation.

CHAPTER III – Materials & Methods

1. Materials

Surgery procedures

Surgery reagents

<i>Ketamine hydrochloride 10% (Ketamine)</i>	Bremer Pharma GmbH, Warburg, Germany
<i>Xylarium 20 mg (Xylazine)</i>	Riemser Arzneimittel AG, Greifswald-Insel Riems, Germany
<i>Forene (Isoflurane)</i>	Abbott AG, Baar, Switzerland
<i>Sterile artificial mouse cerebrospinal fluid (aCSF)</i>	<p>Solution A:</p> <p>8,66 g NaCl (Merck)</p> <p>0,224 g KCl (Merck)</p> <p>0,206 g CaCl₂ · 2H₂O (Sigma-Aldrich)</p> <p>0,163 g MgCl₂ · 6H₂O (Sigma-Aldrich)</p> <p>Solution B:</p> <p>0,214 g Na₂HPO₄ · 7H₂O (Merck)</p> <p>0,027 g NaH₂PO₄ · H₂O (Merck)</p> <p>dH₂O ad 500 ml</p> <p>Mixture of solutions A and B in a 1:1 ratio</p>
<i>Bepanthen Augen- und Nasensalbe 5 g (eye cream)</i>	Bayer Vital GmbH, Leverkusen, Germany
<i>Ringerlösung Fresenius KabiPac (Ringer's solution)</i>	Fresenius KaBI Dtl., Bad Homburg, Deutschland
<i>Cutasept F Lösung 250 ml (disinfectant spray)</i>	Bode Chemie GmbH & Co, Hamburg, Germany
<i>Agarose</i>	Sigma-Aldrich® Chemie GmbH, 82024 Taufkirchen, Germany

Surgical tools and materials

<i>Wella contura W7807 (Hair clipper)</i>	Wella, Darmstadt, Germany
<i>Syringe 3pc 5 ml Omnifix™ luer slip (syringe for injection of Ringer's solution)</i>	B. Braun Melsungen AG, Melsungen, Germany
<i>BD Plastipak Hypodermic luer slip syringe 1 ml (syringe for Ketamine/Xylazine and Ptx injection)</i>	Becton, Dickinson and Company, Franklin Lakes (New Jersey), USA
<i>Feather stainless steel blade (surgical blade)</i>	pfm medical ag, Cologne, Germany
<i>Noyes Spring Scissors (Large spring scissors)</i>	Fine Science Tools GmbH, Heidelberg, Germany
<i>Vannas-Tübingen Spring Scissors (Small angled spring scissors)</i>	Fine Science Tools GmbH, Heidelberg, Germany
<i>Dumont Mini Forceps – Inox Style 3 (Small forceps)</i>	Fine Science Tools GmbH, Heidelberg, Germany
<i>Dumont Mini Forceps – Inox Style 5 (Small forceps, smaller tip than Inox style 3)</i>	Fine Science Tools GmbH, Heidelberg, Germany
<i>Hypodermic Needles BD Microlance 3 30 Gauge (0,3 mm, yellow) for subcutaneous injection of Ringer's solution and anesthesia</i>	Becton, Dickinson and Company, Franklin Lakes (New Jersey), USA
<i>Ethicon Ethilon monofil 6-0 size, 667H (skin suture)</i>	Johnson & Johnson Medical GmbH, Norderstedt, Germany
<i>Ethicon Vicryl 4-0 size, MIC101H (intracorporal suture)</i>	Johnson & Johnson Medical GmbH, Norderstedt, Germany
<i>Sugi (absorbent triangles)</i>	Kettenbach GmbH & Co. KG, Eschenburg, Germany
<i>Metal plate</i>	Custom-made
<i>Cast Alnico Button Magnets</i>	Eclipse Magnetics Ltd, Sheffield, UK
<i>Rubber bands</i>	
<i>Support cushion</i>	Custom-made

Devices

<i>Olympus KL 1500 LCD (cold light source for stereomicroscopy)</i>	Olympus Deutschland GmbH, Hamburg, Germany
<i>Olympus Stereo Microscope SZ51</i>	Olympus Deutschland GmbH, Hamburg, Germany
<i>FST 250 Hot Bead Sterilizer (sterilizer for surgical instruments)</i>	Fine Science Tools GmbH, Heidelberg, Germany
<i>T/Pump (Heating pad)</i>	Gaymar Industries, Orchard Park (New York), USA

Perfusion and immunohistochemistry

Reagents

<i>PFA (paraformaldehyde) 4%</i>	8% PFA (Sigma-Aldrich) in dH ₂ O, heated up to 55 °C and stirred additional 10 min, filtrated and mixed in a 1:1 ratio with 0.2 M PB (Phosphate buffer), pH adjusted to 7.2-7.8
<i>Triton X-100</i>	Sigma-Aldrich, Chemie GmbH, 82024 Taufkirchen, Germany
<i>Sucrose</i>	Sigma-Aldrich, Chemie GmbH, 82024 Taufkirchen, Germany
<i>PBS 10x (phosphate buffered saline), pH=7,2/7,4</i>	2,6 g NaH ₂ PO ₄ · H ₂ O 14,4g Na ₂ HPO ₄ · 2H ₂ O 87,5g NaCl (Merck) dH ₂ O ad 1l
<i>TBS 10x (Tris buffered saline), pH=7,6</i>	61 g Tris base (121,14 g/mol), (Sigma-Aldrich) 90 g NaCl dH ₂ O ad 1l
<i>0,2 M PB (phosphate buffer)</i>	27,598 g NaH ₂ PO ₄ · H ₂ O, 35,598 g Na ₂ HPO ₄ · 2H ₂ O dH ₂ O ad 1l

<i>Gibco goat serum</i>	Invitrogen GmbH, Darmstadt, Germany
<i>DMSO</i>	Sigma-Aldrich® Chemie GmbH, 82024 Taufkirchen, Germany

Antibodies, vital dyes and tracers

<i>Polyclonal rabbit anti-Iba1</i>	Wako Chemicals GmbH, Neuss, Germany
<i>Monoclonal mouse anti-APC/CC1</i>	Merck Millipore, Darmstadt, Germany
<i>Polyclonal rabbit anti-human MBP</i>	Dako/Agilent Technologies, Santa Clara (California), USA
<i>Goat-anti-rabbit Alexa fluor® 594 antibody</i>	Invitrogen GmbH, Darmstadt, Germany
<i>Goat-anti-mouse Alexa fluor® 635 antibody</i>	Invitrogen GmbH, Darmstadt, Germany
<i>Goat-anti-rabbit Alexa fluor® 488 antibody</i>	Invitrogen GmbH, Darmstadt, Germany
<i>DAPI</i>	Invitrogen GmbH, Darmstadt, Germany
<i>Isolectin GS-IB4 from Griffonia simplicifolia, Alexa Fluor 647 conjugate</i>	Invitrogen GmbH, Darmstadt, Germany
<i>Vybrant CFDA SE Cell Tracer Kit</i>	Invitrogen GmbH, Darmstadt, Germany
<i>NeuroTrace 435/455 blue fluorescent Nissl stain</i>	Invitrogen GmbH, Darmstadt, Germany
<i>NeuroTrace 640/660 deep-red fluorescent Nissl stain</i>	Invitrogen GmbH, Darmstadt, Germany
<i>Nuclear-ID Red DNA Stain</i>	Enzo Life Sciences, ENZ-52406
<i>POPO-1 iodide (434/456)</i>	Invitrogen GmbH, Darmstadt, Germany
<i>SYTO 64 red fluorescent nucleic acid stain</i>	Invitrogen GmbH, Darmstadt, Germany
<i>Cell Trace BODIPY TR Methyl Ester</i>	Invitrogen GmbH, Darmstadt, Germany
<i>DiOC6(3) (3,3'-Dihexyloxacarbocyanine Iodide)</i>	Invitrogen GmbH, Darmstadt, Germany
<i>FluoroMyelin red fluorescent myelin stain</i>	Invitrogen GmbH, Darmstadt, Germany
<i>FluoroMyelin green fluorescent myelin stain</i>	Invitrogen GmbH, Darmstadt, Germany
<i>MitoTracker Red CMXRos</i>	Invitrogen GmbH, Darmstadt, Germany
<i>Amplex UltraRed reagent</i>	Invitrogen GmbH, Darmstadt, Germany
<i>Tetramethylrhodamine, methyl ester,</i>	Invitrogen GmbH, Darmstadt, Germany

<i>perchlorate - TMRM</i>	
<i>Rabies virus SAD ΔG (CVS G)</i>	Provided by Karl-Klaus Conzelmann, Gene Center LMU, Munich

Tools and materials for histology

<i>Microscope slides 76x26 mm</i>	Gerhard Menzel Glasbearbeitungswerk GmbH & Co. KG, Braunschweig, Germany
<i>Microscope cover slips 24x60 mm</i>	Gerhard Menzel Glasbearbeitungswerk GmbH & Co. KG, Braunschweig, Germany
<i>Parafilm</i>	Brand GmbH & Co. KG, Wertheim Germany
<i>Pipettes, pipette tips and tubes (2ml and 1,5 ml)</i>	Eppendorf AG, Hamburg, Germany
<i>12-well cell culture plates</i>	Becton, Dickinson and Company, Franklin Lakes (New Jersey), USA
<i>Tissue Tek Cryomold Standard, 25x20x5 mm</i>	Sakura Finetek Europe B.V. , Alphen aan den Rijn, The Netherlands
<i>Tissue Tek Cryomold Biopsy, 10x10x5 mm</i>	Sakura Finetek Europe B.V. , Alphen aan den Rijn, The Netherlands
<i>Tissue Tek optimal cutting temperature (O.C.T.)</i>	Sakura Finetek Europe B.V. , Alphen aan den Rijn, The Netherlands
<i>Vectashield Mounting Medium</i>	Vector Laboratories, Inc., Burlingame (California), USA
<i>Paper filters (185 mm Ø circles)</i>	Whatman Schleicher & Schuell GmbH, Dassel, Germany
<i>50 ml centrifuge tubes</i>	Greiner Bio-One GmbH, Frickenhausen, Germany

Technical devices

<i>Leica CM1850 cryostat</i>	Leica Microsystems GmbH, Wetzlar, Germany
------------------------------	---

<i>Vibratome 1000Plus</i>	Intracel LTD, Shepreth, Royston, Great Britain
<i>Vortex-Genie 2</i>	Scientific Industries, Inc., Bohemia (New York), USA
<i>KERN EW 150-3M (scales)</i>	Kern & Sohn GmbH, Balingen-Frommern, Germany
<i>Laboratory pH meter inoLAB</i>	WTW Wissenschaftlich-Technische Werkstätten, Weilheim, Germany
<i>Magnetic stirring hotplate MR 3001K and stirring bars</i>	Heidolph Instruments GmbH & Co. KG, Schwabach, Germany
<i>Ismatec IP high precision multichannel pump (pump for perfusions)</i>	ISMATEC SA, Labortechnik - Analytik, Glattbrugg, Switzerland
<i>Olympus IX71 inverted fluorescence microscope</i>	Olympus GmbH, Hamburg, Germany

Imaging

Imaging devices

<i>FV1000 confocal system mounted on an upright BX61 microscope</i>	Olympus GmbH, Hamburg, Germany
<i>Olympus FV1000 MPE multiphoton Microscope, equipped with femtosecond- pulsed Ti:Sapphire laser (Mai Tai HP, Newport/Spectra Physics) and opto- electrical intensity regulation</i>	Olympus GmbH, Hamburg, Germany
<i>Objectives: x4/0.13, x10/0.4 air objectives; x25/1.05 water immersion objective; x40/0.85, x60/1.42 oil immersion objectives</i>	Olympus GmbH, Hamburg, Germany
<i>Small animal ventilator</i>	Harvard Apparatus
<i>Intratracheal cannula (1.0 mm OD, 13 mm length)</i>	Harvard Apparatus
<i>Spinal clamping device (spinal adaptor for a stereotaxic frame)</i>	Narishige STS-A

<i>Gravity superfusion system containing in-line heater</i>	Warner Instruments
<i>vacuum system with suction tube</i>	Custom-built
<i>Stage for spinal clamping device</i>	Luigs & Neumann SM 5-9 stage and controller unit

EAE induction

Reagents for immunization

<i>Purified recombinant MOG (from E. Coli)</i>	Stock solution, produced by laboratory of Doron Merkler (Universität Göttingen, University of Geneva)
<i>Purified MOG peptide (N35-55)</i>	Schafer-N Copenhagen, Denmark
<i>Mycobacterium Tuberculosis H37 RA</i>	Sigma-Aldrich® Chemie GmbH, 82024 Taufkirchen, Germany
<i>Incomplete Freund's adjuvant (IFA)</i>	Sigma-Aldrich® Chemie GmbH, 82024 Taufkirchen, Germany
<i>Pertussis toxin from Bordetella pertussis, inactivated</i>	Sigma-Aldrich® Chemie GmbH, 82024 Taufkirchen, Germany

Tools for immunization

<i>10 ml syringes</i>	Hamilton
<i>Hypodermic Needles BD Microlance 3 23 Gauge (0,6 mm, blue) for subcutaneous emulsion immunization</i>	Becton, Dickinson and Company, Franklin Lakes (New Jersey), USA

Electron Microscopy

Reagents for tissue preparation

<i>Glutaraldehyde 50%</i>	Electron Microscopy Sciences, Hatfield, PA 19440, USA
<i>Formaldehyde 16% (PFA)</i>	Electron Microscopy Sciences, Hatfield, PA 19440, USA
<i>Sorensen's Phosphate buffer 0.2M pH 7.2 (PBS)</i>	Electron Microscopy Sciences, Hatfield, PA 19440, USA

Software

Data analysis

<i>Adobe Creative Suite CS6 (Photoshop, Illustrator)</i>	Adobe Systems, Inc., San Jose, California, USA
<i>ImageJ</i>	General Public License http://rsbweb.nih.gov/ij/download.html
<i>Graphpad Prism</i>	GraphPad Software, La Jolla, California, USA
<i>Microsoft Office (Powerpoint, Excel, Word)</i>	Microsoft Corporation, Redmond, Washington, USA
<i>Panoramic viewer 1.15</i>	General Public License http://www.3dhistech.com/panoramic_viewer
<i>Reconstruct</i>	General Public License http://synapses.clm.utexas.edu/tools/reconstruct/reconstruct.stm
<i>Imaris</i>	Imaris® Analytical Image Processing Solutions for the Life Science, Bitplane

2. Methods

Experimental animals

All the animals were bred in our institute animal facility kept under controlled standard housing conditions. For the purpose of this study I have used several transgenic as well as wild-type mouse lines. In particular C57/Bl6 were ordered from Janvier Labs while BiozziABH mice were obtained from Harlan Laboratories, and consequently breed and crossed with different already established transgenic mice: Thy1-MitoCFP-P in which CFP expression is selectively directed to neuronal mitochondria (*Misgeld et al., 2007b*); Thy1-XFP mice, with fluorescently labelled neurons (*Feng et al., 2000*); in CX₃CR1^{gfp/+}, GFP is expressed by resident microglia (*Jung et al., 2000*); in PLP-GFPm mice the PLP promoter localizes the GFP specifically to the oligodendrocyte lineage (*Mallon et al., 2002*); CCR2^{rfp/+} show circulating monocytes labelled with RFP (*Saederup et al., 2010*); FcR quadruple knockout animals (kindly received from Dr. Verbeek at Leiden University Medical Center, The Netherlands). For the experiments only adult animals were used (between 6 and 12 weeks of age) and both sex were equally distributed in controls and experimental groups. Animals were kept in Eurostandard Type II long cages 365x207x140 mmH (Tecniplast, Hohenpeißenberg, Germany) stored in IVC rack system with a maximum of five mice per cage. Autoclaved food (regular food “Maus” from Ssniff, Soest, Germany) and autoclaved tap water were supplied ad libitum. Mice were held at a 12 h light/12 h dark cycle. All animal experiments were performed in accordance with regulations of the animal welfare act and protocols approved by the Regierung von Oberbayern (permit numbers 55.2-1-54-2532-73-13; 55.2-1-54-2532-25-08).

Induction of experimental autoimmune encephalomyelitis (EAE)

Acute and chronic EAE were induced in adult animals (6-12 weeks) as previously reported (*Abdul-Majid et al., 2000; Baker et al., 1990*). The protocols were slightly different according to the mouse line and the experimental design. Briefly, mice with a B16 genetic background were injected with a total of 250 μ l of an emulsion comprised of 200-300 μ g of purified recombinant myelin oligodendrocyte glycoprotein (MOG, N1-125, expressed in *E. Coli*) in complete Freund's adjuvant with 5 mg/ml mycobacterium tuberculosis H37 Ra. The mice received 200-400 ng of Pertussis Toxin at day 0 and day 2 after immunization. BiozziABH and BiozziABH/B16 animals were immunized following the protocol described previously (*Baker et al., 1990*), according to which the mice are injected with an emulsion containing purified recombinant MOG (50 μ g) in complete Freund's adjuvant at day 0 and day 7. On day 0, 1, 7, and 8 following immunizations, pertussis toxin (50 ng) was administered intraperitoneally.

For the antibody transfer experiment, Thy1-YFP/B16 animals were immunized with MOG peptide (N35-55). They received a total of 200 μ g of MOG emulsified with complete Freund's adjuvant with 10 mg/ml mycobacterium tuberculosis H37 Ra. Pertussis toxin was injected at day 0 and day 2 after immunization at a concentration of 400 ng.

Mice were weighed daily and the severity of the neurological deficits was expressed with a score: 0, no detectable clinical signs; 0,5, partial tail weakness; 1, tail paralysis; 1,5, gait instability or impaired righting ability; 2, hind limb paresis; 2,5, hind limb paresis with dragging of one foot; 3, total hind limb paralysis; 3,5, hind limb paralysis and fore limb paresis; 4, hind limb and fore limb paralysis; 5, death.

Immunohistochemistry

Animals were lethally anesthetized with isofluorane and perfused transcardially with 20 ml of saline solution followed by 30 ml of 4% paraformaldehyde (PFA) in 0.1 M phosphate buffer. Spinal cords were dissected out and post-fixed in 4% PFA overnight at 4°C. To cryoprotect the tissue, the tissue was transferred to 30% sucrose for at least 48hrs before embedding the specimens in Tissue-Tek optimal cutting temperature (O.C.T.) compound and freezing it at -20°C. Subsequently I cut 20-30 µm longitudinal spinal cord sections and stained free-floating. The sections were rinsed 3 times for 10 minutes in 1x PBS at room temperature and then incubated for 1 hr at room temperature with 10% goat serum. The following primary antibodies were applied and incubated overnight at 4°C in a solution containing 1% goat serum/0.1% NaN₃/0.5% Triton/1x PBS: rabbit anti-Iba1 (1:200); mouse anti-APC/CC1 (1:100); rabbit anti-MBP (1:200, cold methanol pre-treatment was necessary to obtain a sharp staining). The sections were later washed three times with PBS and incubated with a secondary antibody at 4°C in a solution containing 1% goat serum/0.1% NaN₃/0.5% Triton/1x PBS: goat anti-rabbit Alexa 594 (1:1000), goat anti-mouse Alexa 633 (1:1000), goat anti-rabbit Alexa 488 (1:1000). All the samples were counterstained with Nissl-staining Neurotrace 640/660 (1:500) or DAPI (1:10000).

After staining, the samples were mounted with Vectashield and covered with a coverslip glass sealed with nail polish.

Confocal microscopy

Fixed tissue samples previously stained were then scanned on a FV1000 confocal system mounted on an upright BX61 microscope (Olympus). The system was equipped with a

10x/0.4 water immersion objective, 20x/0.85 and 60x/1.42 oil immersion objectives, and with standard filter sets. Images were processed with ImageJ or AdobePhotoshop.

In vivo imaging

Animals were first anesthetized with ketamine and xylazine (ketamine 87 mg/kg, xylazine 13 mg/kg) and placed on a heating pad. To ensure a stable rate and minimize breathing artefacts, I performed a tracheotomy on the mice and attached them to a small ventilator. I then surgically exposed the dorsal spinal cord as previously described (*Misgeld et al., 2007a; Nikic et al., 2011; Romanelli et al., 2013*) removing 2-3 vertebrae; the opening was constantly superfused with artificial cerebrospinal fluid (aCSF). For the imaging session, the vertebral column was fixed using a spinal clamping device which allows a controlled movement of the mouse in *x-y* and *z*. I then created a well surrounding the spinal opening using 4% agarose: this helps to hold aCSF throughout the entire imaging sessions, as well as allows the incubation with vital dyes (*Romanelli et al., 2013*). *In vivo* imaging was performed using two-photon microscopes, either a custom-built setup based on Olympus FV300 or a commercially available Olympus FV1000 MPE. Both microscopes were equipped with femto-second pulsed Ti:Sapphire lasers, and the power was attenuated by a polarization-based beam splitter or acoustic-optical modulators.

For the imaging of vital dyes, **Table 1** shows the optimal wavelengths necessary to obtain the best imaging quality *in vivo*.

To study myelin alterations *in vivo*, I used *Thy1-YFP16/B16xBiozziABH* previously immunized; only mice with a score of ≥ 2.5 were used for the study. After bath application with MitoTracker Red at a concentration of 8 μM for 30 min, the spinal cord was carefully washed with aCSF before the imaging session. The laser was tuned at 910 nm in order to simultaneously excite both YFP (axons) and MitoTracker Red (myelin), and fluorescence

was collected using a green/red filter set (BA495-540, BA575-630). Imaging was focused within lesions, which were determined by the presence of morphologically altered axons; alternatively, I applied the nuclear dye POPO-1 Iodide (*Romanelli et al., 2013*) to visualize density of nuclei in order to define a lesion. To follow the change in myelin morphology over time, I acquired image stacks every 10 mins for several hours. The animal was kept anesthetized by injections of KX every 2 hours. Time-lapse images were acquired with a 25x/1.25 water immersion objective at 1024 by 1024 pixel resolution, with a pixel dwell time of 2 μ s/pixel.

The experiment was also performed in healthy animals to make sure that the morphological changes in myelin structures were not due to phototoxicity or dye toxicity; in control mice no signs of myelin alterations were detected even after several hours of imaging.

Tissue fixation and processing for electron microscopy

Thy1-YFP16/B16xBiozziABH animals with a score of ≥ 2.5 were transcardially perfused with 2.5% electron microscopy grade glutaraldehyde (GA) and 2% PFA in 0.1 M phosphate buffer (pH 7.2). The spinal cords were microdissected and post-fixed in 2.5%GA/2%PFA overnight. The tissue was then embedded in 4% agarose and cut into thick sections (100-150 μ m) using a vibratome. In order to visualize myelin and have a staining pattern comparable to the *in vivo* situation, I applied MitoTracker Red (8 μ M for 5 hours at room temperature); after the incubation, the sections were carefully washed 3 times for 15 min in PBS and then mounted in PBS under a coverslip in imaging chambers built with parafilm spacers on a glass slide.

Near infrared branding (NIRB) and correlated serial electron microscopic reconstruction

I imaged the samples on an Olympus FV100 MPE using confocal lasers 515 and 559 nm (ExDM405/488/559/635, BA505-540, BA575-620) in order to detect myelinosomes. Once the structure of interest was distinguished, NIRB marks were performed using the infra-red laser tuned at 910 nm, with a 640by640 pixel ratio and a pixel dwell time of 10 μ s/pixel, using the water immersion 25x/1.05 objective. To subsequently locate the myelinosome with EM, I burned a big box of 100 μ m x 100 μ m around the structure, 2 μ m superficial to the area of interest.

Low- and high-resolution stacks were collected with the confocal microscope (Olympus FV1000) to document the structure of interest and the NIRB lines, using 4x/0.13, 20x/0.85 and 60x/1.42 objectives.

For the serial cutting, the sections were first transferred in Sylgard-line 35 mm Petri dishes. The samples were then bathed in diaminobenzidine in 0.1 M Tris buffer (pH 7.4) and the NIRB marks photo-oxidized by excitation with 520-560 nm. The photo-oxidized sections were then processed for EM and stained with 1% osmium tetroxide reduced in 1.5% potassium ferrocyanide, washed in 0.1 M sodium cacodylate buffer, and dehydrated in ascending ethanol series. After dehydration, tissue blocks were transferred in 100% propylene oxide and later embedded into embedding capsules and polymerized at 60°C for 48 hrs. Thick sections (0.5-1 μ m) were cut with a glass knife; when the photo-oxidized NIRB marks became visible with the transmitted light and therefore the region of interest was identified, thin sections (50-70 nm) were serially cut (for detailed protocol see *Bishop et al., 2011*). Sample processing for EM was performed by Prof. Dr. Derron Bishop (Indiana University School of Medicine, Muncie, USA).

Electron micrographs were obtained using at 120KV using a JEOL JEM-1400 equipped with a Gatan Ultrascan 1000XP camera. Images were then processed with the free software Reconstruct (<http://synapses.clm.utexas.edu/tools/reconstruct/reconstruct.stm>), while for the rendering it was used 3DMax.

Histopathological analysis

For the histopathological analysis I immunized and treated according to the specific experiment BiozziABH, BiozziABH/B16 and Thy1-YFP16/B16 mice, and perfused them with 4% PFA. Prof. Dr. Doron Merkler (Univ. Geneva) and his team performed the stainings. Briefly: 3-4 μm thick sections were cut at the vibratome. Stainings were done on cross-sections of lumbar, thoracic and cervical spinal cords. For the histopathological analysis of the inflammatory index, sections were treated with H&E staining and the total number of inflammatory foci was counted. To characterize the immune cells, macrophages were labelled with anti-Mac3 antibody, while for T cells it was used anti-CD3 antibody. For the demyelination analysis, the sections were stained with LFP/PAS; the area of demyelination was calculated as % of total white matter within a given section. To assess axonal pathology, sections were stained with Bielschowsky silver impregnation. Images were captured with a confocal laser scanning microscope (LSM510Meta) equipped with an upright Zeiss Axio Imager Z1 microscope; processing and quantification was performed using Panoramic Viewer 1.15 (http://www.3dhitech.com/pannорamic_viewer).

For the human study, eight brain samples from biopsies of multiple sclerosis patients and three control cases without neurological diseases were provided by Prof. Dr. Wolfgang Brück (Univ. Goettingen). Brains were immediately fixed in PFA. For immunohistochemistry, biopsies were incubated with antibodies against myelin (anti-MBP), axons (anti-NF200),

oligodendrocytes (anti-NOGO-A), microglia/macrophages (anti-Iba1), and counterstained with the nuclear dye DAPI.

Single cell labelling and quantification

PLP-GFPm/Bl6xBiozziABH healthy and immunized animals were used to study oligodendrocyte morphology. At d7 post immunization, animals were first anesthetized with ketamine and xylazine (ketamine 87 mg/kg, xylazine 13 mg/kg); a laminectomy was then performed at the level of the lumbar spinal cord (*Romanelli et al., 2013; Misgeld et al., 2007b; Nikic et al., 2011*). Rabies Virus SAD Δ G mCherry was injected undiluted in the white matter of the lumbar spinal cord with a glass capillary. Specifically, I injected 0.5 μ l of virus at a depth of 0.2-0.4 mm into the white matter. Each mouse received two infusions. Temgesic was administered intraperitoneally before the surgery and for two consecutive days. All the animals were weighed and scored daily and sacrificed 9 days after Rabies Virus injections.

Quantification of the number and length of single oligodendrocytes as well as the 3D rendering, were obtained using the software Imaris Scientific 3D/4D Image processing. In details: the total number of the primary processes exiting the cell soma (not the secondary branches) were counted and expressed as the average number of processes per OL; the length of all the processes (primary and branches) was traced and measured in mm.

Antibody transfer experiment

To assess the role of antibodies during demyelination, I injected the anti-MOG monoclonal antibody 8.18C5 (2.8 μ g/ μ l produced and kindly provided by Dr. Krishnamoorthy, Max-Planck Institute of Neurobiology). The animals were subdivided into two groups: the

experimental group received 250 µg of antibody intraperitoneally for three days, at weight loss, one and two days after onset of clinical symptoms (*Urich et al., 2006; Pöllinger et al., 2009*); the control group was injected intraperitoneally at the same time points with 10 µg of IgG1 Isotype control.

The mice were weighed and scored daily for EAE severity and were sacrificed three days after onset of clinical signs.

B cells depletion protocol

C57Bl6 and BiozziABH/Bl6 mice were treated with anti-hCD20 antibody. To ensure efficient B-cell depletion, the animals were injected weekly (for three consecutive weeks) with 200 µg of anti-hCD20 monoclonal antibody (at a stock concentration of 28.98 µg/µl), prior to immunization with recombinant MOG protein. The control group received instead 200 µg of antiragweed immunoglobulin IgG2a-isotype control monoclonal antibody (at a stock concentration of 5.6 µg/µl). Both anti-CD20 and isotype control were kindly provided by Prof. Dr. Martin Weber (Univ. Goettingen).

Serum was collected in order to check the antibody titers and ELISA assay was performed by Prof. Dr. Martin Weber and his group.

Fixed tissue quantification

Sequence of myelin loss: PLP-GFPm/Bl6xBiozziABH mice were immunized and perfused with 4% PFA two days after onset. The sections were then cut longitudinally and stained free floating for anti-MBP as described earlier. For each animal, three areas respectively comprised of three lesion centers, three lesion borders and three normal appearing white matter regions, were selected to count. ImageJ was used for the processing and quantification

of the areas. Specifically, the “cell counter” plugin was used to count the number of oligodendrocytes and the number of nuclei. The length of myelin was traced using the “freehand line” tracing tool and the “measure” plugin, and expressed in mm.

Myelinosome quantification: Myelinosomes analysis both in Thy-YFP16/bl6xBiozziABH and in Thy1-YFP16/bl6 treated with 8.18C5, were performed in the same way. Sections were stained with anti-MBP and a nuclear dye to visualize the lesion areas. High magnification images were taken with confocal lasers using 60x/1.42 oil objective at a zoom of 4 fold at the border of the lesions. Quantification was performed using ImageJ and its “trace and measure” plugins: the length of each axon was measured and the frequency of myelinosomes appearance (detected with the MBP signal) was expressed as density of myelinosomes per mm of axon.

Quantification of human brain samples: For the analysis of the human samples, images were opened with the software Panoramic Viewer and consequently exported as .tif files in ImageJ. To count the number of DAPI+ cells and the number of oligodendrocytes, I used the “cell counter” plugin. Length of myelin was measured with the “trace and measure” plugins, as described before.

Myelinosome quantification was performed in the same way as described for the murine model.

Statistics

Results are expressed as mean \pm SEM, unless indicated otherwise.

Data set were tested for normal distribution with the D’Agostino-Pearson normality test using GraphPad Prism Software. When normal distribution could be assumed the data were

compared using student *t*-test or, if there were more than two samples, analysed using ANOVA followed by Bonferroni's multiple comparison tests. When normal distribution could not be assumed, the nonparametric Mann-Whitney test, or if there were more than two samples, the Kruskal-Wallis followed by Dunn's multiple comparison tests were chosen. Statistical analyses were performed with GraphPad Prism software.

CHAPTER IV – Results

1. *In vivo* imaging of the spinal cord using vital dyes

Over the past decades, there has been a growing interest in the use of *in vivo* imaging techniques at least partly due to the development of new transgenic mouse lines that express genetically encoded fluorescent proteins or sensors (see Chapter I, section 3). However, the generation of new transgenic lines requires a lot of time and resources, and when the labeling needs to be combined or used in disease models, complex breeding strategies are necessary. In this scenario, synthetic dyes represent a good alternative or complement: they can be easily combined with transgenic labeling and are available in variants that cover a broad range of the wavelength spectrum. The majority of these dyes has already been tested and so far mainly used in *in vitro* studies, with few exceptions used *in vivo*, such as sulforhodamine 101 (Nimmerjahn *et al.*, 2004; Nimmerjahn *et al.*, 2009) or calcium indicator dyes (Stosiek *et al.*, 2003; Johannssen *et al.*, 2010; Grienberger *et al.*, 2012). In my first project I have tested several vital dyes and evaluated their potential for *in vivo* labeling. During this process I have also established a novel technique to label myelin, which allowed me to follow demyelination *in vivo* in my second project.

Surgical procedure and imaging setup

In vivo imaging requires surgical exposure of the spinal cord. To access the dorsal spinal cord, I performed a laminectomy using spring scissors, as described in previous reports (Misgeld *et al.*, 2007a; Davalos *et al.*, 2008; Davalos *et al.*, 2012). Once the region of interest is accessible, the animal must be stabilized under the microscope in order to allow a

controlled movement of the tissue in x - y and z . This is achieved by use of a spinal clamping device to fix the position of the spinal cord, thus minimizing movements and breathing artifacts (**Fig. 8 a-b**).

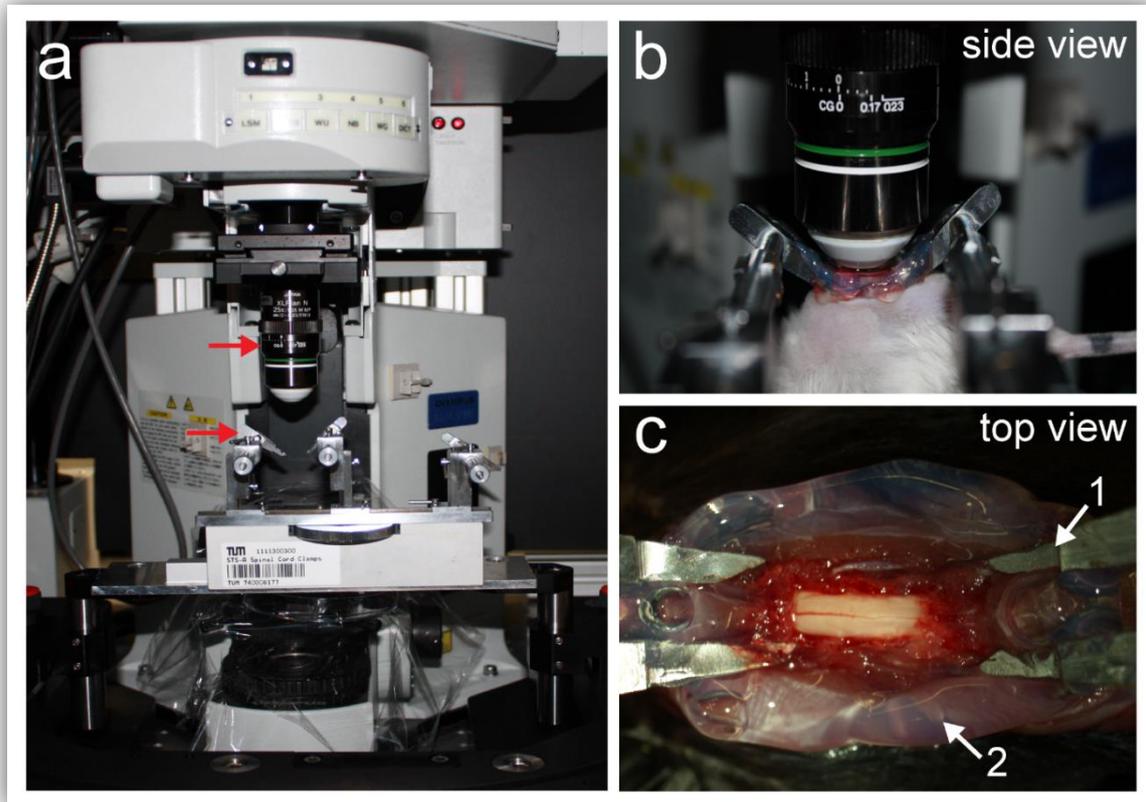


Figure 8 - Experimental setup. (a) Imaging setup of FV1000MPE including custom-built stage to hold spinal stabilization device. (b) Side view of the mouse held by the spinal stabilization device to show the position of the 25x/1.05NA objective between the clamps and within the liquid filling the agarose well. (c) View from above of exposed lumbar spinal cord that has been clamped (1) and agarose well has been built surrounding the cord to allow for dye application without leakage (2).

To improve the imaging quality and, as I will explain in the next section, to obtain a deeper penetration of the vital dye, the meninges (dura mater and arachnoidea) must be carefully removed using a needle and fine forceps. The intact meninges in fact represent an obstacle for the labeling with vital dyes, which would only stain the structures within the dura mater and the arachnoidea and not the spinal tissue beneath (**Fig. 9**).

It is also important to keep the laminectomy opening covered with artificial cerebrospinal fluid, both to avoid damage of the exposed spinal cord and for an optimal dye exposure. Thus, before the imaging session begins, an agarose well can be formed around the spinal opening, taking extra care to avoid any leakage (**Fig. 8c**).

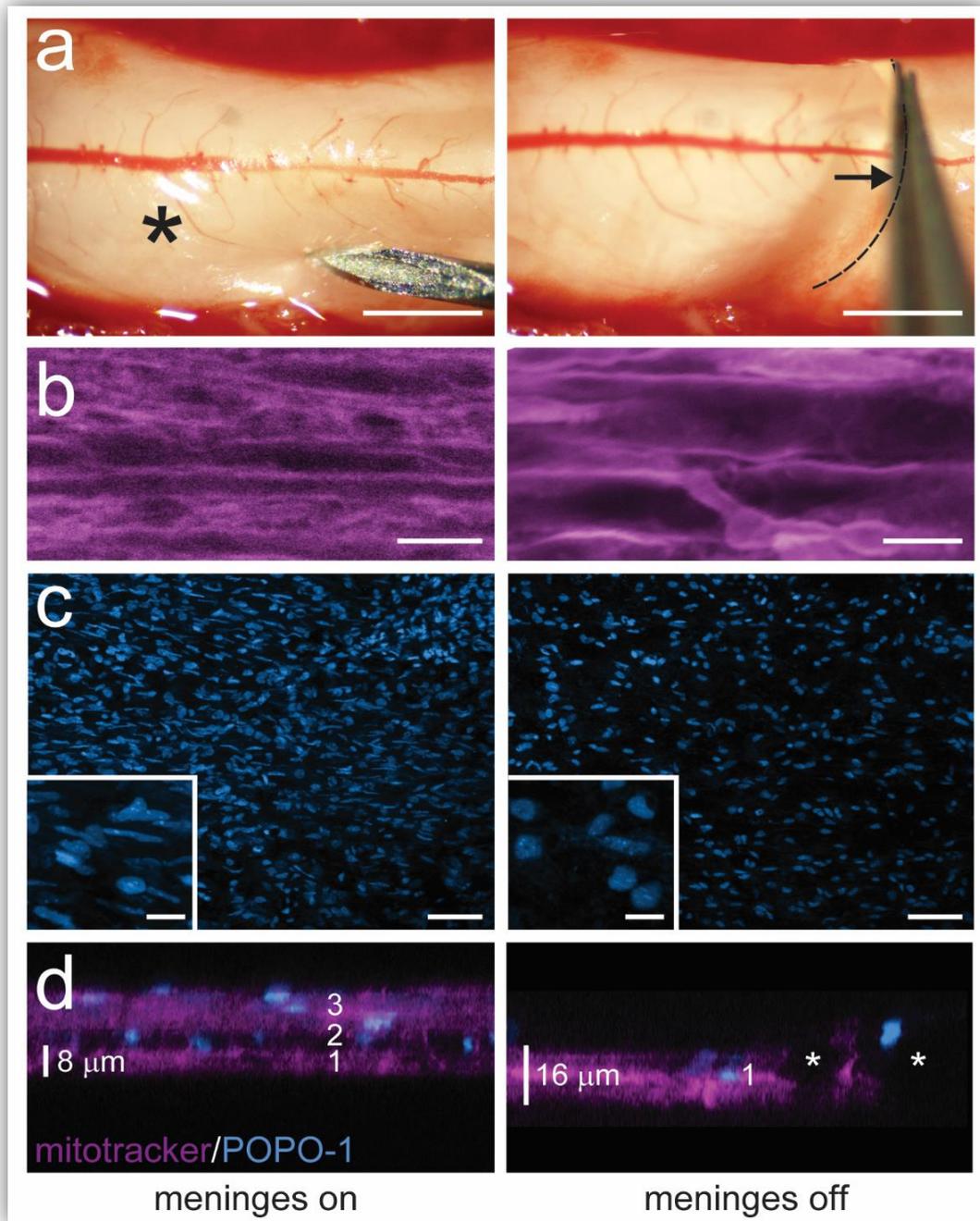


Figure 9 - Removal of the meninges. (a) After laminectomy, the meninges are first punctured with the tip of a hypodermic needle to allow access with surgical tools. The reflective surface, labeled by an asterisk, is indicative of an intact dura and is absent in the right panel where the meninges (dura and arachnoidea) have been peeled off using fine forceps. The direction in which the meninges have

been pulled is indicated by the arrow. The free margin of the meninges is outlined by a dotted line. Removal of the meninges substantially improves the quality of labelling, e.g. by MitoTracker Red (**b**, **magenta** images equalized to full dynamic range so note higher noise level in left panel), as well as nuclear labelling with POPO-1 iodide (**cyan**), which will stain primarily cells in the meningeal layers if the meninges are left on (**c**), as opposed to when the meninges are removed (**right panel**). X-z projection of an image stack with (**left**) or without (**right**) the dura and arachnoidea in place (**d**) shows that penetration into spinal cord is doubled when the dura is removed; (1) dorsal spinal cord; (2) subarachnoideal space; (3) dura mater and arachnoidea. Scale bar in **a**, 1 mm; scale bar in **b**, 10 μm ; scale bar in **c**, 50 μm ; scale bar in **c** inset, 10 μm . Images taken from *Romanelli et al.*, 2013.

Concentration dependence and reliability of vital dyes

Together with Dr. Catherine Sorbara and Dr. Ivana Nikic, we have tested a range of commercially available vital dyes and identified the optimal application and imaging conditions (**Table 2**: in bold font the best suited for *in vivo* imaging, based on reliability, brightness, longevity during imaging and ability to be fixed). The vital dyes have been classified in structural (cell-type specific or targeted to a specific subcellular compartment), and functional.

Finding the appropriate concentration is particularly important, as some of the dyes might label different structures depending on their dilution. For example, as shown in **Fig. 10**, MitoTracker Red labels mitochondria when used at low concentration (**Fig. 10 a**); a moderate increase labels both mitochondria and myelin (**Fig. 10 b**), while if used at high concentration it labels exclusively myelin (**Fig. 10 c**).

For each dye, I have studied the penetration and the labeling efficiency. Most of the dyes penetrate up to 30 μm into the spinal cord (the depth that can be imaged in the heavily myelinated spinal cord is around 40 μm , therefore more limited than in the cortex) (**Table 2**).

Direct comparison of these dyes with established transgenic or immunohistochemical markers has allowed me to determine the labeling efficiency, which is nearly 100% for the nuclear dyes, as well as for myelin (MitoTracker Red) and for activated macrophages/microglia (Isolectin B4), while it is at least 40% for the rest of the dyes.

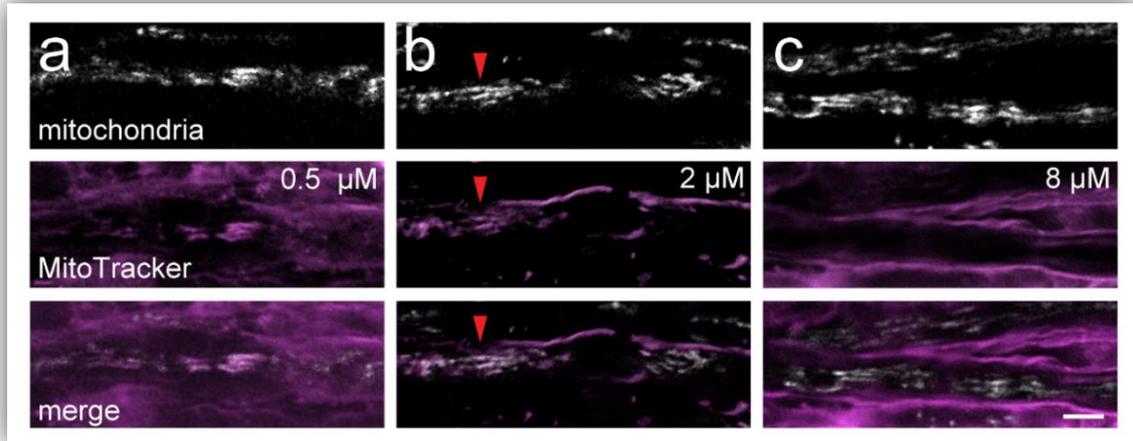


Figure 10 - Concentration dependence. The vital dye MitoTracker Red can be used to label different structures depending on the concentration: (a) sparse mitochondrial labelling is achieved following application of 0.5 μM MitoTracker Red (**magenta**), which co-localizes with genetically labelled mitochondria in MitoMice (described in Misgeld et al., 2007b) (**merge**); (b) increase of the dye concentration to 2 μM reveals myelin, while only few mitochondria remain visible (**arrowhead**); (c) after further increase of the dye concentration to 8 μM only myelin is visible, likely because the intensity of myelin labelling increases compared to the mitochondrial labeling. Scale bar in **a**, 5 μm ; scale bar in **b**, 5 μm ; scale bar in **c**, 5 μm . Image taken from *Romanelli et al., 2013*.

Another feature of the vital dyes is their extreme reliability when re-applied over time. To evaluate this aspect, Dr. Catherine Sorbara has applied two spectral versions of a nuclear dye at different timepoints (NeuroTrace 435/455 at 0h and NeuroTrace 640/660 at 1h). The comparison of the obtained staining patterns revealed nearly identical labeling structures, with $94 \pm 5\%$ of NeuroTrace 435/455+ nuclei subsequently relabeled with NeuroTrace 640/660 (**Fig. 11 a**). A similar result was obtained with the re-application of the same dye (carboxyfluorescein -CFDA-) after photobleaching ($97 \pm 2\%$ of bleached cells were relabeled with CFDA) (**Fig. 11 b**). These results show that the same cells can be reliably relabeled and followed over extended periods of time thus facilitating long imaging sessions and detection of changes in the cellular or subcellular composition.

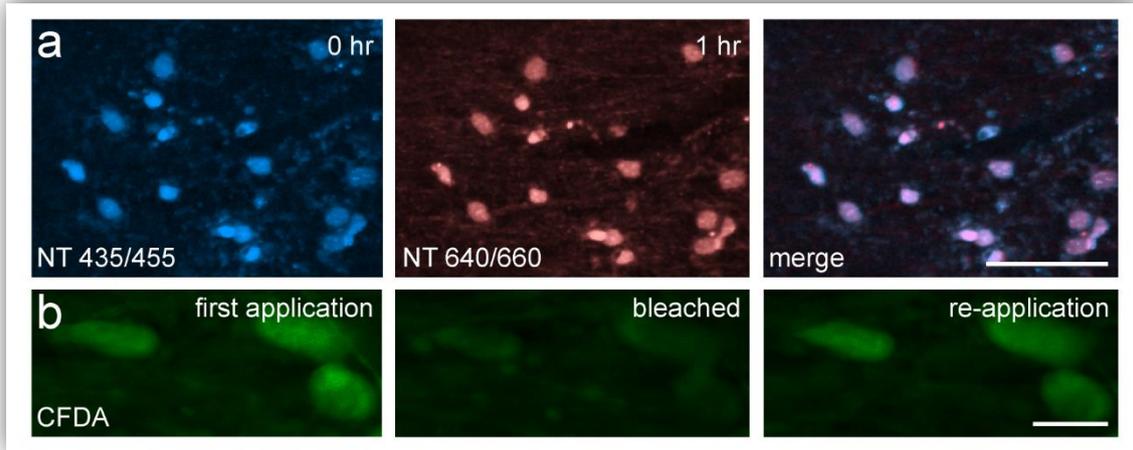


Figure 11 - Reliability of relabeling. Consecutive labeling of the same dorsal spinal cord at two time points (0 and 1 hr) with two spectrally distinct versions of a nuclear dye, Neurotrace (NT) 435/455 (**a, left**) and NT 640/660 (**a, middle**) reveal a near exact labeling pattern (**a, right, merge**). Vybrant CFDA was applied to a healthy spinal cord (**b, left**) and bleached with a two-photon laser (**b, middle**). Following reapplication of the vital dye, the same cells were labelled (**b, right**). Scale bar in **a**, 50 μm ; scale bar in **b**, 10 μm . Image taken from *Romanelli et al., 2013*.

Dye	Company, Order No.	Labeled structure	Dilution/ Concentration	Incubation time	Optimal Excitation (nm)	Persistence of label	Penetration Depth, Comparison to Genetic label ¹	Labeling Efficiency ²	Fixation (in 4% PFA)
Structural Dyes									
<i>Cell- type specific dyes</i>									
Isolectin GS-IB4 from Griffonia simplicifolia, Alexa Fluor 647 conjugate	Invitrogen I32450	activated microglial cells (macrophages)	200 µM	1 hr	840 (2P)	> 2hr	14 ± 2 µm, 35 ± 2 %	87 ± 5% ³	yes
Vybrant CFDA SE Cell Tracer Kit	Invitrogen V12883	OLs	25 µM	30 min	800 (2P)	> 2hr	18 ± 4 µm, 45 ± 4 %	54 ± 7% ⁴	Yes
<i>Subcellular compartment dyes</i>									
NeuroTrace 435/455 blue fluorescent Nissl stain	Invitrogen N-21479	Nuclei	1:250	30 min	850 (2P)	> 2hr			yes
NeuroTrace 640/660 deep-red fluorescent Nissl stain	Invitrogen N-21483	Nuclei	1:250	30 min	740 (2P)	> 2hr			yes
Nuclear-ID Red DNA Stain	Enzo Life Sciences ENZ-52406	Nuclei	1:250	45 min	740 (2P)	> 2hr	20 ± 1 µm, 50 ± 1 %	96 ± 4% ⁵	yes
POPO-1 iodide (434/456)	Invitrogen P3580	Nuclei	1 µM	30 min	850 (2P)	> 2hr	16 ± 3 µm, 40 ± 3 %	100% ⁶	yes
SYTO 64 red fluorescent nucleic acid stain	Invitrogen S11346	nuclei	2.5 µM	45 min	700 (2P)	> 2hr			yes
Cell Trace BODIPY TR Methyl Ester	Invitrogen C34556	myelin	100 µM	40 min	780 (2P)	re-apply after 2hr			yes, but weak signal
DiOC6(3) (3,3'-Dihexyloxacarbocyanine Iodide)	Invitrogen D273	myelin	5 µM	45 min	910 (2P)	> 2hr			yes, but weak signal

FluoroMyelin red fluorescent myelin stain	Invitrogen F34652	myelin	1:50	30 min	940 (2P)	> 2hr			yes, but weak signal
FluoroMyelin green fluorescent myelin stain	Invitrogen F34651	myelin	1:50	30 min	910 (2P)	> 2hr			yes, but weak signal
MitoTracker Red CMXRos	Invitrogen M7512	myelin and mitochondria	0.5 μ M	30 min	740 (2P)	> 2hr	14 \pm 1 μ m, 35 \pm 1%	43 \pm 6% ⁷	no
MitoTracker Red CMXRos	Invitrogen M7512	myelin	8 μ M	30 min	740 (2P)	> 2hr	18 \pm 2 μ m, 45 \pm 2%	95 \pm 2% ⁸	no
Functional Dyes									
Amplex UltraRed reagent	Invitrogen A36006	hydrogen peroxide sensor (extracellular)	200 μ M	30 min	RFP excitation (1P) 740 (2P)	~20min	31 \pm 4 μ m, 78 \pm 4%		n/a
Tetramethyl rhodamine, methyl ester, perchlorate - TMRM	Invitrogen T-668	mitochondrial potential	0.6 μ M	30 min	910 (2P)	> 2hr	20 \pm 2 μ m, 50 \pm 2%	60. \pm 10% ⁹	n/a

¹Percentage based on comparison to the imaging depth of transgenic mouse line, thy1-YFP¹⁶MitoP.

²Labeling efficiency calculated as percentage of a well-established immunohistochemical or transgenic marker double-labeled with a given vital dye (n=3 animals per dye, see methods for labeling procedure).

³Percentage of Anti-Iba1 (rabbit antibody, WAKO) positive cells double-positive for Isolectin.

⁴Percentage of Anti-APC (mouse monoclonal antibody clone CC-1, Calbiochem) positive cells double-positive for CFDA.

⁵Percentage of DAPI (4', 6-diamidino-2-phenylindole, Invitrogen) positive cells double-positive for Nuclear ID.

⁶Percentage of NT 530/615 (Neurotrace red fluorescent nissl stain, Invitrogen) positive cells double-positive for POPO-1 iodide.

⁷Percentage of mitochondria in a thy1-MitoS, double-positive for MitoTrackerRed.

Table 2 - Vital dyes for cellular, subcellular and functional imaging. Table taken from *Romanelli et al., 2013*.

Structural dyes

As shown in **Table 2**, the vital dyes have been categorized in structural and functional dyes. Among the structural ones, some show high cell-type specificity. For example, it appears that Vybrant CFDA SE Cell Tracer labels preferentially oligodendrocytes. I have applied CFDA on the spinal cord of *Plp-CreERT2xTdTomato* mice, in which the *Plp* promoter drives the expression of the fluorescent protein selectively to oligodendrocytes (*Leone et al., 2003*): the vital dye colocalizes with transgenic somata and processes (**Fig. 12 a**). An advantage of this dye is that it can be fixed after the imaging session, allowing further analysis to be performed. To assess the specificity of the dye, I stained the tissue with the oligodendrocyte marker APC-CC1 (*Fancy et al., 2010*) which showed that about half of the APC-CC1+ oligodendrocytes were also CFDA+; in the same analysis, only a small portion of astrocytes (stained with the marker S100) and microglia cells (identified by Iba1 staining) were labeled with CFDA (**Fig. 12 b, c**).

Another example of a dye that results in cell-type specific labeling is Isolectin GSA-B4. Previous studies have shown that it can be successfully used to label microglia in fixed tissue and living slices (*Moreira et al., 2009; Dailey et al., 1999*). I tested its use *in vivo* in a mouse in which I previously induced EAE. **Fig. 12 d** shows a lesion with a high density of activated macrophages/microglia; after fixation with paraformaldehyde, the co-staining with a macrophages/microglia marker (Iba1) showed that more than 80% of the cells were double positive for Isolectin GSA-B4 (**Fig. 12 f**). The application of Isolectin GSA-B4 in a $CX3CR1^{GFP/+}$ transgenic mouse in which resident macrophages/microglia are labeled with GFP (*Jung et al., 2000*) show co-labeling of the same cells after EAE induction. The same vital dye seems not to stain resting microglial cells (**Fig. 12 e**).

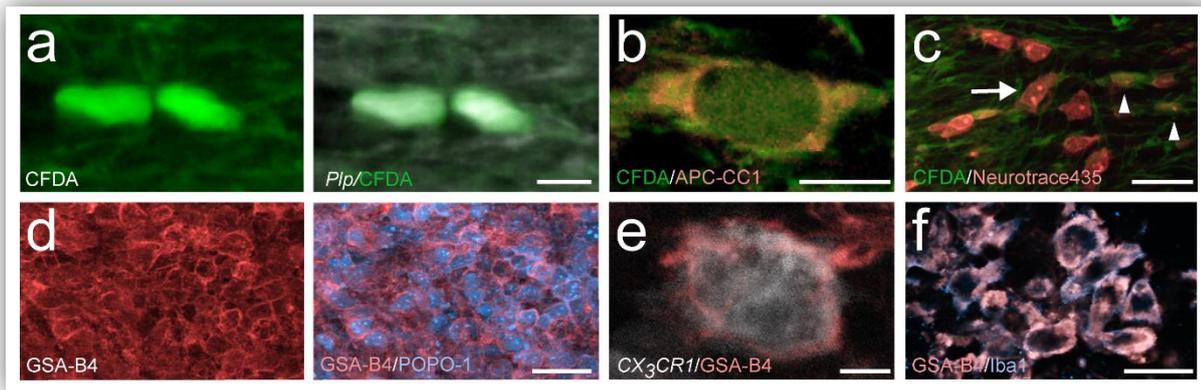


Figure 12 - Cell-type specific dyes. (a) The dye CFDA (**green**) co-localizes with somata and processes of transgenically labeled oligodendrocytes in a tamoxifen-injected Plp-CreERT2 x TdTomato mouse. (b) Post-imaging fixation of CFDA (**green**) stained with an anti-APC (CC-1) antibody (**red**) to label mature oligodendrocytes. (c) Low magnification of a spinal cord stained with CFDA (**green**) and the nuclear dye Neurotrace 435 (**red**). Some nuclei are CFDA positive (**arrowheads**) while others are not co-labeled (**arrows**). (d) Activated microglia/macrophages stained with Isolectin GSA-B4 (**red**) and counterstained with the nuclear dye, POPO-1 iodide (**cyan**), in a C57BL/6 mouse, 2 days after onset of EAE. (e) In vivo labelling of Isolectin GSA-B4 (**red**) in a CX₃CR₁ transgenic mouse. (f) Isolectin GSA-B4 was applied in vivo and consecutively fixed (**red**); the tissue was then counterstained with an anti-Iba1 antibody (**cyan**) to label activated and resting microglia. Scale bar in **a**, 10 μ m; scale bar in **b**, 10 μ m; scale bar in **c**, 20 μ m; scale bar in **d**, 50 μ m; scale bar in **e**, 20 μ m; scale bar in **f**, 25 μ m. Image taken from *Romanelli et al., 2013*.

Some vital dyes stain specific subcellular compartments. Nuclei for example can be easily labeled with a wide range of dyes, using relatively low concentration and short incubation time. Their labeling efficiency is nearly 100% when comparing the *in vivo* labeling with postmortem staining using the nuclear dye DAPI (**Fig. 13 a**). The most reliable results were obtained with POPO-1 Iodide and Nuclear ID Red, both are easy to apply and extremely reliable.

For my work, it was also essential to find a suitable dye for labelling myelin. In my hands, MitoTracker Red gave the best results. As shown in **Fig. 13 b**, MitoTracker Red gives a bright and clear myelin labeling, and also clearly depicting nodes of Ranvier; notably, the dye labels the outermost layers of myelin, as shown by the gap between the myelin stain and the cytoplasmic labeling of the axon. Another dye commonly used *in vitro* is Fluoromyelin (*Watkins et al., 2008; Monsma et al., 2012*). Its application *in vivo* appears to be a good alternative to MitoTracker Red (**Fig. 13 c**); the labeling pattern of the two dyes is in fact very

comparable, though Fluoromyelin requires a higher concentration. One advantage of Fluoromyelin over MitoTracker Red is its fixability allowing further studies after the imaging session. As myelin dyes are very sensitive, a general rule is to pay extra attention to the removal of blood clots and meninges in order to ensure a good penetration of the dye.

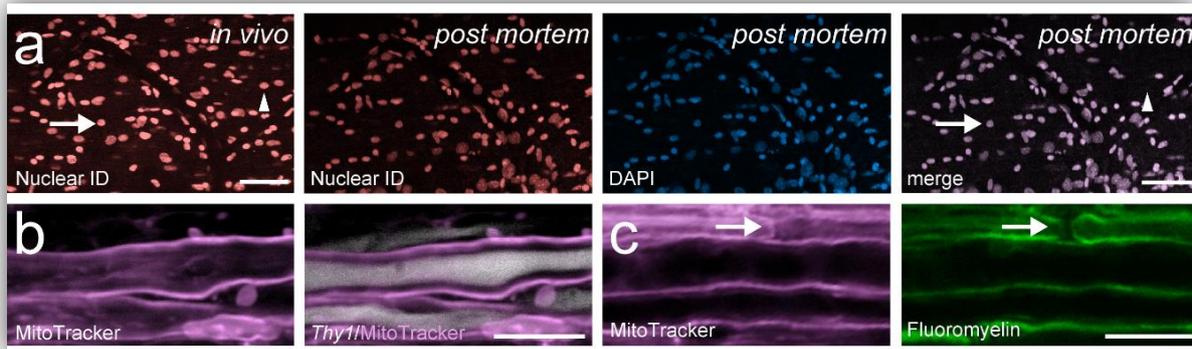


Figure 13 - Dyes specific for subcellular compartments. **(a)** Overview of a healthy spinal cord in vivo, where NuclearID Red is used to visualize nuclei (**red**). The same spinal cord was fixed post-imaging and imaged by confocal microscopy to reveal nearly identical staining (**arrows** identify examples of identical cells in vivo and post mortem; **arrowheads** indicate differences in the labelling pattern, probably due to minor changes in the way the spinal cord is angled). Counter-stain with DAPI (**cyan**) post mortem confirms specific nuclear localization of the in vivo NuclearID label (**merge**). **(b)** High magnification view of a healthy axon and its myelin, labeled with MitoTracker Red (**magenta**). **(c)** In vivo co-labeling of myelin with MitoTracker Red (**magenta**) and Fluoromyelin (**green**). The **arrow** identifies a node of Ranvier. Scale bar in **a**, 50 μm ; scale bar in **b**, 10 μm ; scale bar in **c**, 10 μm . Image modified from *Romanelli et al., 2013*.

Functional dyes

Dr. Ivana Nikic and Dr. Catherine Sorbara have tested some vital dyes to detect the release of toxic mediators. Amplex UltraRed, for example, detects extracellular hydrogen peroxide. Nikic et al. have used it in their study, and they showed that Amplex signal is increased in acute inflammatory lesions of EAE animals (*Nikic et al., 2011*) (**Fig. 14 a**).

A different functional dye can be used to assess mitochondria function. Tetramethylrhodamine (TMRM) works nicely *in vivo* and can be used to study mitochondrial potential in axons. The penetration of TMRM is however limited and only a subset of axonal

mitochondria is labelled by this dye when compared with the fluorescent pattern observed in transgenic MitoMice (*Misgeld et al., 2007b*). Interestingly, the application of cyanide m-chlorophenyl hydrazone (CCCP), a protonophore, immediately release TMRM from mitochondria (**Fig. 14 b**).

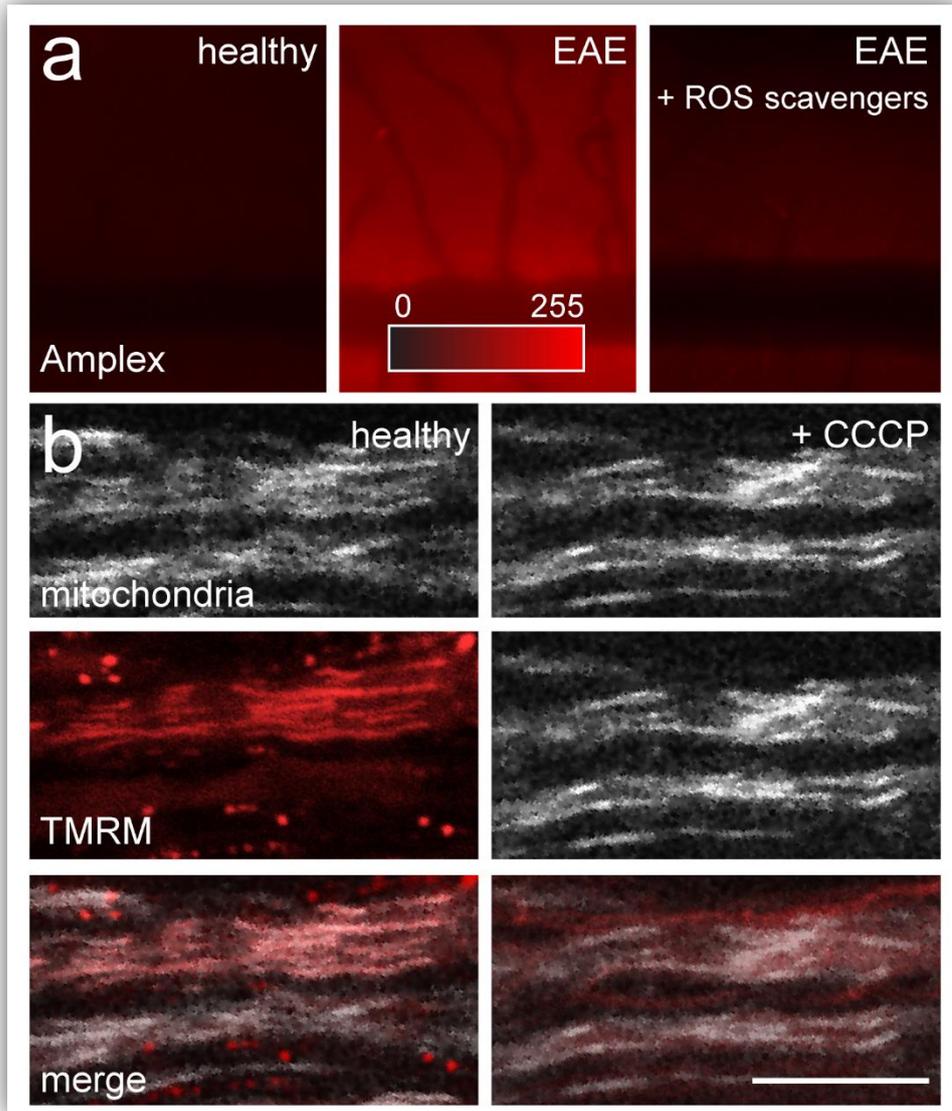


Figure 14 - Functional dyes. Measurement of extracellular H_2O_2 concentration detected with Amplex UltraRed (**a, red**) in the dorsal spinal cord of healthy (**a, left**), EAE untreated (**a, middle**; 2 days after onset) and EAE mouse treated intraperitoneally with a cocktail of reactive oxygen species (ROS) scavengers beginning at weight loss (**a, right**; 2 days after onset). Mitochondrial potential was assessed by bath application of TMRM (**b, red**). Mitochondrial labelling disappears immediately after application of 100 μ M CCCP (**right**). Scale bar in **a**, 250 μ m (calibration bar); **b**, 50 μ m. Image taken from *Romanelli et al., 2013*.

Use of vital dyes to assess disease models in the spinal cord

I screened a number of vital dyes in order to find the most suitable candidates to use *in vivo*, because the final aim of this project was to combine the use of these dyes with transgenic mouse strains. This approach increases the number of questions that can be addressed in a single *in vivo* experiment and represents a relatively easy way to avoid the generation of new transgenic lines or crosses.

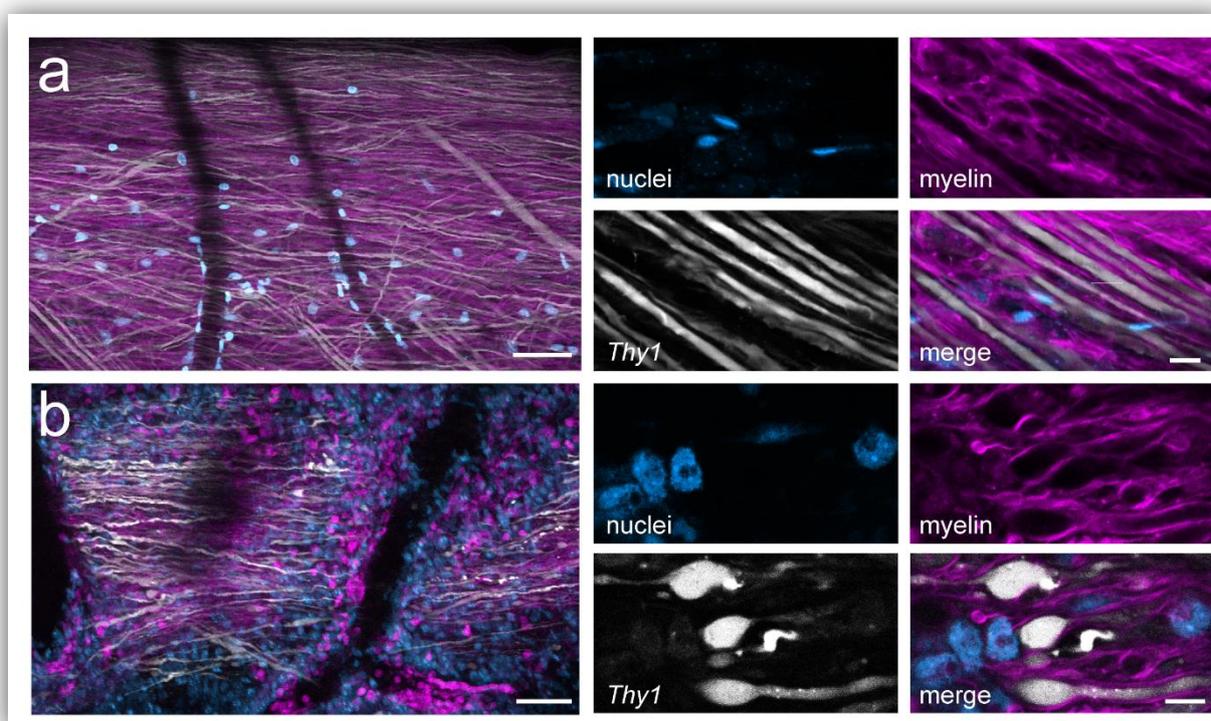


Figure 15 - Anticipated results. (a) Overview of the spinal cord of a healthy Thy1-YFP¹⁶ mouse, where Mitotracker Red (**magenta**) and POPO-1 iodide (**cyan**) have been applied to stain myelin and nuclei, respectively. Nuclei, myelin and axons appear normal. (b) Overview of a Thy1-YFP¹⁶ mouse labelled with the same dye combination at 2 days after onset of EAE. Here, infiltrating nuclei, myelin and axonal damage are indicative of an inflammatory lesion. Note that some inflammatory cells also label with the MitoTracker Red dye. Higher magnification views shown on the right. Scale bar in **a**, **b**, overview, 50 μm ; scale bar insets, 10 μm . Image taken from *Romanelli et al., 2013*.

This method is versatile and can be applied to different disease models. In the work described here I have used several transgenic mouse lines in combination with myelin and nuclear dyes, in the EAE model for MS. **Fig. 15** shows a *Thy1*-YFP transgenic mouse in which I have

labeled myelin with MitoTracker Red and nuclei with POPO-1 iodide: in the control mouse, axons and myelin appear healthy and only few cells are present in the imaging area; in the EAE animal instead axons and myelin are damaged which results in some of the axons showing swellings and beading, and myelin debris becoming apparent in the lesion area. The high density of nuclei is also indicative of an inflammatory lesion.

2. *In vivo* analysis of myelin in multiple sclerosis and its animal model

Although demyelination represents the major histopathological hallmark of MS, currently very little is known about the mechanisms that mediate myelin damage. My second project aimed at understanding how myelin is damaged in EAE, by combining two-photon *in vivo* imaging with confocal microscopy and correlated ultrastructural analysis.

Characterization of the animal model

As reviewed in section Chapter I - section 1, several animal models are available to study inflammation and demyelination in the CNS. For my experiments, I have induced EAE induced in Biozzi ABH mice crossed with different transgenic reporter lines. The Biozzi ABH strain develops relapsing-remitting EAE which in later stages results in a steady progression of the disease, and therefore represents a good model for the study of both relapsing-remitting as well as secondary progressive MS. Conversely to the commonly used C57/Bl6 animals, Biozzi ABH mice manifest a strong antibody response and extensive demyelination indicating that they are well suited to investigate myelin damage.

In order to visualize neurons and their axons, or oligodendrocytes, it was necessary to breed Biozzi ABH mice with already described Bl6 transgenic lines. To assess whether the interstrain crossing (Biozzi ABH/Bl6) affects disease presentation in the F1 hybrids

compared to the pure line (Biozzi ABH), I have performed histopathological analysis to assess the extent of the demyelinated area, axonal survival and the number of inflammatory loci.

First, the mice were immunized with 50 µg of recombinant MOG protein at day 0 and day 7, and pertussis toxin (50 ng) was injected at day 0, 1, 7 and 8. Ten to twelve days after the induction of EAE, the mice showed the first clinical symptoms. The peculiar clinical course of the disease which characterizes Biozzi ABH strain was reflected also in Biozzi ABH/Bl6 (F1 generation): the first 20 to 30 days are characterized by an alternation of relapses and periods of remission, with the first relapse being considered as the acute timepoint of the disease. Following the initial relapsing-remitting phase, the pathology progresses steadily in the chronic phase (**Fig. 16**).

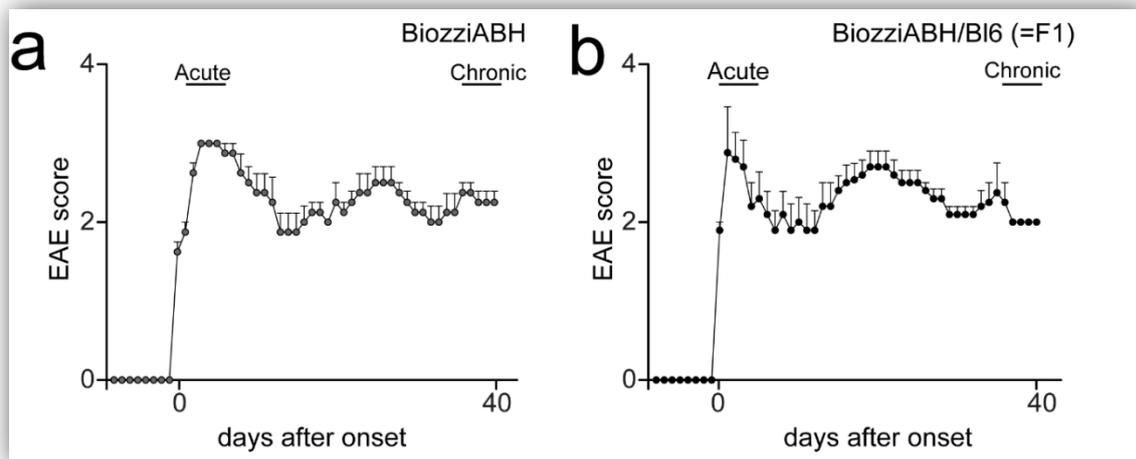


Figure 16 - Clinical course of EAE in BiozziABH (a) and BiozziABH/Bl6 (b). The disease progression is nearly identical, and characterized by a relapsing-remitting period where the first relapse represents the acute phase, and a chronic progression of the symptoms (BiozziABH, n=5 mice; Biozzi/Bl6, n=5 mice).

The mice were then analyzed for inflammation, demyelination and axon density. Histopathological staining was performed on PFA-fixed cross-section of lumbar, thoracic and cervical spinal cord. The number of inflammatory lesions per spinal cord cross-section was quantified by H&E staining and expressed as inflammatory index. Demyelination was

quantified by measuring the demyelinated area on LFB/PAS stained sections and expressed as % of total analyzed area of white matter within a given section. Bielschowsky silver impregnation was used to assess the axonal density. I performed the study both at the acute and at the chronic timepoints. As shown in **Fig. 17** and **Fig. 18**, there is no significant difference in the pathology of the EAE disease between pure Biozzi ABH and F1 generation Biozzi ABH x C57/BL6 mice. Furthermore the area of demyelination continues to increase between the acute and the chronic timepoint suggesting an ongoing demyelination process.

Taken together these results confirm that the chosen model is suitable for our study of inflammatory demyelination, and that the breeding with a transgenic BL6 mouse line does not affect the typical Biozzi ABH disease pathology.

The histopathological stainings were kindly performed by Prof. Dr. Doron Merkler (Univ. Geneve).

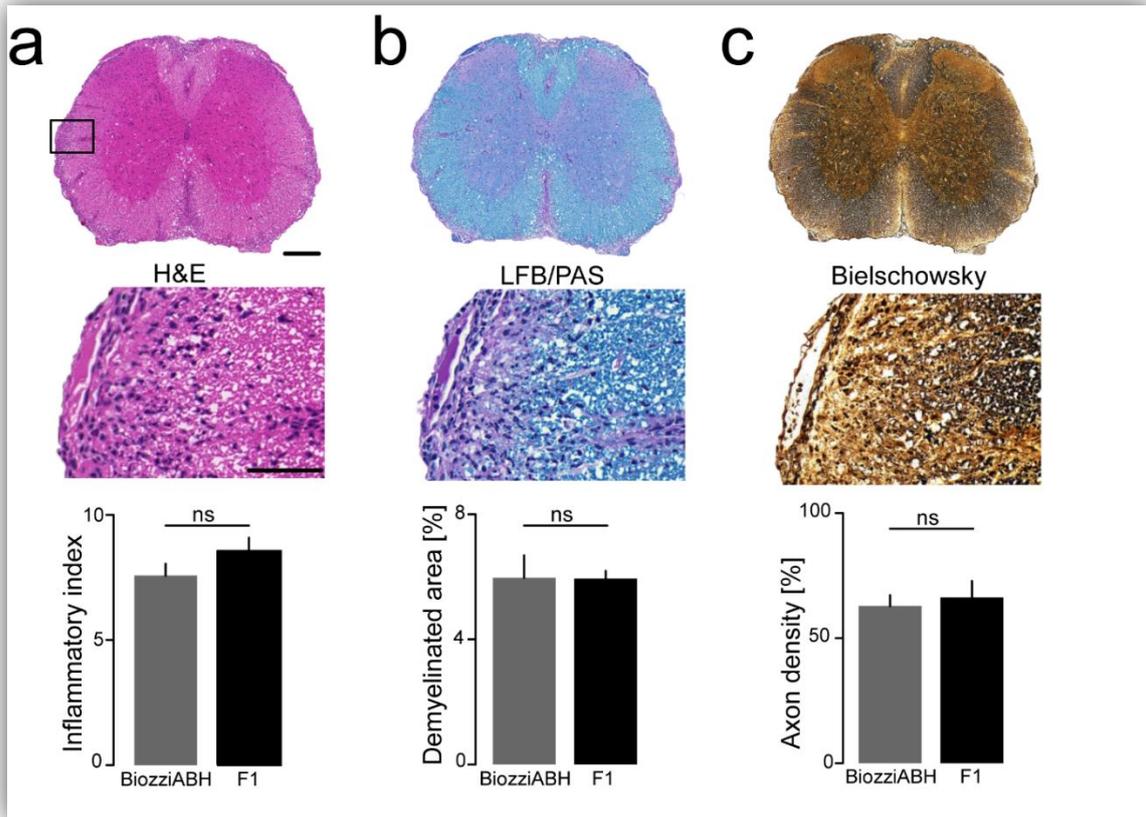


Figure 17 - Histopathological analysis at the acute timepoint. Here is shown the same cross-section from the lumbar spinal cord of a Biozzi/B16 animal. **(a)** The inflammatory index is expressed by the number of inflammatory loci within a cross-section, identified by H&E staining. **(b)** LFB/PAS staining is used to determine the demyelinated area, expressed as a % total analyzed area of white matter in the given section. **(c)** The axon density shows the % of surviving axons, quantified with Bielschowsky silver impregnation. (BiozziABH, n=5 mice; Biozzi/B16, n=5 mice). Scale bars in **(a)** 200 μm (overview) and 50 μm (inset).

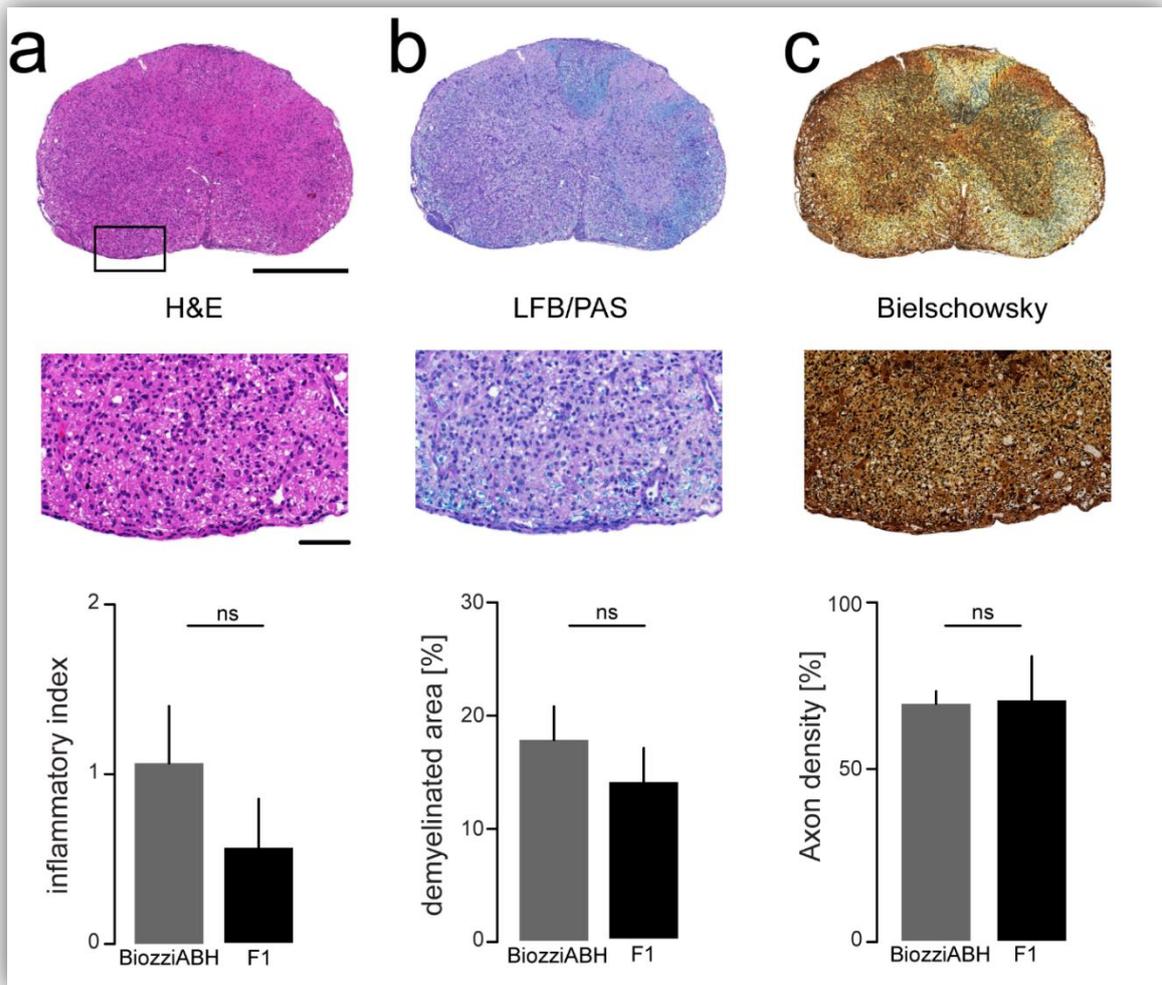


Figure 18 - Histopathological analysis at the chronic timepoint. Here is shown the same cross-section from the lumbar spinal cord of a Biozzi/Bl6 animal. The inflammatory index (a), the demyelinated area (b), and the axon density (c), are analyzed as described before. (BiozziABH, n=5 mice; Biozzi/Bl6, n=5 mice). Scale bars in (a) 200 μ m (overview) and 50 μ m (inset).

Cellular sequence of demyelination in acute EAE

As outlined in the introduction section it is well established that MS lesions are characterized by oligodendrocyte pathology and myelin loss (see Chapter I – Pathology of MS), yet it is currently still debated where oligodendrocyte damage starts and whether oligodendrocyte pathology thus follows an “outside-inside” or “inside-outside” gradient.

I first tried to address this question in our EAE model. To characterize the lesions observed in this model, *PLP-GFPm*/Bl6 x BiozziABH mice were bred in our animal facility; in these mice, the PLP promoter drives the expression of green fluorescence protein (GFP), allowing to visualize OLs cell bodies and their processes. After immunization with MOG, I quantified the density of OLs and the length of myelin within a given lesion and its surroundings. The lesion area was determined by the number of infiltrating cells, with the lesion center characterized by a high density of cells, decreasing towards the rim (**Fig. 19 a-b**).

The results observed in BiozziABH/Bl6 mice seem to indicate an outside-inside gradient of oligodendrocyte damage: while myelin is lost not only at the center of the lesion but also at its border, OL cell loss is significant only in the lesion center while their density is nearly identical to the healthy animals at the rim of the lesion (**Fig. 19 c**).

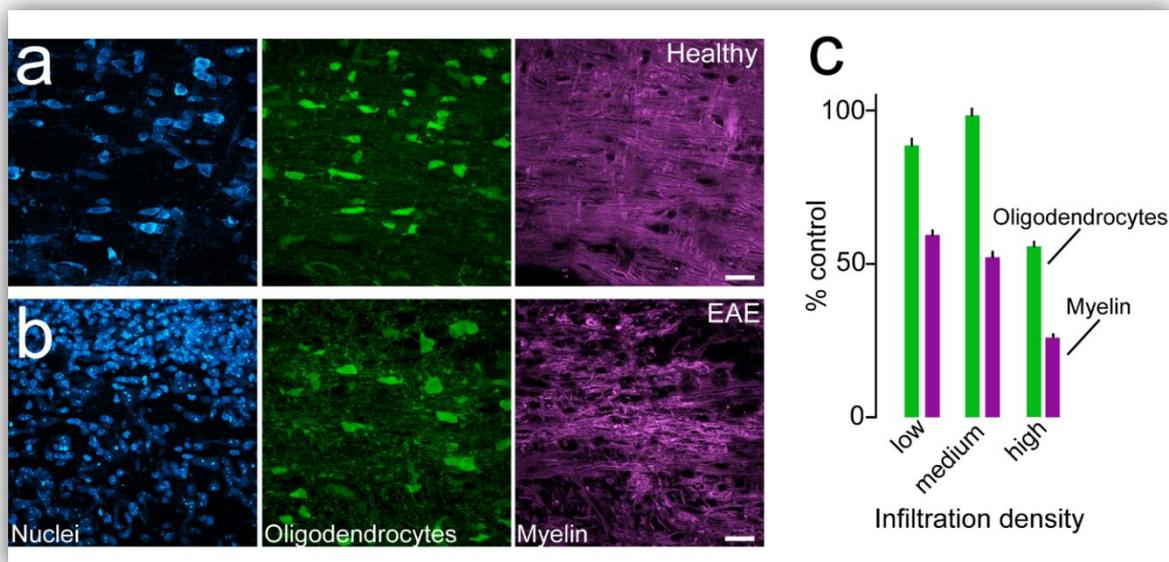


Figure 19 - Sequence of demyelination. Overview of a *PLP-GFPm* X BiozziABH mouse spinal cord in a healthy control (**a**) and EAE (**b**), stained with the nuclear dye Neurotrace (cyan) and MBP (magenta), while oligodendrocytes are transgenically GFP positive (green). In healthy example, the cells look organized and myelin intact; on the contrary, in the EAE animal it is visible a clear lesion with a high density of infiltrating cells, and where myelin appears damaged and debris are scattered within the lesion. (**c**) Quantification of the OLs number and myelin length performed at the peak of the disease (2 days after the appearance of the first symptoms, On+2) at the center of the lesion (high infiltration), at the border (medium infiltration) and far from the lesion site (low infiltration); the data are normalized to the controls. Scale bar in **a**, **b**, 25 μ m. (For the quantification: EAE, n=6 mice; Healthy, n=3 mice).

To confirm the outside-inside spread of OL pathology, I next reconstructed the morphology of single OLs. The PLP-GFPm strain is a highly efficient reporter in which nearly 100% of the OLs and their processes are positive for GFP. Consequently, the visualization of single cells is virtually impossible. Thus, for this purpose I have injected Rabies Virus SAD Δ G mCherry in the lumbar spinal cord. Rabies virus is normally used as a virus for neuronal tracing as it spreads trans-synaptically in retrograde direction (*Wickersham et al., 2007a; Wickersham et al., 2007b; Mebatsion et al., 1996; Etessami et al., 2000*). In my experiment, I have injected a low concentration of the virus in the dorsal white matter of PLP-GFPm x BiozziABH immunized mice, resulting in only few mCherry positive cells. I was then able to selectively choose OLs based on the co-expression of GFP and mCherry, and perform analysis and 3D reconstruction on these OLs (**Fig. 20 a-b**).

With this strategy of labeling, it was easy to study the morphology of the OLs: the cell body does not seem to be altered in EAE mice compared to non-immunized controls. However, OLs processes appear damaged and visibly fragmented. The quantification shows that OL processes were fewer, as well as significantly shorter than in controls groups (**Fig. 21 a-b**).

Taken together, these data suggest that in our mouse model the neuroinflammatory process damages myelin first, then it spreads to OLs processes and only at the later stages affects the somata, thus following an outside-inside gradient.

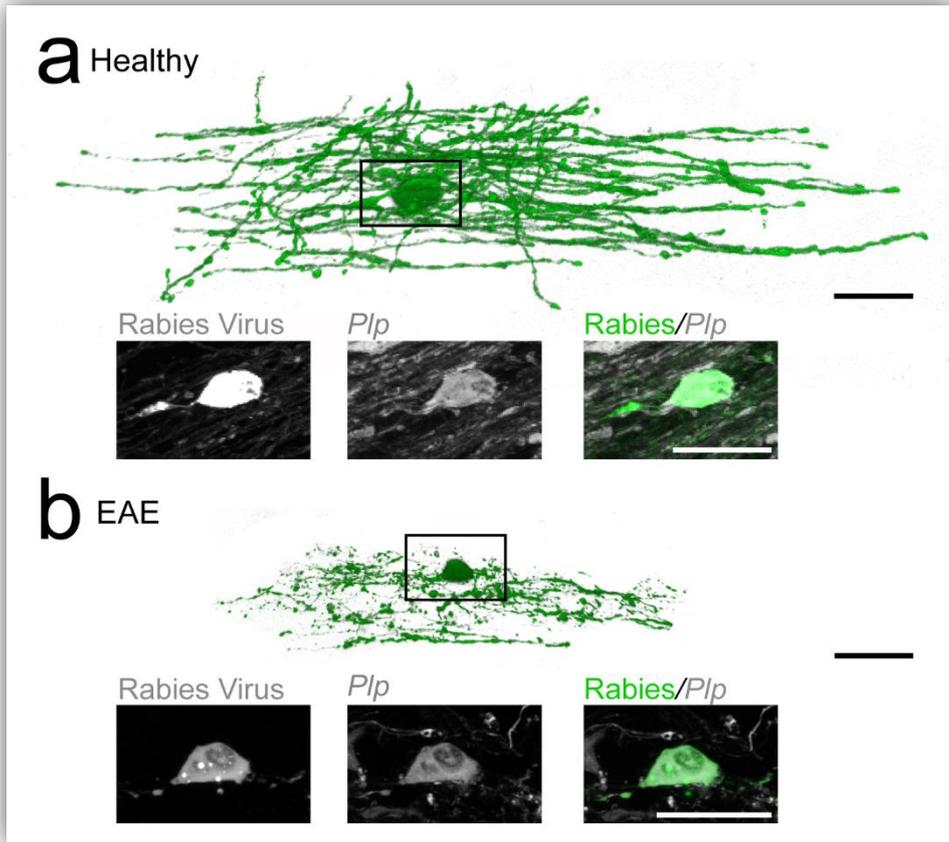


Figure 20 - Single cell labeling. Reconstruction of a single OL infected with Rabies Virus and transgenically positive for GFP. (a) Healthy OL, with straight and long processes; (b) OL from a sick animal, with short and damaged processes. Scale bar in **a**, 100 μ m (rendering) and 20 μ m (inset); in **b**, 100 μ m (rendering) and 20 μ m (inset).

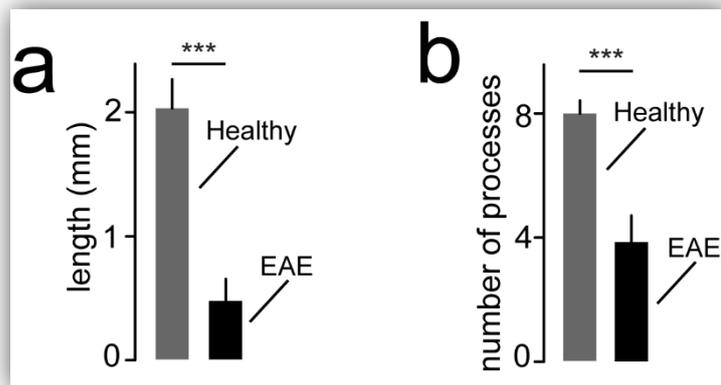


Figure 21 - Analysis of OLs processes. The OLs processes of immunized animals at On+2 are significantly shorter (a) and less in number (b) than those in healthy animals. (Controls, n=8 mice; EAE, n=8 mice) (***) $P < 0.001$).

Imaging myelin loss *in vivo*

As myelin is the first target of the inflammatory attack in the EAE model I established an *in vivo* imaging approach to study myelin damage in EAE. For this purpose the animals were immunized with MOG protein and imaged two days after the onset of the disease (acute timepoint). The lumbar spinal cord was exposed as discussed in section 1 of the Results and MitoTracker Red was applied to label myelin, while POPO-1 Iodide was used to visualize nuclei. **Fig. 22 a** shows the *in vivo* appearance of an inflammatory lesion, with YFP+ axons looking damaged, numerous infiltrating immune cells and ongoing myelin fragmentation. Analysis of the myelination status showed that in the center of an acute EAE lesion, roughly 80% of the axons are either fully or partially demyelinated; when we look at the border of the lesion, we can observe that half of the axons are still myelinated indicating that demyelination is ongoing (**Fig. 22 b**).

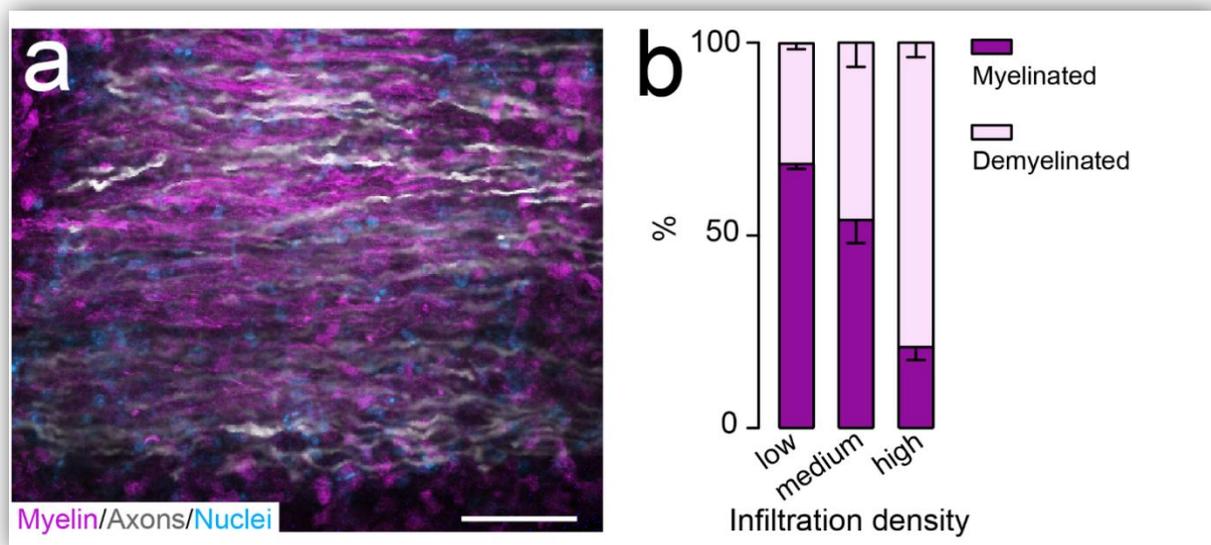


Figure 22 - (a) *In vivo* image of an acute lesion in an YFP16xBiozziABH animal; axons show swellings and myelin appears fragmented. (b) Quantification in fixed tissue of the myelination status in axons of YFP16xBiozziABH two days after the disease onset. In the lesion center, where the infiltration density is high, the majority of the axons are demyelinated; the further you go from the lesion center, the more axons show an intact myelin sheath. Scale bar in **a**, 50 μ m.

By continuously imaging lesion border areas over time, I observed the formation of peculiar myelin structures characterized by a bulb-like shape, which we named “myelinosomes”. These myelin outfoldings grow in size over time and can be observed in EAE animals but not in non-immunized control animals. I have quantified their presence at different timepoints of the disease, and I found the highest density at the acute timepoint (two days after onset) correlating with disease severity, while none of these structure are observed in healthy animals, leading to the assumption that myelinosomes formation might be a mechanism of myelin removal (**Fig. 23**). Myelinosomes were also found, though with a much lower frequency, at the onset of the clinical symptoms and at chronic timepoint of EAE (20 days after the onset of the second relapse).

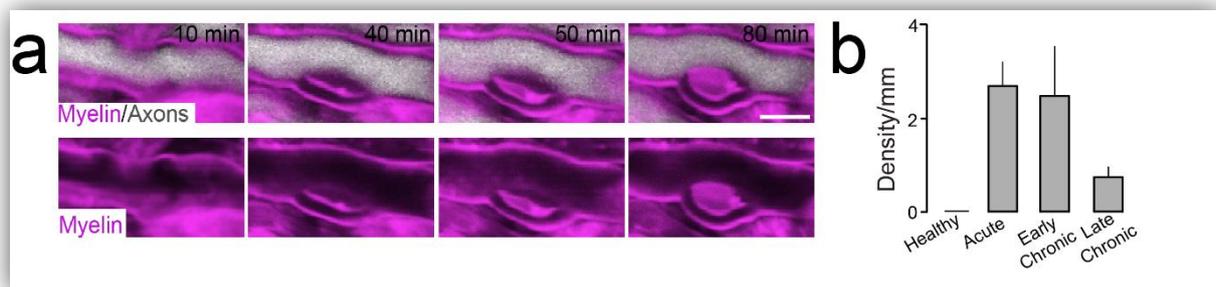


Figure 23 - *In vivo* time lapse and quantification. (a) In sick animals I have noticed the formation of myelin outfoldings that become bigger and bigger with the progression of the time. We have named these myelin structures “myelinosomes”. Myelinosomes can carry inside myelin debris, to which I refer as myelin inclusion. (b) fixed tissue quantification show that myelinosomes have the highest frequency at the peak of EAE disease, acute timepoint. (Healthy, n=3 mice; Acute, n=6 mice; Early chronic, n=3; Late chronic, n=5). Scale bar in a, 5 μ m.

Correlated light and electron microscopy of myelinosomes

In 2011 Bishop and colleagues (*Bishop et al., 2011*) described near-infrared branding (NIRB) as a method to successfully correlate light microscopy and electron microscopy (EM). I have used the same technique to confirm our *in vivo* findings and correlate them with an ultrastructural analysis.

Briefly, I used an infra-red laser to create “branding” marks in the proximity of myelin structures of interest. These marks become autofluorescent and visible through photo-oxidation; thus, the targeted area could be easily identified in serial ultrathin sections (for a detailed protocol see *Bishop et al., 2011*). **Fig. 24 a** shows a myelinosome detected with light microscopy; branding lines are visible and surround the structure of interest. The sample was then processed for EM and ultrathin sections were serially cut. The 3D reconstruction is shown in **Fig. 24 b**.

This ultrastructural study confirmed that myelinosomes are formed by myelin leaflets and that the debris inside the myelinosome, often seen during *in vivo* imaging sessions or fixed tissue quantification, are themselves part of the myelin sheath (**Fig. 24 c and d**).

This study at the electron microscope was possible thanks to the help of Prof. Dr. Bishop at the Indiana University School of Medicine, IN (USA). Prof. Dr. Bishop performed the tissue processing and the ultrathin serial cut of the sample, while I took care of scanning it with the electron microscope and actively helped with the 3D reconstruction.

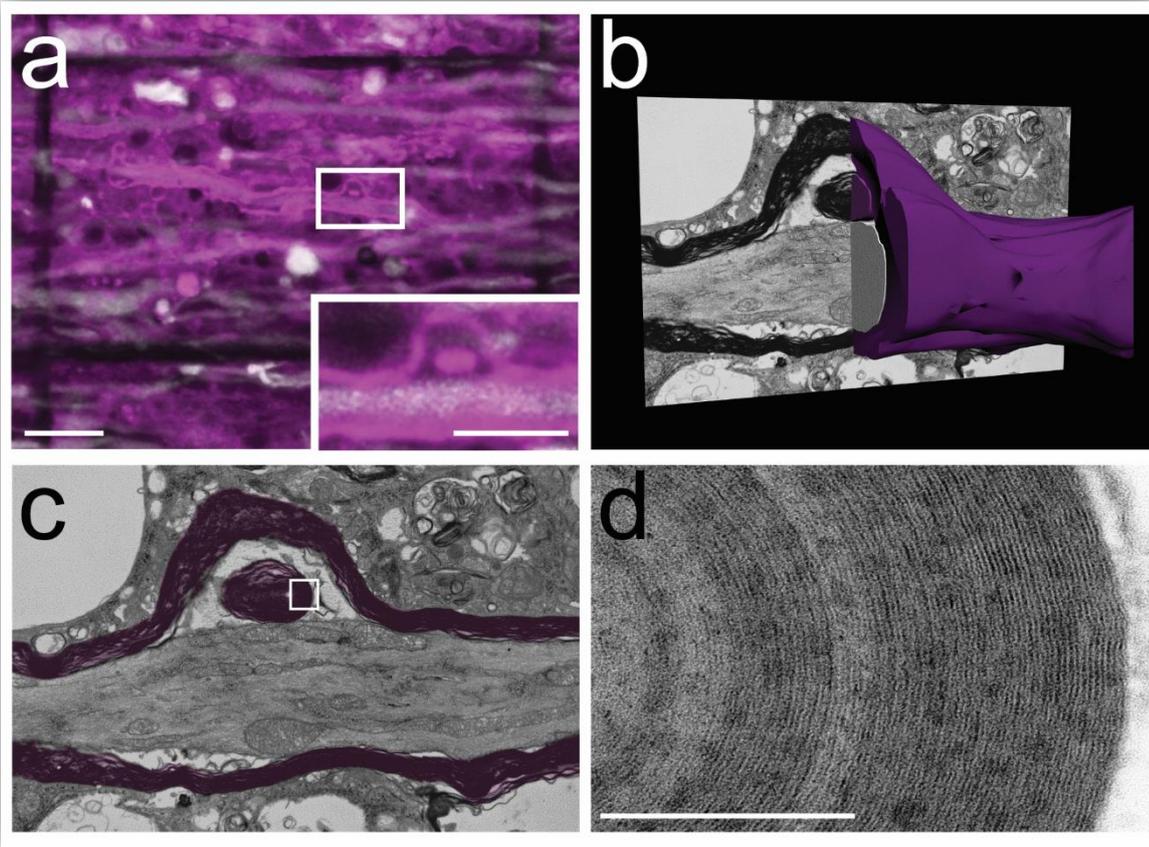


Figure 24 - Correlated light and electron microscopy. **(a)** Example of a myelinosome detected in a spinal cord lesion of a YFP16xBiozziABH sick animal; myelin is stained with MitoTracker Red and shown here in magenta. NIRB marks are boxing the myelinosome in order to allow to find the targeted area while performing the serial cut for EM. **(b)** The sample was first serially cut and then reconstructed to obtain a 3D image of the structure. **(c)** EM image showing the targeted myelinosome and its inclusion. Myelin is colored in magenta. **(d)** High magnification of the inclusion confirms that it is made of myelin. Scale bar **a**, 20 μm (overview) and 10 μm (inset); **d**, 200 nm.

Insight into the mechanism of myelinosome formation

Ultrastructural analysis

The ultrastructural analysis of myelinosomes helped us to better characterize the morphology and composition of these myelin outfoldings. In fact, sometimes the myelinosome encompass the entire myelin sheath, as shown in **Fig. 24**. Some other times, it appears to be formed only by one or few myelin leaflets (**Fig. 25 insets**).

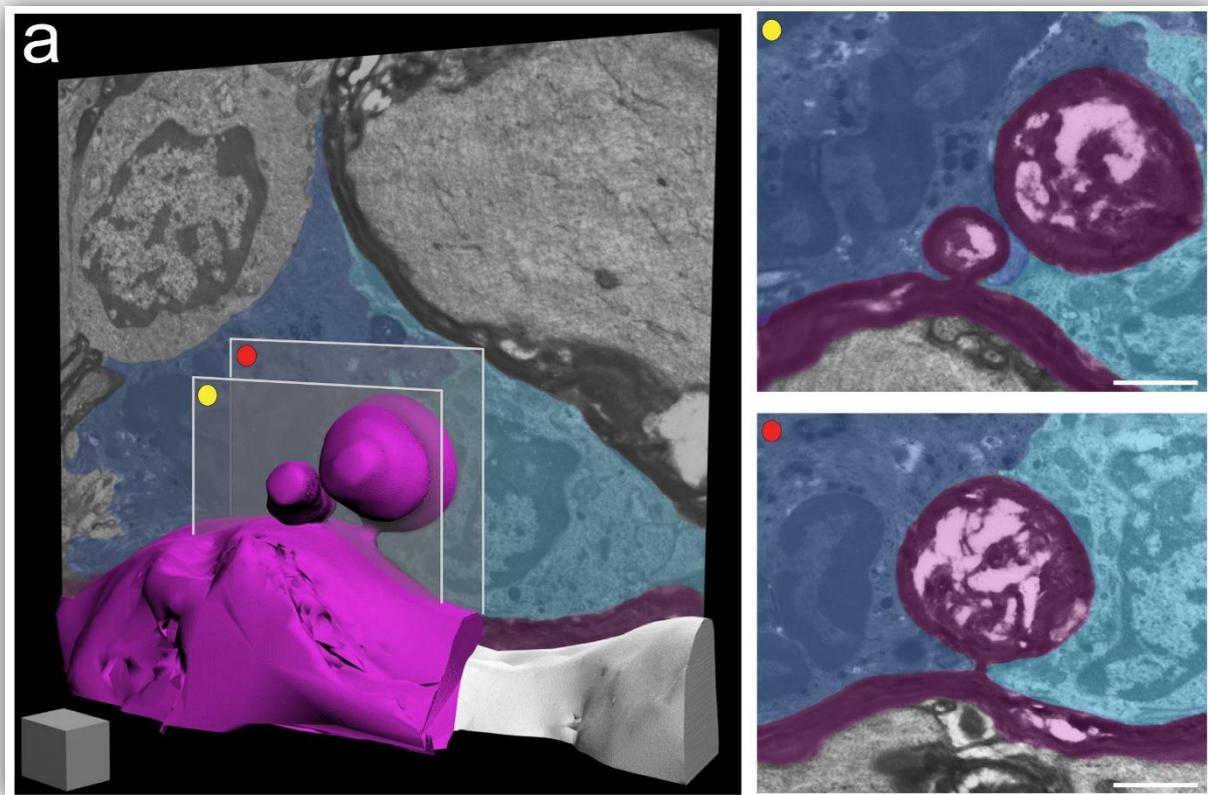


Figure 25 - Ultrastructural analysis. **(a)** On the left, 3D reconstruction of two myelinosomes on the same axon found at the acute peak of EAE. On the right, EM images of higher magnification of the myelinosomes. From the upper example we can note that sometimes myelinosomes are composed by single (or few) myelin sheath. Interestingly, the structures are surrounded by two big cells, likely monocyte-derived macrophages, which are wrapping and engulfing the myelinosomes. Myelin is colored in magenta, while the immune cells in cyan and blue. Scale bar in **a**, 1 μm (cube) and 1 μm (insets).

Interestingly, myelinosomes usually appear in direct contact with other cells. As already discussed previously, lesions in the EAE model are generally characterized by a high density

of immune cells, mainly infiltrating macrophages, granulocytes and leukocytes but also activated resident microglia. **Fig. 25** shows the 3D reconstruction of two myelinosomes forming on the same axon. It is interesting to see that those two myelin outfoldings are still attached to the axon by a small myelin bend. However, the cells processes wrapping the two structures are highly suggestive of an active process of myelinosome engulfment and phagocytosis. To characterize the cell type that contacts the myelinosomes, I used CCR2-RFPxBiozziABH animals, in which monocytes-derived macrophages express red fluorescent protein. In all cases studied (n=3 mice), the myelinosome was surrounded by MDMs, which suggests that those cells that I observed at the ultrastructural level are most likely invading phagocytes.

Antibodies transfer experiment

In our working hypothesis phagocytic cells interact with myelin in order to form a myelinosome, pull it off and consequently engulf it, therefore directly contributing to the demyelination process. Considering the high amount of autoantibodies that are likely present in an EAE lesion, we hypothesized that the formation of myelinosomes is initiated by an antibody-mediated process. While autoantibodies can recognize specific myelin proteins, macrophages express the Fc receptors which can bind the Fc fragment of an antibody, thus opsonizing the marked cellular structures. To determine whether our assumption is correct, I have used an antibody transfer approach. The experiment involves the injection of specific antibodies (in this case I injected the anti-MOG monoclonal antibody 8.18C-5, kindly provided by Dr. Krishnamoorthy) at given time points during the course of EAE (*Urich et al., 2006; Pöllinger et al., 2006*). Importantly, this experiment was carried out in the B16 strain, in which anti-CNS inflammation is dominated by CD4⁺ T cells, while the involvement of antibodies and B cells is very limited (*Lyons et al., 1999*). In order to visualize neurons and

their axons, this EAE model was induced in Thy1-Y16/Bl6 mice. Following immunization with MOG₃₅₋₅₅ peptide, the anti-MOG monoclonal antibody 8.18C-5 was injected i.p. for 3 consecutive days starting at the day of the onset, while the controls were treated with an IgG isotype control. The animals were sacrificed at onset+3. Prof. Dr. Merkler at the University of Geneva and his group helped me with the classical histopathological stainings, which I then analyzed for demyelinated area, inflammatory index and axonal density, as discussed before. The results show that the animals treated with anti-MOG antibodies show significantly more demyelination compared to the EAE controls which received an isotype control antibody, in line with previous publications showing that anti-MOG mAbs administration significantly exacerbates EAE and myelin pathology (*Piddlesden et al., 1993; Linington et al., 1988; Litzemberger et al., 1998; Morris-Downes et al., 2002*) (**Fig. 26 a**). As expected from this EAE model, the axon pathology is very severe, with less than 50% of axons surviving the insult; however there was no difference between the anti-MOG treated animals and the controls in terms of axon damage (**Fig. 26 b**).

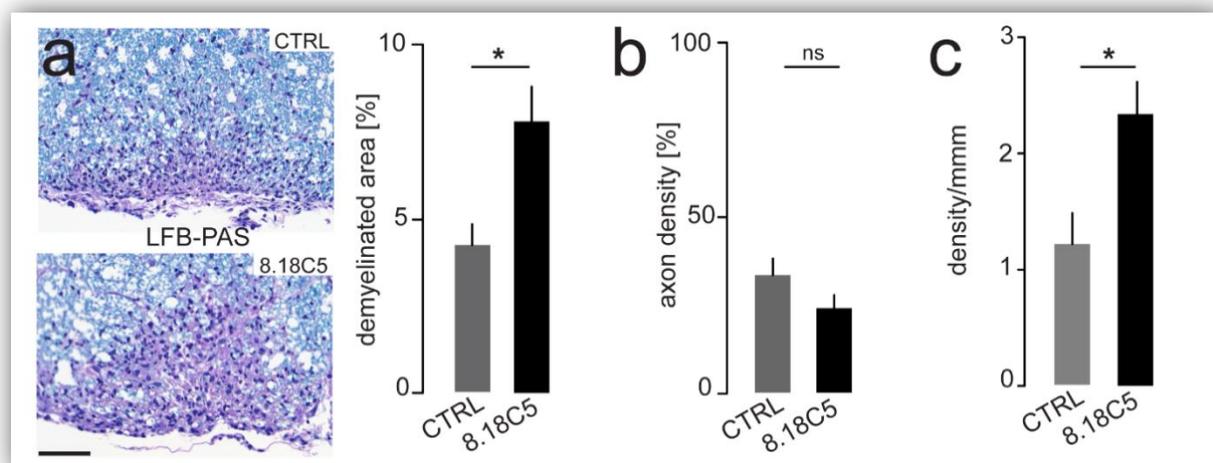


Figure 26 - Histopathological analysis and myelinosomes quantification. As shown in **a**) animals treated with 8.18C5 Abs have a significantly higher demyelination, in line with previous studies. The axonal pathology (**b**) is severe and no difference is seen among the groups. **c**) The quantification of the number of myelinosomes shows that the density is higher in 8.18C5 treated samples. (Ctrl=8 mice; 8.18C5 treatment=8 mice). Scale bar **a**, 50 μ m. (* $P < 0.005$).

Particularly interesting was the quantification of the density of myelinosomes: anti-MOG treatment led to a more pronounced demyelination and also doubled the density of myelinosomes (2.3 ± 0.2 myelinosomes/mm compared to 1.2 ± 0.3 myelinosomes/mm) compared to isotype control administration (**Fig. 26 c**).

The inflammatory index shows that the 8.18C5 treated mice have an higher number of inflammatory loci; to determine whether there is a difference in the inflammatory cells that compose the lesions, I further quantified the number of T cells (CD3+) and macrophages (Mac3+) within a given area (stainings were performed by Prof. Dr. Merkler): no difference in the composition of inflammatory cells could be observed among the different experimental groups (**Fig. 27**).

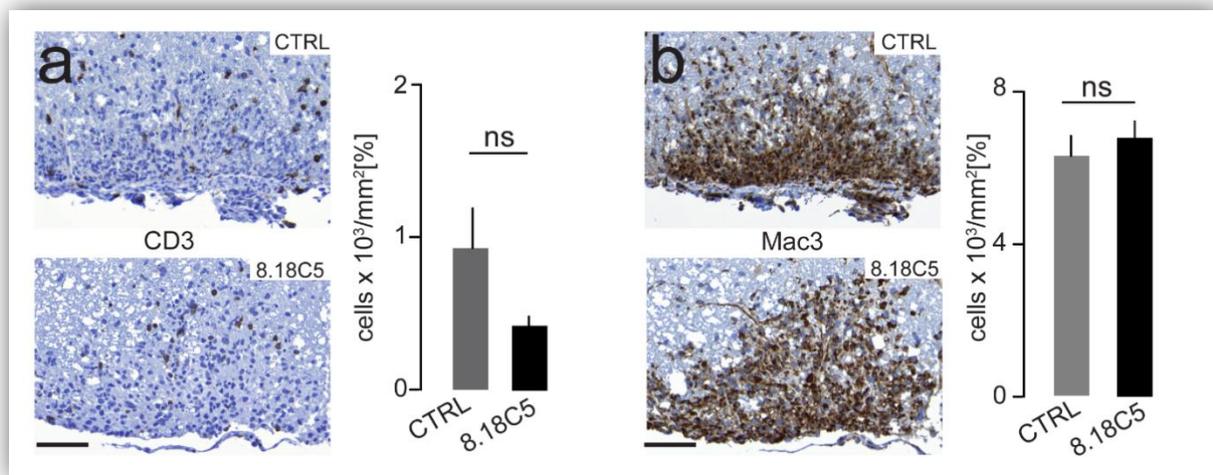


Figure 27 - Inflammatory cell composition. Inflammatory cells that characterize a lesion are mainly T lymphocytes and macrophages/microglia. To assess whether there is a difference in the cell types that form the lesions, I have quantified the density of CD3+ and Mac3+ cells. As shown in **a)** and **b)**, there is no significant difference between controls and treated animals, although a decrease is observed in the number of CD3+ cells. Scale bar **a** and **b**, 50 μ m.

All together, these data suggest that autoantibodies may play a major role in the formation of myelinosomes and consequently on demyelination.

B cell depletion approach

To further investigate and confirm the role of antibodies in myelinosome formation, I have tried to manipulate the number of circulating antibodies: if the antibody titer is lowered and our hypothesis is correct, then I should observe a less severe demyelination and lower number of myelinosomes.

Rituximab, one of the new agents currently under investigation as potential therapy for MS, targets CD20 protein on B cells thus inducing cell death. I have used the same approach and injected anti-CD20 antibody as previously described (*Weber et al., 2010; Simmons et al., 2013*). In the latter studies, treatment with anti-CD20 antibodies ameliorated EAE clinical symptoms in C57/Bl6 mice. While I successfully reproduced these results in a test round of experiments using MOG-immunized C57/Bl6 animals, I failed to obtain a satisfying B cell depletion in BiozziABH/Bl6 mice. Probably due to the genetic background of this mixed mouse strain, B cell depletion in these mice is not fully effective and the antibody titer is only partially reduced. I have repeated the experiment several times to confirm this result which, unfortunately precluded further analysis of the B cell depletion approach in the Biozzi ABH model.

Complement depletion experiment

Antibodies can mediate their action through the activation of the complement cascade, with C1q recognizing the Fc fragment of Abs and initiating the classical pathway. To test whether this mechanism of action is responsible for the formation of myelinosomes and consequent demyelination, I injected Cobra Venom Factor (CVF). A single i.p. injection of CVF is enough to deplete experimental animals (*Vogel and Fritzinger, 2010; Hundgeburth et al., 2013; Ramaglia et al., 2012*). Thy1-Y16/Bl6 mice were immunized with MOG₃₅₋₅₅, and injected with CVF to deplete the complement followed by 3 consecutive injections with

8.18C-5 anti-MOG to induce an Abs response, starting at the onset of clinical symptoms. Two control groups were added, respectively injected either only with 8.18C-5 anti-MOG or with Isotype control. Both groups injected with 8.18C-5 show a stronger disease and higher scores (**Fig. 28 a**). Interestingly, complement depleted animals have a low density of myelinosomes comparable to the control group (CVF-treated animals 1.17 ± 0.2 myelinosomes/mm, Isotype control 1.08 ± 0.3 myelinosome/mm), thus indicating a crucial role of the complement system in demyelination (**Fig. 28 b**).

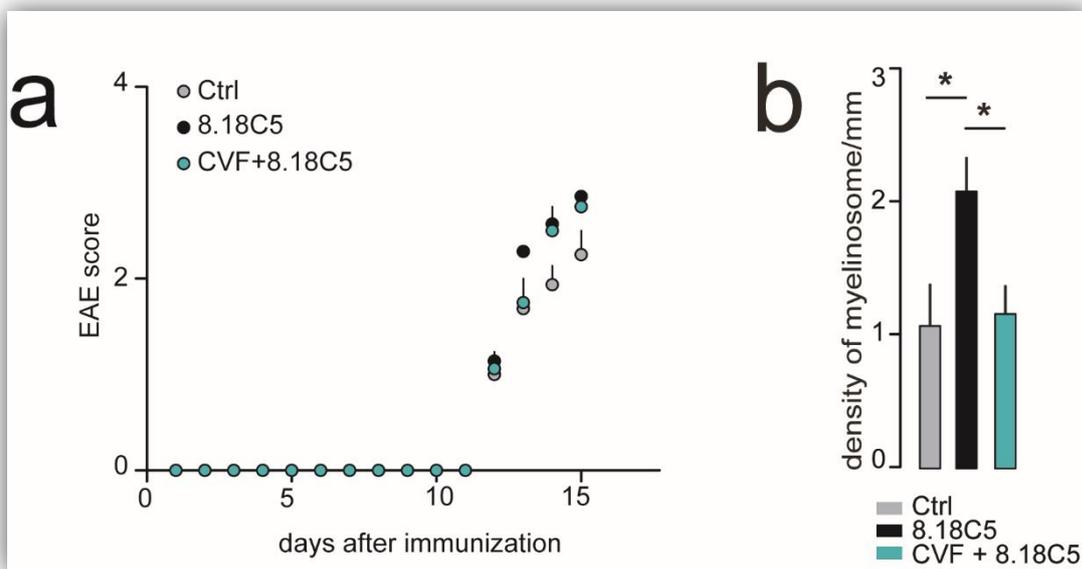


Figure 28 – Complement depletion experiment. a) After immunization, animals injected with CVF and consequent 8.18C-5 anti-MOG show severe EAE symptoms compared to the isotype control group. b) The density of myelinosomes in animals depleted of the complement system is instead quite low, thus indicating that the complement plays a crucial role in the formation of myelinosome and consequent demyelination. (Ctrl=8 mice; 8.8C5=7 mice; CVF+8.8C5=8 mice). (* P<0.05).

Relevance for the human pathology

Sequence of demyelination in MS

The results from the animal models should in the end help to better understand how the process of demyelination occurs in the human pathology. I therefore received biopsies from patients affected by MS (kindly provided by Prof. Dr. Wolfram Brück, Univ. Göttingen, and stained by Prof. Dr. Merkler, Univ. Geneve) and characterized their pathology. All the biopsies show active demyelinating lesions, characterized by ongoing myelin loss, high number of infiltrating cells and presence of myelin debris in the cytoplasm of macrophages.

For my work, I have quantified the number of OLs within the lesion area, at the lesion border and in the NAWM. Interestingly, while myelin is mostly lost in the lesion center and preserved in NAWM regions, the OLs number is comparable between the different areas (**Fig. 29**). These results suggest that myelin is the first target of the immune attack also in human MS lesions.

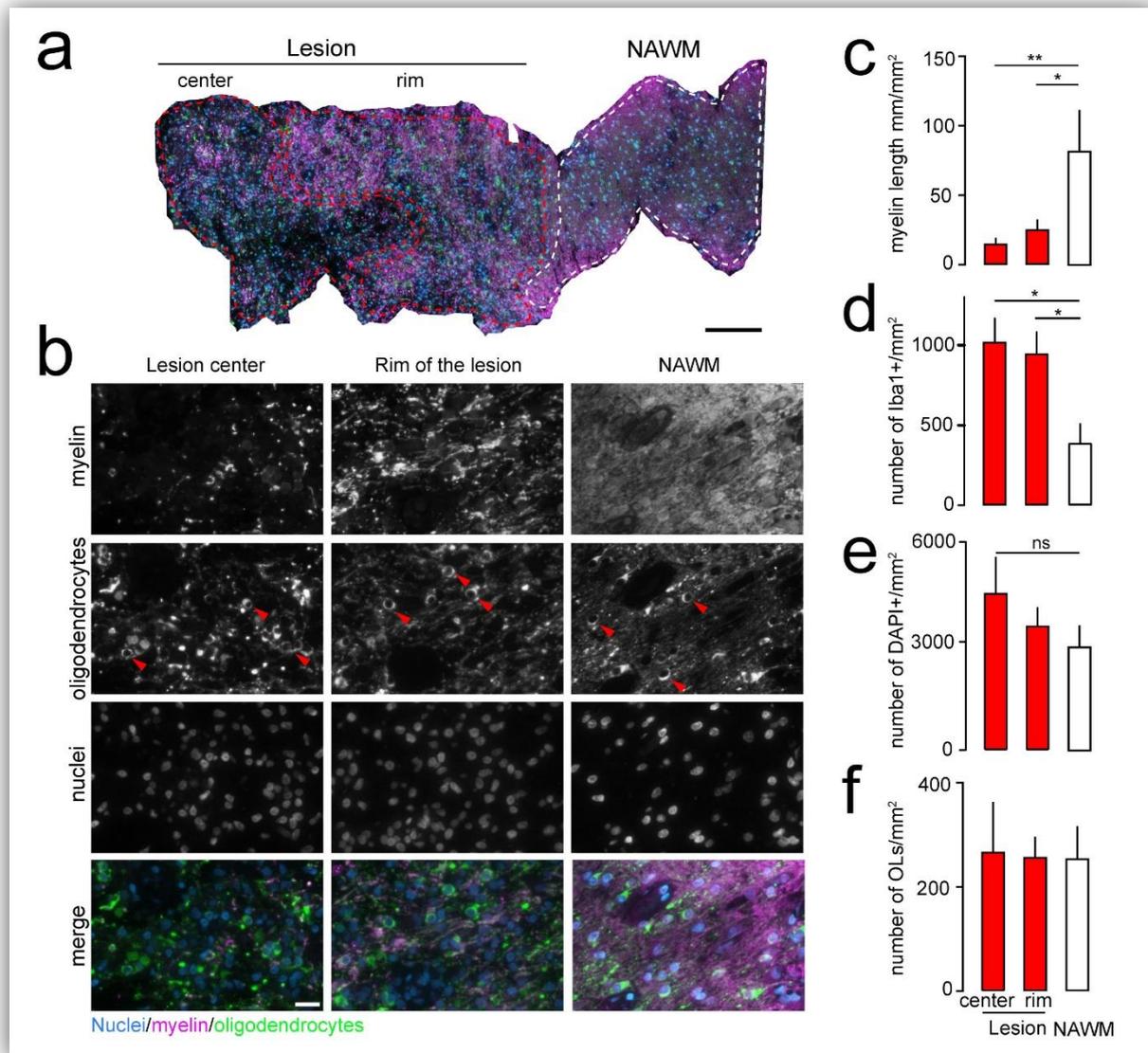


Figure 29 - Pathology of MS lesions. **a**) Overview of an active demyelinating MS biopsy stained for OLs marker NOGO-A (green), for myelin marker MBP (magenta) and with the nuclear dye DAPI (cyan). There can be distinguished three different areas, defined as the lesion center, the lesion rim and the NAWM. **b**) Higher magnification of OLs, myelin and nuclei, in the lesion center, rim and NAWM. **c**) Quantification of the total myelin length shows a significant decrease in the lesion areas compared to the NAWM. **d**) The density of activated microglia was quantified counting Iba1+ cells; as expected, the graph shows a higher density within the lesion. **e**) The total number of cells indicates a slight higher density in the center and rim of the lesion, probably due to the high number of infiltrating cells. **f**) Interestingly, OLs density appears to be rather consistent within the different areas, suggesting that OLs damage happens secondarily to myelin loss. (Biopsies n=6) (** P<0.01; * P<0.05). Scale bar in **a**, 200 μ m, **b**, 20 μ m.

Parallelism with the murine myelinosomes

Interestingly, high resolution confocal analysis of the myelin structure in MS biopsies, revealed the presence of structures that are very similar to the myelinosomes observed in the EAE model. I could detect bulb-like myelin outfoldings in different areas of the biopsies: the highest density was found in the center of the lesion, while a smaller number of myelinosomes was also noted in the normal appearing white matter (NAWM). Although these areas are called “normal-appearing”, they can potentially show different preclinical pathological changes (Allen *et al.*, 2001). Importantly, analysis of myelin in control tissue from patients not affected by any demyelinating disease, failed to reveal presence of myelinosomes, thus indicating that their presence is restricted to pathological inflammatory conditions in which myelin represents one of the main immune targets (**Fig. 30**).

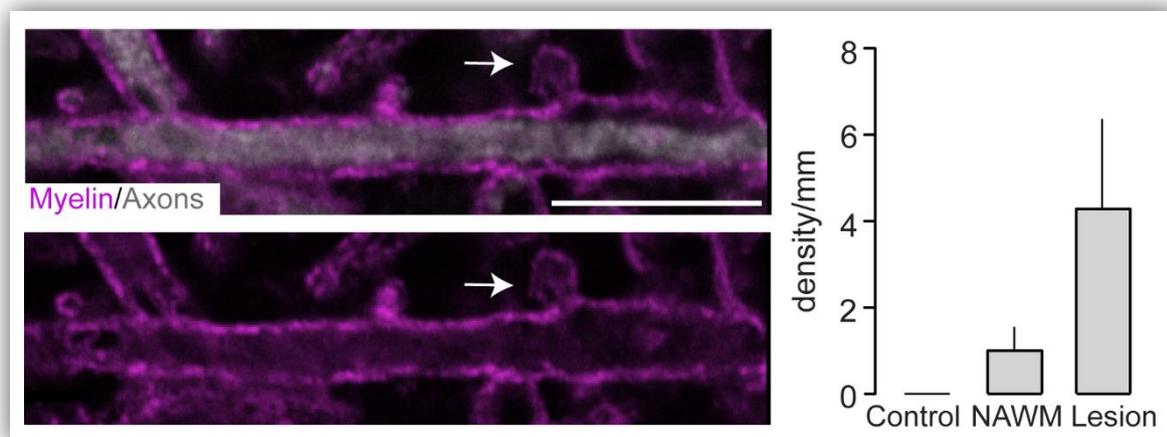


Figure 30 - MS myelinosomes. Density of myelinosomes was quantified in control biopsies, NAWM and lesion center. The results show a high frequency in the lesion, while the control myelin looks fully healthy. (Biopsies, MS n=4, control n=3). Scale bar 10 μ m.

CHAPTER V – Discussion

1. Key findings

- Part I: *In vivo* imaging as a tool to study demyelination and neuroinflammation

Important recent advances in the field of neuroscience come from the use of *in vivo* microscopy techniques combined with novel transgenic strategies. In the past years the combined use of these new tools allowed the study of healthy CNS as well as neurological disorders, allowing for example to investigate axon degeneration and regeneration in the injured spinal cord (*Kerschensteiner et al., 2005; Ertürk et al., 2007; Debarbieux et al., 2009*), or cellular interactions and axonal pathology during neuroinflammation (*Bartholomäus et al., 2009; Nikic et al., 2011; Siffrin et al., 2010; Breckwoldt et al., 2014; Sorbara et al., 2014*).

The first project presented in this thesis, helped to further expand the range of tools available for *in vivo* microscopy. To achieve this I have determined the ideal concentration and the best *in vivo* imaging settings for a set of commercially available vital dyes that have previously been primarily used in *in vitro* studies. I could show that the application of vital dyes provides a comparably easy and efficient way to label specific cellular and subcellular compartments, as well as to assess the release of toxic mediators in the living nervous system (*Romanelli et al., 2013*).

- Part II: Pathogenesis of demyelination in EAE and MS

The aim of this part of my thesis was to better understand the process of demyelination in EAE and MS. In fact, although demyelination represents one of the classical hallmarks of this disease, the mechanisms mediating it are not clear. The experiments presented in this thesis led to the following conclusions:

- In the EAE model oligodendrocyte damage follows an outside-inside gradient: myelin is the first target of the immune attack; secondly, OL processes are lost and lastly, the OL soma is damaged.
- Continuous imaging over several hours in an EAE lesion area showed that myelin is removed by formation of myelin bulb-like structures that we named “myelinosomes”. These myelin outfoldings are not observed in control animals, but are found in the EAE model where they appear with particularly high frequency at the peak of disease (2 days after onset).
- EM studies helped to further characterize the morphology of myelinosomes: they can encompass the entire myelin sheath, or they can be formed by single or few myelin leaflets.
- EM analysis also showed that myelinosomes are closely contacted by cells, which I further characterized to be primarily monocyte-derived macrophages. Those cells engulf and phagocytose the myelinosome, leaving a patch of axon myelin-free.

- Antibodies play a crucial role in the formation of myelinosomes, likely through complement binding and interaction with the complement receptor on the phagocytic cell.
- In human samples, the mechanism of demyelination shares some similarities with our animal model: while myelin is lost in the center of the lesion as well as drastically reduced in perilesion areas, OLs somata are consistently preserved in both regions and in NAWM. Furthermore myelinosome-like structures were also found in MS samples, suggesting that the mechanisms underlying demyelination in the human disease might be similar to those described in the mouse model.

2. Vital dyes: a new tool for *In vivo* imaging studies

In my first project I described a new approach to efficiently label different cell types (such as macrophages/microglia or oligodendrocytes), subcellular compartments (such as myelin) and organelles (such as mitochondria), or to detect the release of toxic mediators (such as reactive oxygen species), by the local application of vital dyes previously described in *in vitro* studies. Vital dyes can thus be easily used to complement genetic labeling approaches. While numerous reporter mouse lines suitable for imaging of immune cells, neurons (*Singbartl et al., 2001; Jung et al., 2000; Feng et al., 2010*), or myelin producing cells (*Karram et al., 2008; Hirrlinger et al., 2005; Mallon et al., 2002; Viganò et al., 2013*) are now available, the creation of new transgenic lines especially if different labels are to be combined, is often time-consuming and expensive. Thus the combined application of one or more vital dyes to a specific reporter mouse line could help to address several questions in a single *in vivo* experiment. For example, in my second project focused on the study of demyelination in EAE, I have used a specific vital dye to label myelin in conjunction with a well established transgenic mouse line that provides a spectrally distinct labeling of neurons and their connections.

Considering the increasing interest in the use of *in vivo* microscopy to study CNS disease models (*Siffrin et al., 2010; Mues et al., 2013; Nikic et al., 2011; Sorbara et al., 2014; Misgeld and Kerschensteiner, 2006; Sorbara et al., 2012*), a fast and reliable labeling technique, such as the hereby described application of vital dyes, represents a useful strategy to further enhance and expand the available toolset for such experiments (*Romanelli et al., 2013*).

3. Oligodendrocyte damage and demyelination in mice

Since its first description in 1933 (*Rivers et al., 1933*), EAE has been the most commonly used model to study MS pathogenesis. Among others it helped to understand, which cell types are involved in the initiation of a neuroinflammatory lesion. However, some open questions remain to be addressed; in particular it is still debated which mechanisms drive OLs impairment and demyelination in neuroinflammatory lesions. Here I suggest that the detriment starts at the myelin level and consequently spreads towards the OLs cell body in an “outside-to-inside” gradient (**Fig. 31**). Furthermore, I provide *in vivo* evidence for a novel mechanism of myelin damage, and suggest that myelin removal might be a multistep process mediated by the binding of autoantibodies to the myelin that activate mononuclear phagocytes via complement.

Demyelination as an outside-inside process

The sequence of events that characterizes oligodendrocyte damage remains unclear and different hypothesis have been proposed regarding the site where damage to OLs is initiated: myelin and its proteins (MBP, MOG, MAG, PLP), OLs processes that mediate the communication between OLs soma and myelin, or the cell body itself. To answer this question, I have used mice on a BiozziABH genetic background in which, contrarily to the widely used C57Bl6 animals, extensive primary demyelination occurs over the course of EAE (*Biozzi et al., 1972; Baker et al., 1990; Amor et al., 2005*). Two days after the onset of the clinical EAE symptoms, the results show extensive myelin damage not only in the lesion center but also at the lesion border. On the contrary OLs loss, is only observed in the lesion center (**Fig. 19**). It is known that with disease progression there is a significant loss of all three OLs compartments (myelin, OLs processes and OLs cell bodies). However our findings

imply that 1) the damage to myelin is not secondary to OLs death but it rather is the primary target; 2) myelin loss correlates with the number of infiltrating cells, reinforcing the already known notion that immune cells act as mediators of demyelination.

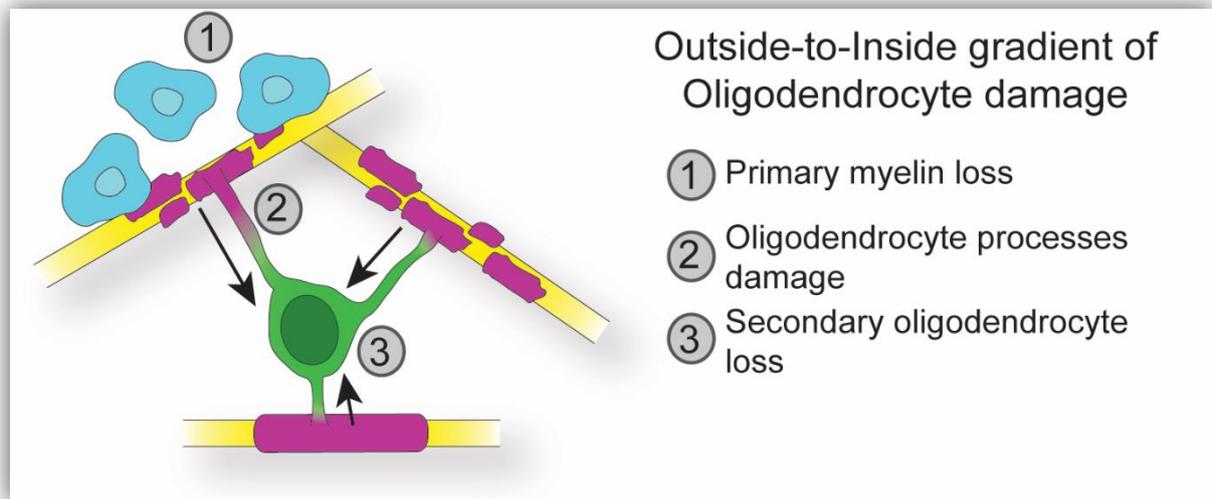


Figure 31 – Oligodendrocyte damage follows an outside-to-inside gradient starting with myelin loss, spreading towards oligodendrocytes processes and finally to oligodendrocyte cell bodies.

The finding that myelin represents the first target of the immune attack and not OLs cell bodies as suggested previously (*Barnett and Prineas, 2004*), is in line with the studies describing that in the majority of MS cases demyelination appears to follow an “outside-to-inside” gradient (*Lucchinetti et al., 2000; Lassman et al., 2001*). It is likely that myelin itself can be an target for the immune attack; its proteins are well-known autoantigens in experimental models and autoantibodies against MOG, PLP and MBP are described in subsets of MS patients (*Pröbstel et al., 2011; Derfuss and Meinl, 2012; Quintana et al., 2012*). Work in animal models would also suggest that autoreactive myelin-specific T lymphocytes play an important role in the pathogenesis of MS (*Babbe et al., 2000; Skulina et al., 2004*).

The reconstruction of single OLs reconstruction in EAE and healthy animals, achieved through the injection with Rabies Virus SADΔG-mCherry (*Wickersham et al., 2007a*;

Wickersham et al., 2007b; Mebatsion et al., 1996; Etessami et al., 2000; Wickersham et al., 2010) in a transgenic PLP-GFP mouse line (*Mallon et al., 2002*), confirmed the centripetal direction of OLs damage (**Fig. 20**). Distal and proximal oligodendrocyte processes in EAE lesions appeared fragmented, and were fewer in number and shorter than those in the controls (**Fig. 21**).

All together our data support the hypothesis that OLs death is not the primary event in the process of demyelination. Although primary OLs damage is commonly seen in different pathologies, such as virus-induced inflammatory demyelination (*Johnson and Ludwin, 1981; Rodriguez et al., 1995*) and white matter ischemia (*Aboul-Einen et al., 2003*), and in the past years many efforts were made to find drugs aimed to enhance OLs survival and increase their differentiation (i.e. Benzotropine, *Deshmukh et al., 2013*), our data encourage instead the development of new therapeutic strategies focused on preserving myelin from the immune attack.

Time lapse *in vivo* imaging reveals myelin abnormalities

In order to learn how demyelination occurs in EAE, I have used an *in vivo* imaging approach that has previously helped us to investigate axons dynamics and mitochondria transport in a similar disease model (*Nikic et al., 2011; Sorbara et al., 2014*). To directly visualize the demyelination process I applied the vital dye MitoTracker Red to label myelin (*Romanelli et al., 2013*) in a Thy1-XFP transgenic line (*Feng et al., 2010*) that revealed the axonal counterparts. As described previously (*Nikic et al., 2011; Romanelli et al., 2013; Sorbara et al., 2014*) when looking at the spinal cord of an immunized animal, axons show swellings and often appear fragmented, while intact myelin sheaths in these areas are partially lost and replaced by myelin debris. The local application of a nuclear dye allowed the visualization of infiltrating cells *in vivo* (*Romanelli et al., 2013*), which made the identification of EAE

lesions easier. When I then imaged the same area with higher resolution over time, myelin appears damaged and bulb-like structures are visible within the lesion. Such structures, which we named myelinosomes, are frequently found 2 days after the disease onset when demyelination is particularly severe. Their morphology is similar to myelin outfoldings which appear to increase over the time (**Fig. 23**), and likely represent the initial stage of demyelination. Although the data reported in this thesis represent the first report of an *in vivo* time course of myelin outfoldings formation in EAE, the findings that such myelin abnormalities can be in dysmyelinating diseases is not fully new. In fact, biopsies from patients affected by Charcot-Marie-Tooth Type 4H, a neurological disorders that damages Schwann cells (responsible for the myelination of axons in the peripheral nervous system) and reduces nerve conduction velocity, have revealed profound myelin abnormalities, characterized by myelin infoldings and outfoldings (*De Sandre-Giovannoli et al., 2005; Stendel et al., 2007; Fabrizi et al., 2009*). Mice lacking Fabrin/Fgd4, a member of the family of Cdc42-specific guanine nucleotide exchange factors (*Nakanishi and Takai, 2008*), show dysmyelination during early peripheral nerve development with the formation of aberrant myelin structures (*Horn et al., 2012*). Same myelin abnormalities also appear when Mtmr2, the myotubularin-related 2 gene, is inactivated in Schwann cells (*Bolino et al., 2012; Pereira et al., 2012*). While myelin outfoldings have usually been linked to pathological disorders, a recent paper described the presence of redundant myelin also at early stages during development in the optic nerve; this accumulation of excess membrane spreads out along the myelin sheath during development and gradually disappears in adult life (*Snaidero et al., 2014a*). Comparable structures were also previously found in the proximity of nodes of Ranvier in EAE by ultrastructural examination (*Yamasaki et al., 2014*).

In our animal model, the formation of myelinosomes correlates with disease progression, with only few myelinosomes observed at the onset of EAE and an increased frequency 2 days

after disease onset when demyelination reaches its peak. Myelinosomes are also seen with a high density two days after a disease relapse, while they decrease at a chronic time point when the majority of the axons have already been demyelinated. In the healthy adult spinal cord myelinosomes are never seen, thus reinforcing that their presence is restricted to the pathological condition.

An interesting point to mention is the relationship between axonal and myelin degeneration. Despite the widely held view that MS is a primary demyelinating disease in which axon damage happens secondarily to myelin loss, studies have suggested that in some remyelinating and inactive MS lesions (*Bitsch et al., 2000; Kornek et al., 2000; Kuhlman et al., 2002*) as well as in EAE (*Nikic et al., 2011*), axons can be damaged independently from their myelinating/demyelinating status. My results support this notion, as I find myelinosomes surrounding normal appearing axons as well as axons undergoing degeneration. This further confirms that axonal pathology and demyelination might occur independently from each other and might indeed be triggered by different mechanisms. These results must be kept in mind when developing new therapeutic strategies, because a drug which is effective for the prevention of myelin destruction, might not automatically protect axons from degeneration.

Ultrastructural analysis of myelinosomes

The *in vivo* visualization of myelin is based on the application of the vital dye MitoTracker Red (*Romanelli et al., 2013*). Being a highly lipophilic dye, it can easily penetrate membranes, therefore sometimes its labeling is not only restricted to myelin. Hence, an argument that could be raised is that myelinosomes might be artefacts of the labelling itself. Considering that I did not detect myelinosomes in control animals even after long imaging sessions and even though we were confident that myelinosomes are not artefacts of the

labelling, to fully exclude this possibility I performed electron microscopic analysis of myelinosomes. This helped not only to clarify their composition but also to better characterize their morphology and interaction with adjacent cells.

Part of this study was conducted based on a novel technique previously described to correlate light and electron microscopy (“near-infrared branding (NIRB)”) (*Bishop et al., 2011*), that relies on the use of fiducial “branding” marks which photo-oxidize after exposure to diaminobenzidine (DAB), thus allowing to be recognized at the electron microscopic level (*Bishop et al., 2011*). With this method, I excluded the possibility of myelinosomes being artefacts and confirmed that they are indeed outfoldings of the myelin sheath which sometimes carry inside fragments of myelin debris (inclusions) (**Fig. 23 - 24**).

Further EM studies also shed light on the composition of myelinosomes, showing that they can encompass the entire myelin sheath or they can be made up of only few myelin leaflets (**Fig. 25**). This might be explained by the original thickness of the myelin sheath. It is indeed known that there is a correlation between myelin and axon diameter (*Friede and Samorajski, 1967; Elder et al., 2001*): thinner axons have a thinner myelin sheath, while big caliber axons require a thicker myelin. Thus, on the one hand when the axon is thin, myelinosomes might be formed by the whole myelin sheath; on the other hand, when the axon is thick, the removal of myelin might require more steps and the formation of several myelinosomes each composed by few myelin layers. However, myelin is a very tightly packed structure and in order for the single-leaflets myelinosomes to form, the interactions among myelin stacks must be loosened. It was recently proposed that MBP, one of the major components of compact myelin (*Privat et al., 1979*), thanks to its capacity to go through phase transition is responsible for myelin assembly and aggregation (*Aggarwal et al., 2013*). On the contrary, when MBP changes from a condensed to a dispersed phase, it might induce myelin

disassembly, leading to detachment among myelin leaflets which in turns might favor the formation of single-leaflet myelinosomes.

4. Involvement of the immune system

As I already summarized in the Introduction (see section “Animals model of demyelination and inflammation”), different components of the immune system are involved in the formation of new lesions in EAE. However macrophages, derived either from resident microglia (MiDMs) or from circulating monocytes (MDMs), are the main cells that compose a classic neuroinflammatory lesion and their density usually correlates to EAE severity (*Huitinga et al., 1990, 1993; Ajami et al., 2011*). Here I show that they also play a crucial role in the initiation of demyelination. Specifically through the interaction with anti-MOG antibodies they contribute to the formation of myelinosomes and consequently to myelin loss.

Macrophages interaction

The electron microscopic study was helpful to show the relationship of myelinosomes with the surrounding cells. Here I observed that adjacent cells always reach out to contact and engulf myelinosomes (**Fig. 25**). Myelinosomes are formed predominantly 2 days after onset, when demyelination is known to be particularly severe and the density of infiltrating immune cells significantly high. Given their preferential occurrence at the demyelination peak and the close contact with phagocytic cells, we propose that myelinosomes are a mechanism of myelin removal which is responsible for demyelination in the EAE model. To understand which cells initiate myelinosome formation, I used a transgenic mouse line that allows to discriminate between MiDMs and MDMs (*Saederup et al., 2010; Mizutani et al., 2012*). The finding that phagocytes contacting myelinosomes always belong to the monocytes-derived-

macrophages family (MDMs) means that those cells are likely involved in the process of myelinosome formation. The result is in line with the data presented by Yamasaki and colleagues, suggesting that MDMs and MiDMs exert different roles in EAE pathology, with MDMs responsible for the initiation of demyelination starting in the proximity of the node of Ranvier, while MiDMs are involved in the removal of myelin debris (*Yamasaki et al., 2014*). Macrophages are known to act as mediators of axon damage and mitochondrial dysfunction (*Smith and Lassman, 2002; Lin et al., 2006; Nikic et al., 2011*) through the release of toxic factors, which may also be responsible for myelin destruction (*Bitsch et al., 2000*). However our data argue for a rather active and mechanic role of macrophages in myelin removal. In fact, due to the peculiar morphology of myelinosomes and their close vicinity to phagocytic cells, we can speculate that a tight interaction between myelin and the cell itself does exist. This bond helps the macrophage to physically pull off myelinosomes, engulf them and leave a patch of axon myelin-free. Given the presence of potential phagocytic signals, such as immunoglobulins and opsonins (*Nauta et al., 2004*) or eat-me signals (*Hochreiter-Hufford and Ravichandran, 2013*), which can be recognized by specific receptors on macrophages implicated in phagocytosis like the scavenger receptor SRA-I/II, Fc Receptor, C1q and C3b receptors (*Winther et al., 2012; Hogarth and Piertersz, 2012; Hadas et al., 2012; Smith, 2001; Reichert and Rotschenker, 2003*), it will be important to identify the molecular mechanism initiating the formation of myelinosomes, and eventually to selectively manipulate it in order to prevent demyelination.

Antibodies and myelinosomes formation

Although MS is recognized as a T cell-mediated autoimmune disease, the presence of oligoclonal Igs and plasma cells in the CSF is widely used to diagnose the disease (*Egg et al., 2001; Warren et al., 1994*), suggesting that antibodies (Abs) might play a role in the

pathology of MS. I have hypothesized that Abs might as well be involved in demyelination and myelinosome formation identifying surface myelin proteins as antigens and consequently interacting with the surrounding macrophages/phagocytes.

I have injected anti-MOG mAb in Y16/Bl6 mice after immunization with MOG₃₅₋₅₅, a model in which normally the role of B cells and Abs is very limited and the disease is predominantly driven by T cells. I found that the treatment with anti-MOG mAbs induces exacerbation of demyelination, in accordance with previous reports (*Piddlesden et al., 1993; Linington et al., 1988; Litzemberger et al., 1998; Morris-Downes et al., 2002*). Of particular interest was the finding that the density of myelinosomes is significantly increased after anti-MOG Abs injection (**Fig. 26**). From former studies, it is known that in the EAE model the role of Abs and their producing cells is still controversial, with some evidence suggesting a pro-inflammatory role with amelioration of the clinical symptoms after B-cells depletion (*Lyons et al., 1999; Weber et al., 2010*), and others describing a rather protective role (*Weber et al., 2010; Simmons et al., 2013*). My findings point in the direction of a destructive action of anti-myelin Abs and suggest that myelinosome formation and demyelination are antibody-mediated processes. Specifically MOG, one of the few surface proteins that is exposed on the myelin sheath, seems to be the target of the autoantibodies attack. Indeed, anti-MOG autoantibodies have also been described in the serum of a subgroup of (pediatric) MS patients (*Pröbstel et al., 2011*).

A potential confounder in this experiment could be that the higher density of myelinosomes observed after anti-MOG Abs injections might be due to a different density of macrophages and T cells within the lesions after Ab application. However, analysis of inflammatory lesions revealed no difference both in the density of T cells (CD3+) and macrophages/microglia (Mac3+) between the treated animals and the controls. This further confirms that myelinosome formation is dependent on the number of antibodies capable of

binding MOG proteins. If we want to spare axons from demyelination we therefore need to act on 1) reducing the titer of Abs that can potentially bind myelin proteins and 2) interfere with the mechanism of action of the Abs, thus preventing them to interact with macrophages/phagocytes.

Myelinosome formation as an antibody-complement mediated mechanism

In order to prevent demyelination a question that will be helpful to answer, is throughout which pathways and receptors Abs exert their function.

Abs can elicit their effector function through activation of the complement system initiating the classical complement pathway (*Botto et al., 1998; Kishore et al., 2000*). By injecting with cobra venom factor (CVF), commonly used to deplete experimental animals (*Vogel and Fritzingler, 2010; Hundgeburth et al., 2013; Ramaglia et al., 2012*), I studied the role of the complement system in regard to its interaction with antibodies in the EAE model and its contribution to demyelination and myelinosome formation. My data suggest that the complement system plays a crucial role in the formation of myelinosomes, as demonstrated by the low density of myelin abnormalities in the animals treated with CVF (**Fig. 28**). This is in agreement with previous studies, which lean on a major role of the complement system during demyelination (*Urich et al., 2006; Ingram et al., 2009*). A role for the complement in MS is known since 1971, when C3 deposits were described in the brains of MS patients (*Lumsden, 1971*); since then, numerous studies in the animal models have been aimed to investigate the role of the complement system in EAE pathogenesis. Recently the complement was the subject of a study performed in BiozziABH mice, which reported that it is highly activated when demyelination is ongoing during the acute, relapsing and progressive disease stages, while its activation is markedly diminished during remission (*Ramaglia et al., 2015*).

The constant region of immunoglobulins can also be recognized by the FcR on macrophages and this bond is usually responsible for antibody-directed cell-mediated cytotoxicity (ADCC) (Ravetch and Clynes, 1998). Although few studies have already been conducted on the role of FcγRs in the pathogenesis of demyelination, which concluded that FcγRs are not involved in the processes leading to the myelin loss (Urich *et al.*, 2006; Breij *et al.*, 2005), we are currently performing experiments using FcγR quadruple knockout mice (deficient in both the activatory and inhibitory FcγRs - I, II, III and IV -). This will help to clarify whether FcγRs play a role in the formation of myelinosomes or not.

The finding that complement system is involved in myelin damage opens new feasible therapeutic strategies to prevent myelin destruction and suggests the complement system as a new potential target for drug development.

5. Relevance for MS

Considering that the current literature does not provide a conclusive answer on the sequence of demyelination in MS, during my PhD work I have analyzed several active demyelinating MS biopsies in collaboration with the group of Doron Merkler (University of Geneva). My work suggests that demyelination in MS shares important similarities with the animal model, both in regards to the sequence that leads to myelin loss and to the mechanisms that drives it.

Demyelination in MS lesions

As previously investigated in the animal model, I first studied the sequence of myelin loss by measuring the density of OLs cell bodies as well as myelin length in lesion (active lesion center and border of the lesion) and in NAWM regions. The results show that there is a substantial reduction of myelin within the lesion areas compared to the NAWM regions, but

the density of OLs is constant among the different areas (**Fig. 29**). This sequence of OL damage is similar to the one observed in the animal model and supports the hypothesis that the most common demyelinating pattern in MS follows an outside-to-inside gradient. Lucchinetti et al. suggested that there is a profound heterogeneity in the immunopathological composition of the lesions, with the majority of the MS patients showing a “centripetal” damage, in which the autoimmune attack starts at the myelin level and later spreads towards the OLs bodies (pattern II), while in about 30% of MS cases the damage to oligodendroglia follows a “centrifugal” gradient where OLs death is the primary hallmark (pattern III) (*Lucchinetti et al., 2000; Lassman et al., 2001*) (**Fig. 32**). Albeit previous reports also describe a “variable” loss of OLs at the active lesion border with high number of OLs in the inactive plaque (*Lucchinetti et al., 2000; Popescu et al., 2013; Storch et al., 1998*), in my work there was no such difference.

Although we cannot exclude that some of the OLs observed within the lesion might be newly-formed OLs, no sign of OLs apoptosis or degeneration are seen in the area. This finding is in contrast with another study describing that the formation of new MS lesions always starts with OLs death, microglia activation but not macrophage infiltration, and no structural myelin alterations (so called “pre-phagocytic lesions”) (*Barnett and Prineas, 2004*). An interesting point to note is that in my data the density of Iba1+ cells is considerably higher in the lesions compared to NAWM areas, suggesting that not only resident microglia is activated but also a substantial number of macrophages has infiltrated the area. The fact that the lesions described in my study show an outside-to-inside gradient with prominent macrophages infiltration, indicates that they belong to the previously described patterns I or II (**Fig. 32**). In light of these results, the need to develop new treatments aimed to protect myelin from degeneration is emerged, though drugs focused on enhancing OPCs differentiation or promoting remyelination (benztropine, antibody against LINGO-1,

monoclonal IgM antibody 22, quetiapine, etc...) (Deshmukh et al., 2013; Mi et al., 2005; Warrington et al., 2007; Bi et al., 2012; Kremer et al., 2014), might still be useful at later stages of the disease when demyelination has already reached OLs somata.

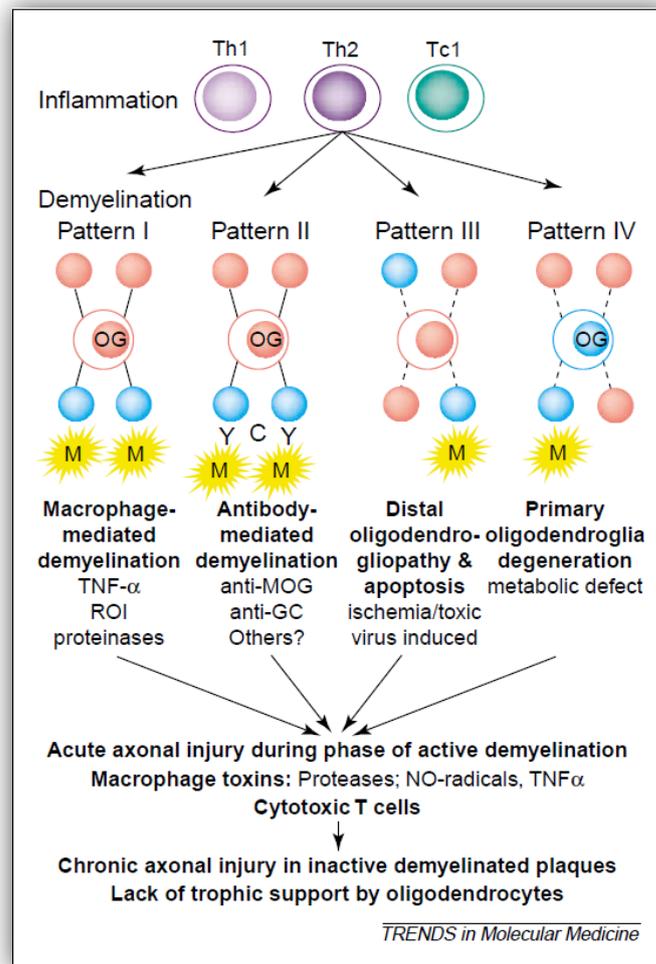


Figure 32 – Mechanisms involved in the formation of multiple sclerosis lesions. In active lesions, four distinct patterns can be distinguished: demyelination is induced by macrophages and their toxic factors (pattern I), by antibodies against myelin proteins and complement (pattern II), by distal oligodendroglial gliopathy followed by apoptosis (pattern III), or by primary OL death followed by myelin damage (pattern IV). Scheme taken from Lassman et al., 2001.

When I looked at the myelin sheaths in the MS biopsies at higher resolution using confocal microscopy, I observed myelin outfoldings that were similar to the myelinosomes described in the animal model lesions (**Fig. 30**). The density was particularly high in the lesion center and at the rim of the lesion, where demyelination is ongoing. Myelinosomes are also

detectable, although with a much lower frequency, in NAWM regions. This is not fully unexpected; in fact, even though they are supposed to be normal-looking areas, often NAWM appears mildly compromised in MS, showing astrogliosis, microglial activation, reduced myelin density and axonal loss (*Matthews et al., 1999; Allen et al., 1979; Allen et al., 2001*). Contrarily, when white matter areas from control patients not affected by demyelinating neurological diseases were analyzed, no signs of myelinosomes were found. This is consistent with the notion that in MS, the presence of myelin outfoldings is common and represents an early stage of demyelination. It is therefore crucial to study myelinosomes and the mechanisms that lead to their development, in order to interfere with the process and prevent demyelination.

In my experiments in the animal model I have studied the role of antibodies directed against MOG and found that they mediate myelinosome formation and consequent demyelination. Considering that my findings from the human samples share similarities with EAE in terms of the sequence of events leading to myelin destruction and morphology of myelin abnormalities, one could assume that similar molecular mechanisms may also be responsible for demyelination in MS. Antibodies against myelin proteins, particularly MOG, are found in the serum of MS patients and have been described to be implicated in demyelination in a subgroup of MS lesions (*Storch et al., 1998; Lucchinetti et al., 2000; Reindl et al., 2006*). Knowing which antibodies are involved in a specific disease is important not only to develop new therapeutic agents, but it can also be useful to diagnose and classify disease subtypes. In fact, the humoral response is critically involved in several inflammatory demyelinating CNS diseases, e.g. neuromyelitis optica (NMO) in which antibodies against aquaporin-4 are a characteristic and likely pathogenic component of the disease (*Lennon et al., 2005*). Although MOG is the best-characterized autoantigen, it cannot be excluded that antibodies in MS patients may also recognize other non-myelin proteins (such as KIR4.1, or antibodies to

paranodal proteins) (*Srivastava et al., 2012; Meinel et al., 2011*), therefore leading to secondary demyelination.

Patients affected by NMO benefit from B cells/antibody-targeted drugs which raises hopes that similar targeted treatment might be valuable also for the therapy of MS. At the moment, few similar approaches are used in the treatment of MS. Removal of pathogenic antibodies by plasma exchange has been proved efficacious in a subgroup of MS patients showing pattern II lesions during relapses (*Keegan et al., 2005*), while new drugs aimed to deplete B cells are now under consideration for the treatment of MS (i.e. Rituximab, Ocrelizumba, etc..) (*Krumbholz et al., 2012*). In addition to the already available agents, I hope that the results presented in this thesis will help to design more effective therapeutic strategies to protect myelin from immune attack e.g. by limiting the interaction between myelinosomes and phagocyte.

ACKNOWLEDGEMENTS

I have to admit it: there has been a time (actually, more than one...) during the past years when I thought that this day would never come! Well...here I am, writing the acknowledgements of my thesis and thanking everyone who has been part of this long ride.

*My first big “thank you” goes to **Prof. Martin Kerschensteiner**, who gave me the chance to be part of his outstanding team and work on such an interesting project. You have walked me through this journey and your true passion for science has always been an inspiration. Thank you for your precious advices, thank you for taking the time to talk to me and thank you for being such a good teacher!*

*Thanks to **Prof. Hans Straka**, my supervisor at the biology faculty, who took the time to discuss my work and showed interest in my research.*

*I want to truly thank also **Prof. Thomas Misgeld** for his important feedback and input at any time during my PhD.*

*I was lucky enough to work with amazing people!! So the next round of “thank you” is for my lab mates, former and current. From the bottom of my heart, many thanks to **all of you!!***

*Special mention to: **Ivana**, who is not only a good friend but she is also a fantastic scientist who taught me everything when I started! Thanks to my dear friend **Anne**: without you the past years would have not been so fun; I could have not asked for a better desk-mate! Thanks to **Anja**, for your help in the lab and for the ice-cream breaks! A big grazie goes to my Italian colleague **Beppe**, who is a friend, a good cook and also a talented scientist; thanks to **Cathy**, with whom I shared laughters and many stories over the past years! Big thank you to **Kris**, who helped to give my thesis a pretty look!*

*A big thanks goes to my friends outside the lab, in particular to **Clara, Giulia, Martina, Frido, Vale, Fabi, Laura, Vale, Viwi, Lore, Luca, Niky, Chiara, Cenzo, Miryam** and many others!!*

*Next round of thanks is for my family: thanks to my big **brothers** and my **sisters**, my beautiful nephews **Nicolò** and **Riccardo**, my grandmothers **Nonna Stella** and **Nonna Lucia**, and the biggest thank you to my fantastic **Mom and Dad**.*

*Thanks also to my new family, **Enzo** and **Vale**. A special thanks to my mother in-law **Gabriella**, we miss you!*

*It doesn't matter how far I live, you all are always with me, in my heart and in my thoughts!
Non importa se vivo lontano, tutti voi siete sempre con me, nel mio cuore e nei miei pensieri.*

*And the last, but without any doubts the most important “thank you”, is for my husband **Marco**. The past years haven't always been easy, but you were there for me every time I needed it. I could have not done it without your infinite love and support. I love you.*

BIBLIOGRAPHY

- Abdul-Majid, K., & Jirholt, J. (2000). Screening of several H-2 congenic mouse strains identified H-2 q mice as highly susceptible to MOG-induced EAE with minimal adjuvant requirement. *Journal of Neuroimmunology*, *111*(1-2), 23–33.
- Aboul-Enein, F., & Rauschka, H. (2003). Preferential loss of myelin-associated glycoprotein reflects hypoxia-like white matter damage in stroke and inflammatory brain diseases. *The Journal of Neuropathology & Experimental Neurology*, *62*(1), 25–33.
- Aggarwal, S., Snaidero, N., Pähler, G., Frey, S., Sánchez, P., Zweckstetter, M., ... Simons, M. (2013). Myelin membrane assembly is driven by a phase transition of myelin basic proteins into a cohesive protein meshwork. *PLoS Biology*, *11*(6), e1001577.
- Aguirre, A., Dupree, J. L., Mangin, J. M., & Gallo, V. (2007). A functional role for EGFR signaling in myelination and remyelination. *Nature Neuroscience*, *10*(8), 990–1002.
- Aguzzi, A., Barres, B. A., & Bennett, M. L. (2013). Microglia: scapegoat, saboteur, or something else? *Science*, *339*(6116), 156–161.
- Ajami, B., Bennett, J. L., Krieger, C., McNagny, K. M., & Rossi, F. M. V. (2011). Infiltrating monocytes trigger EAE progression, but do not contribute to the resident microglia pool. *Nature Neuroscience*, *14*(9), 1142–9.
- Albrecht, P., Bouchachia, I., Goebels, N., Henke, N., Hofstetter, H. H., Issberner, A., ... Methner, A. (2012). Effects of dimethyl fumarate on neuroprotection and immunomodulation. *Journal of Neuroinflammation*, *9*(1), 163.
- Allen, I. V., McQuaid, S., Mirakhur, M., & Nevin, G. (2001). Pathological abnormalities in the normal-appearing white matter in multiple sclerosis. *Neurological Sciences*, *22*(2), 141–144.
- Allen, I., & McKeown, S. (1979). A histological, histochemical and biochemical study of the macroscopically normal white matter in multiple sclerosis. *Journal of the Neurological Sciences*, (1977), 81–91.
- Amor, S., Smith, P. a., & Baker, D. (2005). Biozzi mice: Of mice and human neurological diseases. *Journal of Neuroimmunology*, *165*(1-2), 1–10.
- Ascherio, A., Munger, K. L., & Lünemann, J. D. (2012). The initiation and prevention of multiple sclerosis. *Nature Reviews. Neurology*, *8*(11), 602–612.
- Babbe, H., Roers, A., Waisman, A., Lassmann, H., Goebles, N., Hohlfeld, R., Friese, M., Schröder, R., Deckert, M., Schmidt, S., Ravid, R., & Rajewsky, K. (2000). Clonal expansions of CD8+ T cells dominate the T cell infiltrate in active multiple sclerosis lesions as shown by micromanipulation and single cell polymerase chain. *The Journal of Experimental Medicine*, *192*(3), 393-404.

- Baker, D., O'Neill, J. K., Gschmeissner, S. E., Wilcox, C. E., Butter, C., & Turk, J. L. (1990). Induction of chronic relapsing experimental allergic encephalomyelitis in Biozzi mice. *Journal of Neuroimmunology*, 28(3), 261–270.
- Baloh, R. H., Schmidt, R. E., Pestronk, A., & Milbrandt, J. (2007). Altered axonal mitochondrial transport in the pathogenesis of Charcot-Marie-Tooth disease from mitofusin 2 mutations. *The Journal of Neuroscience: The Official Journal of the Society for Neuroscience*, 27(2), 422–30.
- Barnett, M. H., & Prineas, J. W. (2004). Relapsing and remitting multiple sclerosis: pathology of the newly forming lesion. *Annals of Neurology*, 55(4), 458–68.
- Barnett, M. H., Parratt, J. D., Cho, E. S., & Prineas, J. W. (2009). Immunoglobulins and complement in postmortem multiple sclerosis tissue. *Annals of Neurology*, 65(1), 32–46.
- Barten, L. J., Allington, D. R., Procacci, K. a., & Rivey, M. P. (2010). New approaches in the management of multiple sclerosis. *Drug Design, Development and Therapy*, 4, 343–366.
- Bartholomäus, I., Kawakami, N., Odoardi, F., Schläger, C., Miljkovic, D., Ellwart, J. W., ... Flügel, A. (2009). Effector T cell interactions with meningeal vascular structures in nascent autoimmune CNS lesions. *Nature*, 462(7269), 94–8.
- Bashir, K., & Whitaker, J. (1998). Current immunotherapy in multiple sclerosis. *Immunology and Cell Biology*, 55–64.
- Baumann, N., & Pham-Dinh, D. (2001). Biology of oligodendrocyte and myelin in the mammalian central nervous system. *Physiological Reviews*, 81(2), 871–928.
- Baxter, A. (2007). The origin and application of experimental autoimmune encephalomyelitis. *Nature Reviews Immunology*, 7(November), 96–99.
- Becher, B., & Antel, J. P. (1996). Comparison of phenotypic and functional properties of immediately ex vivo and cultured human adult microglia. *Glia*, 18(1), 1–10.
- Berard, J. L., Wolak, K., Fournier, S., & David, S. (2010). Characterization of relapsing-remitting and chronic forms of experimental autoimmune encephalomyelitis in C57BL/6 mice. *Glia*, 58(4), 434–445.
- Berer, K., Wekerle, H., & Krishnamoorthy, G. (2011). B cells in spontaneous autoimmune diseases of the central nervous system. *Molecular Immunology*, 48(11), 1332–1337.
- Bi, X., Zhang, Y., Yan, B., Fang, S., He, J., Zhang, D., ... Li, X.-M. (2012). Quetiapine prevents oligodendrocyte and myelin loss and promotes maturation of oligodendrocyte progenitors in the hippocampus of global cerebral ischemia mice. *Journal of Neurochemistry*, 123(1), 14–20.
- Bielekova, B. (2006). Regulatory CD56bright natural killer cells mediate immunomodulatory effects of IL-2R α -targeted therapy (daclizumab) in multiple sclerosis. *Proceedings of the National Academy of Sciences of the United States of America* 103(15), 5941–5946.

- Biozzi, G., Stiffel, C., Mouton, D., Bouthillier, Y., Decreusefond, C., (1972). Cytodynamics of the immune response in two lines of mice genetically selected for “high” and “low” antibody synthesis. *Journal of Experimental Medicine*, *135*, 1071– 1094.
- Bishop, D., Nikić, I., Brinkoetter, M., Knecht, S., Potz, S., Kerschensteiner, M., & Misgeld, T. (2011). Near-infrared branding efficiently correlates light and electron microscopy. *Nature Methods*, *8*(7), 568–70.
- Bitan, M., Weiss, L., Reibstein, I., Zeira, M., Fellig, Y., Slavin, S., ... Vlodavsky, I. (2010). Heparanase upregulates Th2 cytokines, ameliorating experimental autoimmune encephalitis. *Molecular Immunology*, *47*(10), 1890–1898.
- Bitsch, A., Schuchardt, J., Bunkowski, S., Kuhlmann, T., & Bru, W. (2000). Acute axonal injury in multiple sclerosis. Correlation with demyelination and inflammation. *Brain*, *123*, 1174–1183.
- Bolino, A., Bolis, A., Previtali, S. C., Dina, G., Bussini, S., Dati, G., ... Wrabetz, L. (2004). Disruption of Mtmr2 produces CMT4B1-like neuropathy with myelin unfolding and impaired spermatogenesis. *The Journal of Cell Biology*, *167*(4), 711–21.
- Botto, M., Dell’Agnola, C., & Bygrave, A. (1998). Homozygous C1q deficiency causes glomerulonephritis associated with multiple apoptotic bodies. *Nature Genetics*, *19*(1), 56-9.
- Breckwoldt, M. O., Pfister, F. M. J., Bradley, P. M., Marinković, P., Williams, P. R., Brill, M. S., ... Misgeld, T. (2014). Multiparametric optical analysis of mitochondrial redox signals during neuronal physiology and pathology in vivo. *Nature Medicine*, *20*(5), 555–60.
- Breij, E. C., Heijnen, P., Vloet, R., Saito, T., van der Winkel, J. G., Dijkstra, C. D., Amor, S., & Verbeek, S. (2005). The FcRgamma chain is not essential for induction of experimental allergic encephalomyelitis (EAE) or anti-myelin antibody-mediated exacerbation of EAE. *The Journal of Neuropathology & Experimental Neurology*, *64*(4), 304-11.
- Brimnes, M. K., Hansen, B. E., Nielsen, L. K., Dziegiel, M. H., & Nielsen, C. H. (2014). Uptake and presentation of myelin basic protein by normal human B cells. *PloS One*, *9*(11), e113388.
- Bunge, M., Bunge, R., & Ris, H. (1961). Ultrastructural study of remyelination in an experimental lesion in adult cat spinal cord. *The Journal of Biophysical and Biochemical cytology*, *10*, 67-94.
- Busche, M., Eichhoff, G., & Adelsberger, H. (2008). Clusters of hyperactive neurons near amyloid plaques in a mouse model of Alzheimer’s disease. *Science*, *321*(5896), 1686-9.
- Caprariello, A. V., Mangla, S., Miller, R. H., & Selkirk, S. M. (2012). Apoptosis of oligodendrocytes in the central nervous system results in rapid focal demyelination. *Annals of Neurology*, *72*(3), 395–405.

- Carrithers, M. D. (2014). Update on Disease-Modifying Treatments for Multiple Sclerosis. *Clinical Therapeutics*, 1–8.
- Carson, M. J. (2002). Microglia as liaisons between the immune and central nervous systems: functional implications for multiple sclerosis. *Glia*, 40(2), 218–231.
- Chalfie, M., Tu, Y., Euskirchen, G., Ward, W., & Prasher, D. (1994). Green fluorescent protein as a marker for gene expression. *Science*, 263(5148), 802–5.
- Chen, H., Assmann, J., & Krenz, A. (2014). Hydroxycarboxylic acid receptor 2 mediates dimethyl fumarate's protective effect in EAE. *The Journal of Clinical Investigation*, 124(5), 4–8.
- Clanet, M. (2008). The neurology of Jean Cruveilhier. *Medical History*, 17, 343–355.
- Cohen, J., & Barkhof, F., Comi, G., Hartung, H.P., ... Kappos, L. (2010). Oral fingolimod or intramuscular interferon for relapsing multiple sclerosis. *The New England Journal of Medicine*, 362(5), 405–415.
- Coles, A. (2009). Multiple sclerosis. *Practical Neurology*, 9(2), 118–26.
- Compston, A., & Coles, A. (2008). Multiple sclerosis. *Lancet*, 372(9648), 1502–1517.
- Cosburn, M., Pace, a a, Jones, J., Ali, R., Ingram, G., Baker, K., ... Robertson, N. P. (2011). Autoimmune disease after alemtuzumab treatment for multiple sclerosis in a multicenter cohort. *Neurology*, 77(6), 573–579.
- Cua, D., Sherlock, J., Chen, Y., & Murphy, C. (2003). Interleukin-23 rather than interleukin-12 is the critical cytokine for autoimmune inflammation of the brain. *Nature*, 421(February), 9–13.
- Dailey, M. E., & Waite, M. (1999). Confocal imaging of microglial cell dynamics in hippocampal slice cultures. *Methods (San Diego, Calif.)*, 18(2), 222–30, 177.
- Davalos, D., & Akassoglou, K. (2012). In vivo imaging of the mouse spinal cord using two-photon microscopy. *Journal of Visualized Experiments : JoVE*, (59), e2760.
- Davalos, D., Lee, J. K., Smith, W. B., Brinkman, B., Ellisman, M. H., Zheng, B., & Akassoglou, K. (2008). Stable in vivo imaging of densely populated glia, axons and blood vessels in the mouse spinal cord using two-photon microscopy. *Journal of Neuroscience Methods*, 169(1), 1–7.
- De Graaf, K. L., Albert, M., & Weissert, R. (2012). Autoantigen conformation influences both B- and T-cell responses and encephalitogenicity. *The Journal of Biological Chemistry*, 287(21), 17206–13.
- De Sandre-Giovannoli, a, Delague, V., Hamadouche, T., Chaouch, M., Krahn, M., Boccaccio, I., ... Lévy, N. (2005). Homozygosity mapping of autosomal recessive demyelinating Charcot-Marie-Tooth neuropathy (CMT4H) to a novel locus on chromosome 12p11.21-q13.11. *Journal of Medical Genetics*, 42(3), 260–5.

- Deng, B., Wehling-Henricks, M., Villalta, S. A., Wang, Y., & Tidball, J. G. (2012). IL-10 triggers changes in macrophage phenotype that promote muscle growth and regeneration. *Journal of Immunology*, *189*(7), 3669–3680.
- Denk, W., Strickler, J., & Webb, W. (1990). Two-photon laser scanning fluorescence microscopy. *Science*, (April), 73–76.
- Derfuss, T., & Meinl, E. (2012). Identifying autoantigens in demyelinating diseases: valuable clues to diagnosis and treatment? *Current Opinion in Neurology*, *25*(3), 231–8.
- Derfuss, T., Parikh, K., & Velhin, S. (2009). Contactin-2/TAG-1-directed autoimmunity is identified in multiple sclerosis patients and mediates gray matter pathology in animals. *Proceedings of the National Academy of Sciences of the United States of America*, *106*(20), 8302-7.
- Deshmukh, V. a, Tardif, V., Lyssiotis, C. a, Green, C. C., Kerman, B., Kim, H. J., ... Lairson, L. L. (2013). A regenerative approach to the treatment of multiple sclerosis. *Nature*, *502*(7471), 327–32.
- Dhib-Jalbut, S. (2002). Mechanisms of action of interferons and glatiramer acetate in multiple sclerosis. *Neurology*, *58*, S3-9.
- Diaspro, A., Bianchini, P., Vicidomini, G., Faretta, M., Ramoino, P., & Usai, C. (2006). Multi-photon excitation microscopy. *Biomedical Engineering Online*, *5*, 36.
- Dittel, B. N. (2008). CD4 T cells: Balancing the coming and going of autoimmune-mediated inflammation in the CNS. *Brain, Behavior, and Immunity*, *22*(4), 421–430.
- Dittel, B. N., Urbania, T. H., & Janeway, C. a. (2000). Relapsing and remitting experimental autoimmune encephalomyelitis in B cell deficient mice. *Journal of Autoimmunity*, *14*(4), 311–8.
- Dray, C., Rougon, G., & Debarbieux, F. (2009). Quantitative analysis by in vivo imaging of the dynamics of vascular and axonal networks in injured mouse spinal cord. *Proceedings of the National Academy of Sciences of the United States of America*, *106*(23), 9459–64.
- Duffy, S. S., Lees, J. G., & Moalem-Taylor, G. (2014). The Contribution of Immune and Glial Cell Types in Experimental Autoimmune Encephalomyelitis and Multiple Sclerosis. *Multiple Sclerosis International*, *2014*, 1–17.
- Ebbing, B., Mann, K., Starosta, A., Jaud, J., Schöls, L., Schüle, R., & Woehlke, G. (2008). Effect of spastic paraplegia mutations in KIF5A kinesin on transport activity. *Human Molecular Genetics*, *17*(9), 1245–52.
- Egg, R., Reindl, M., Deisenhammer, F., Linington, C., & Berger, T. (2001). Anti-MOG and anti-MBP antibody subclasses in multiple sclerosis. *Multiple Sclerosis*, *7*(5), 285–289.

- Elder, G. a, Friedrich, V. L., & Lazzarini, R. a. (2001). Schwann cells and oligodendrocytes read distinct signals in establishing myelin sheath thickness. *Journal of Neuroscience Research*, 65(6), 493–9.
- Emery, B. (2010). Regulation of oligodendrocyte differentiation and myelination. *Science*, 330(November), 779–783.
- Emery, B. (2010). Regulation of oligodendrocyte differentiation and myelination. *Science*, 330(November), 779–783.
- Ertürk, A., HELLAL, F., Enes, J., & Bradke, F. (2007). Disorganized microtubules underlie the formation of retraction bulbs and the failure of axonal regeneration. *The Journal of Neuroscience : The Official Journal of the Society for Neuroscience*, 27(34), 9169–80.
- Etessami, R. (2000). Spread and pathogenic characteristics of a G-deficient rabies virus recombinant: an in vitro and in vivo study. *Journal of General Virology*, 2147–2153.
- Fabrizi, G., Taioli, F., Cavallaro, T., & Ferrari, S. (2009). Further evidence that mutations in FGD4/frabin cause Charcot-Marie-Tooth disease type 4H. *Neurology*, 1160–1165.
- Fancy, S. P. J., Kotter, M. R., Harrington, E. P., Huang, J. K., Zhao, C., Rowitch, D. H., & Franklin, R. J. M. (2010). Overcoming remyelination failure in multiple sclerosis and other myelin disorders. *Experimental Neurology*, 225(1), 18–23.
- Fancy, S. P. J., Zhao, C., & Franklin, R. J. M. (2004). Increased expression of Nkx2.2 and Olig2 identifies reactive oligodendrocyte progenitor cells responding to demyelination in the adult CNS. *Molecular and Cellular Neurosciences*, 27(3), 247–54.
- Farrar, M. J., Bernstein, I. M., Schlafer, D. H., Cleland, T. a, Fetcho, J. R., & Schaffer, C. B. (2012). Chronic in vivo imaging in the mouse spinal cord using an implanted chamber. *Nature Methods*, 9(3), 297–302.
- Feng, G., Mellor, R. H., Bernstein, M., Keller-Peck, C., Nguyen, Q. T., Wallace, M., ... Sanes, J. R. (2000). Imaging Neuronal Subsets in Transgenic Mice Expressing Multiple Spectral Variants of GFP. *Neuron*, 28(1), 41–51.
- Fenrich, K. K., Weber, P., Hocine, M., Zalc, M., Rougon, G., & Debarbieux, F. (2012). Long-term in vivo imaging of normal and pathological mouse spinal cord with subcellular resolution using implanted glass windows. *The Journal of Physiology*, 590(Pt 16), 3665–75.
- Fillatreau, S., Sweenie, C. H., McGeachy, M. J., Gray, D., & Anderton, S. M. (2002). B cells regulate autoimmunity by provision of IL-10. *Nature Immunology*, 3(10), 944–950.
- Firth, D. (1948). The case of Augustus D' Este. *Cambridge University Press*.
- Flamm, E. (1973). Jean Martin Charcot. *The International MS Journal*, 15, 59–61.
- Franklin, R. J. M., & Ffrench-Constant, C. (2008). Remyelination in the CNS: from biology to therapy. *Nature Reviews. Neuroscience*, 9(11), 839–55.

- Franklin, R. J. M., & Gallo, V. (2014). The translational biology of remyelination: past, present, and future. *Glia*, 62(11), 1905–15.
- Freund, J., Stern, E., & Pisani, T. (1947). Isoallergic encephalomyelitis and radiculitis in guinea pigs after one injection of brain and Mycobacteria in water-in-oil emulsion. *Journal of Immunology*, 57(2), 179-194.
- Friede, R. L. & Samorajski, T. (1967). Relation between the number of myelin lamellae and axon circumference in fibers of vagus and sciatic nerves of mice. *The Journal of the Comparative Neurology*, 130(3), 223-31.
- Fritzsching, B., Haas, J., König, F., Kunz, P., Fritzsching, E., Pöschl, J., ... Wildemann, B. (2011). Intracerebral human regulatory T cells: analysis of CD4+ CD25+ FOXP3+ T cells in brain lesions and cerebrospinal fluid of multiple sclerosis patients. *PloS One*, 6(3), e17988.
- Fu, Y., Sun, W., Shi, Y., Shi, R., & Cheng, J.-X. (2009). Glutamate excitotoxicity inflicts paranodal myelin splitting and retraction. *PloS One*, 4(8), e6705.
- Fuhrmann, M., Bittner, T., Jung, C. K. E., Burgold, S., Page, R. M., Mitteregger, G., ... Herms, J. (2010). Microglial Cx3cr1 knockout prevents neuron loss in a mouse model of Alzheimer's disease. *Nature Neuroscience*, 13(4), 411–3.
- Fünfschilling, U., Supplie, L. M., Mahad, D., Boretius, S., Saab, A. S., Edgar, J., ... Nave, K.-A. (2012). Glycolytic oligodendrocytes maintain myelin and long-term axonal integrity. *Nature*, 485(7399), 517–21.
- Genain, C. P., Nguyen, M., Letvin, N. L., Pearl, R., Davis, R. L., Adelman, M., ... Hauser, S. L. (1995). Rapid Publication Antibody Facilitation of Multiple Sclerosis like Lesions in a Nonhuman Primate. *Journal of Clinical Investigation*, 96, 2966–2974.
- Grienberger, C., & Konnerth, A. (2012). Imaging calcium in neurons. *Neuron*, 73(5), 862–85.
- Groves, A., Barnett, S., & Franklin, R. (1993). Repair of demyelinated lesions by transplantation of purified 0-2A progenitor cells. *Nature*, 362(6419), 453-5.
- Grutzendler, J., Kasthuri, N., & Gan, W. (2002). Long-term dendritic spine stability in the adult cortex. *Nature*, 420(6917), 812-6.
- Hadas, S., Spira, M., Hanisch, U.-K., Reichert, F., & Rotshenker, S. (2012). Complement receptor-3 negatively regulates the phagocytosis of degenerated myelin through tyrosine kinase Syk and cofilin. *Journal of Neuroinflammation*, 9(1), 166.
- Haider, L., Fischer, M. T., Frischer, J. M., Bauer, J., Höftberger, R., Botond, G., ... Lassmann, H. (2011). Oxidative damage in multiple sclerosis lesions. *Brain*, 134(Pt 7), 1914–24.
- Hamann, I., Dörr, J., Glumm, R., Chanvillard, C., Janssen, A., Millward, J. M., ... Infante-Duarte, C. (2013). Characterization of natural killer cells in paired CSF and blood samples during neuroinflammation. *Journal of Neuroimmunology*, 254(1-2), 165–169.

- Hauser, S. L., & Oksenberg, J. R. (2006). The neurobiology of multiple sclerosis: genes, inflammation, and neurodegeneration. *Neuron*, *52*(1), 61–76.
- Helmchen, F., & Denk, W. (2005). Deep tissue two-photon microscopy. *Nature Methods*, *2*(12), 932–40.
- Helmchen, F., & Waters, J. (2002). Ca²⁺ imaging in the mammalian brain in vivo. *European Journal of Pharmacology*, *447*, 119–129.
- Hirrlinger, P. G., Scheller, A., Braun, C., Quintela-Schneider, M., Fuss, B., Hirrlinger, J., & Kirchhoff, F. (2005). Expression of reef coral fluorescent proteins in the central nervous system of transgenic mice. *Molecular and Cellular Neurosciences*, *30*(3), 291–303.
- Hochreiter-hufford, A., & Ravichandran, K. S. (2013). Clearing the dead: apoptotic cell sensing, recognition, engulfment, and digestion. *Cold Spring Harbor perspectives in biology*, *5*(1), a008748.
- Hogarth, P. M., & Pietersz, G. a. (2012). Fc receptor-targeted therapies for the treatment of inflammation, cancer and beyond. *Nature Reviews. Drug Discovery*, *11*(4), 311–31.
- Holtmaat, A., Bonhoeffer, T., Chow, D. K., Chuckowree, J., De Paola, V., Hofer, S. B., ... Wilbrecht, L. (2009). Long-term, high-resolution imaging in the mouse neocortex through a chronic cranial window. *Nature Protocols*, *4*(8), 1128–44.
- Horn, M., Baumann, R., Pereira, J. a, Sidiropoulos, P. N. M., Somandin, C., Welzl, H., ... Suter, U. (2012). Myelin is dependent on the Charcot-Marie-Tooth Type 4H disease culprit protein FRABIN/FGD4 in Schwann cells. *Brain: A Journal of Neurology*, *135*(Pt 12), 3567–83.
- Howng, S. Y. B., Avila, R. L., Emery, B., Traka, M., Lin, W., Watkins, T., ... Popko, B. (2010). ZFP191 is required by oligodendrocytes for CNS myelination. *Genes & Development*, *24*(3), 301–11.
- Huang, J. K., Jarjour, A. a, Nait Oumesmar, B., Kerninon, C., Williams, A., Krezel, W., ... Franklin, R. J. M. (2011). Retinoid X receptor gamma signaling accelerates CNS remyelination. *Nature Neuroscience*, *14*(1), 45–53.
- Hughes, E. G., Kang, S. H., Fukaya, M., & Bergles, D. E. (2013). Oligodendrocyte progenitors balance growth with self-repulsion to achieve homeostasis in the adult brain. *Nature Neuroscience*, *16*(6), 668–76.
- Huitinga, I. (1993). Treatment with anti-CR3 antibodies ED7 and ED8 suppresses experimental allergic encephalomyelitis in Lewis rats. *European Journal of Immunology*, *23*(3), 709–715.
- Huitinga, I., & Rooijen, N. Van. (1990). Suppression of experimental allergic encephalomyelitis in Lewis rats after elimination of macrophages. *The Journal of Experimental Medicine*, *172*(4), 1025-33.

- Hundgeburth, L. C., Wunsch, M., Rovituso, D., Recks, M. S., Addicks, K., Lehmann, P. V., & Kuerten, S. (2013). The complement system contributes to the pathology of experimental autoimmune encephalomyelitis by triggering demyelination and modifying the antigen-specific T and B cell response. *Clinical Immunology (Orlando, Fla.)*, *146*(3), 155–64.
- Huseby, E., Liggitt, D., & Brabb, T. (2001). A pathogenic role for myelin-specific CD8+ T cells in a model for multiple sclerosis. *The Journal of Experimental Medicine*, *194*(5), 669–676.
- Ingram, G., Hakobyan, S., Robertson, N. P., & Morgan, B. P. (2009). Complement in multiple sclerosis: its role in disease and potential as a biomarker. *Clinical and Experimental Immunology*, *155*(2), 128–39.
- Innes, J. R. M. (1951). Experimental allergic encephalitis: attempts to produce the disease in sheep and goats. *Journal of Comparative Pathology*, *61*, 241–250.
- Irvine, K. a, & Blakemore, W. F. (2008). Remyelination protects axons from demyelination-associated axon degeneration. *Brain : A Journal of Neurology*, *131*(Pt 6), 1464–77.
- Jäger, A., Dardalhon, V., Sobel, R. a, Bettelli, E., & Kuchroo, V. K. (2009). Th1, Th17, and Th9 effector cells induce experimental autoimmune encephalomyelitis with different pathological phenotypes. *Journal of Immunology*, *183*(11), 7169–7717.
- Johannssen, H. C., & Helmchen, F. (2010). In vivo Ca²⁺ imaging of dorsal horn neuronal populations in mouse spinal cord. *The Journal of Physiology*, *588*(Pt 18), 3397–402.
- Johnson, E., & Ludwin, S. (1981). Evidence for a “dying-back” gliopathy in demyelinating disease. *Annals of Neurology*, *9*(3), 301–305.
- Jung, S., & Aliberti, J. (2000). Analysis of fractalkine receptor CX3CR1 function by targeted deletion and green fluorescent protein reporter gene insertion. *Molecular and Cellular Biology*, *20*(11), 4106–4114.
- Jurynczyk, M., Jurewicz, A., Bielecki, B., Raine, C. S., & Selmaj, K. (2005). Inhibition of Notch signaling enhances tissue repair in an animal model of multiple sclerosis. *Journal of Neuroimmunology*, *170*(1-2), 3–10.
- Juurlink, B., Thorburne, S., & Hertz, L. (1998). Peroxide-scavenging deficit underlies oligodendrocyte susceptibility to oxidative stress. *Glia*, *22*(4), 371–378.
- Karram, K., Goebbels, S., Schwab, M., Jennissen, K., Seifert, G., Steinhäuser, C., ... Trotter, J. (2008). NG2-expressing cells in the nervous system revealed by the NG2-EYFP-knockin mouse. *Genesis (New York, N.Y. : 2000)*, *46*(12), 743–57.
- Kebir, H., Kreymborg, K., Ifergan, I., Dodelet-Devillers, A., Cayrol, R., Bernard, M., ... Prat, A. (2007). Human TH17 lymphocytes promote blood-brain barrier disruption and central nervous system inflammation. *Nature Medicine*, *13*(10), 1173–1175.

- Keegan, M., König, F., McClelland, R., & Brück, W. (2005). Relation between humoral pathological changes in multiple sclerosis and response to therapeutic plasma exchange. *The Lancet*, 579–582.
- Kerschensteiner, M., Schwab, M. E., Lichtman, J. W., & Misgeld, T. (2005). In vivo imaging of axonal degeneration and regeneration in the injured spinal cord. *Nature Medicine*, 11(5), 572–7.
- Kishore, U., & Reid, K. (2000). C1q: structure, function, and receptors. *Immunopharmacology*, 49, 159–170.
- Kleinschmidt-DeMasters, B.K., Tyler, K.L. (2005). Progressive multifocal leukoencephalopathy complicating treatment with natalizumab and interferon beta-1a for multiple sclerosis. *The New England Journal of Medicine*, 353(4), 369-374.
- Kornek, B., Storch, M. K., Weissert, R., Wallstroem, E., Stefferl, a, Olsson, T., ... Lassmann, H. (2000). Multiple sclerosis and chronic autoimmune encephalomyelitis: a comparative quantitative study of axonal injury in active, inactive, and remyelinated lesions. *The American Journal of Pathology*, 157(1), 267–76.
- Körner, H., & Goodsall, A. (1995). Autoreactive T-cell traffic within the central nervous system during tumor necrosis factor receptor-mediated inhibition of experimental autoimmune encephalomyelitis. *Proceedings of the National Academy of Sciences of the United States of America*, 92(24), 11066–11070.
- Kremer, D., Förster, M., Schichel, T., Göttle, P., Hartung, H.-P., Perron, H., & Küry, P. (2014). The neutralizing antibody GNbAC1 abrogates HERV-W envelope protein-mediated oligodendroglial maturation blockade. *Multiple Sclerosis (Houndmills, Basingstoke, England)*, 1–4.
- Kreutzberg, G. (1996). Microglia: a sensor for pathological events in the CNS. *Trends in Neurosciences*, 2236, 471–474.
- Krishnamoorthy, G. (2006). Spontaneous opticospinal encephalomyelitis in a double-transgenic mouse model of autoimmune T cell/B cell cooperation. *Journal of Clinical Investigations*, 116(9), 2385–2392.
- Krishnamoorthy, G., & Wekerle, H. (2009). EAE: an immunologist's magic eye. *European Journal of Immunology*, 39(8), 2031–5.
- Krumbholz, M., Derfuss, T., Hohlfeld, R., Meinl, E. (2012). B cells and antibodies in multiple sclerosis pathogenesis and therapy. *Nature Reviews. Neurology*, 8(11), 613–23.
- Kuchibhotla, K., Goldman, S., & Lattarulo, C. (2008). A β plaques lead to aberrant regulation of calcium homeostasis in vivo resulting in structural and functional disruption of neuronal networks. *Neuron*, 59(2), 214–225.
- Kuhlmann, T., Lingfeld, G., & Bitsch, A. (2002). Acute axonal damage in multiple sclerosis is most extensive in early disease stages and decreases over time. *Brain*, 2202–2212.

- Lassmann, H., Brück, W., Lucchinetti, C. (2001). Heterogeneity of multiple sclerosis pathogenesis: implications for diagnosis and therapy. *Trends in Molecular medicine*, 7(3), 115-121.
- Lee, J., Gravel, M., Zhang, R., Thibault, P., & Braun, P. E. (2005). Process outgrowth in oligodendrocytes is mediated by CNP, a novel microtubule assembly myelin protein. *The Journal of Cell Biology*, 170(4), 661-73.
- Lee, Y., Morrison, B. M., Li, Y., Lengacher, S., Farah, M. H., Hoffman, P. N., ... Rothstein, J. D. (2012). Oligodendroglia metabolically support axons and contribute to neurodegeneration. *Nature*, 487(7408), 443-8.
- Lennon, V. a, Kryzer, T. J., Pittock, S. J., Verkman, a S., & Hinson, S. R. (2005). IgG marker of optic-spinal multiple sclerosis binds to the aquaporin-4 water channel. *The Journal of Experimental Medicine*, 202(4), 473-7.
- Leone, D. P., Genoud, S. téphan., Atanasoski, S., Grausenburger, R., Berger, P., Metzger, D., ... Suter, U. (2003). Tamoxifen-inducible glia-specific Cre mice for somatic mutagenesis in oligodendrocytes and Schwann cells. *Molecular and Cellular Neuroscience*, 22(4), 430-440.
- Linington, C., & Bradl, M. (1988). Augmentation of demyelination in rat acute allergic encephalomyelitis by circulating mouse monoclonal antibodies directed against a myelin/oligodendrocyte. *The American Journal of Pathology*, 130(3), 443-54.
- Lisak, R. P., Benjamins, J. a, Nedelkoska, L., Barger, J. L., Ragheb, S., Fan, B., ... Bar-Or, A. (2012). Secretory products of multiple sclerosis B cells are cytotoxic to oligodendroglia in vitro. *Journal of Neuroimmunology*, 246(1-2), 85-95.
- Litzenburger, T., & Fässler, R. (1998). B lymphocytes producing demyelinating autoantibodies: development and function in gene-targeted transgenic mice. *The Journal of Experimental Medicine*, 188(1), 169-80.
- Liu, C., Li, Y., Yu, J., Feng, L., Hou, S., Liu, Y., ... Ma, C. (2013). Targeting the shift from M1 to M2 macrophages in experimental autoimmune encephalomyelitis mice treated with fasudil. *PloS One*, 8(2), e54841.
- Locatelli, G., Wörtge, S., Buch, T., Ingold, B., Frommer, F., Sobottka, B., ... Becher, B. (2012). Primary oligodendrocyte death does not elicit anti-CNS immunity. *Nature Neuroscience*, 15(4), 543-50.
- Lock, C., Hermans, G., & Pedotti, R. (2002). Gene-microarray analysis of multiple sclerosis lesions yields new targets validated in autoimmune encephalomyelitis. *Nature Medicine*, 8(5).
- Lublin, F. D., Reingold, S. C., Cohen, J. a, Cutter, G. R., Sørensen, P. S., Thompson, A. J., ... Polman, C. H. (2014). Defining the clinical course of multiple sclerosis: The 2013 revisions. *Neurology*, 83(3), 278-286.

- Lucchinetti, C. F., Brück, W., Rodriguez, M., & Lassmann, H. (1996). Distinct patterns of multiple sclerosis pathology indicates heterogeneity on pathogenesis. *Brain Pathology*, 6(3), 259–274.
- Lucchinetti, C., Bruck, W., Parisi, J., .., Lassmann, H. (2000). Heterogeneity of multiple sclerosis lesions: implications for the pathogenesis of demyelination. *Annals of Neurology*, 47(6), 707–717.
- Luessi, F., Kuhlmann, T., & Zipp, F. (2014). Remyelinating strategies in multiple sclerosis. *Expert Review of Neurotherapeutics*, 14(11), 1315–34.
- Lumsden, C. (1971). The immunogenesis of the multiple sclerosis plaque. *Brain Research*, 28, 365–390.
- Lyons, J. a, San, M., Happ, M. P., & Cross, a H. (1999). B cells are critical to induction of experimental allergic encephalomyelitis by protein but not by a short encephalitogenic peptide. *European Journal of Immunology*, 29(11), 3432–9.
- Mallon, B., & Shick, H. (2002). Proteolipid promoter activity distinguishes two populations of NG2-positive cells throughout neonatal cortical development. *The Journal of Neuroscience*, 22(3), 876–885.
- Marriott, J. J., & Miyasaki, J. M. (2010). Evidence Report: The efficacy and safety of mitoxantrone (Novantrone) in the treatment of multiple sclerosis. *Neurology*, 74(18), 1463-1470.
- Martínez-Rodríguez, J. E., López-Botet, M., Munteis, E., Rio, J., Roquer, J., Montalban, X., & Comabella, M. (2011). Natural killer cell phenotype and clinical response to interferon-beta therapy in multiple sclerosis. *Clinical Immunolog*, 141(3), 348–356.
- Mathey, E. K., Derfuss, T., Storch, M. K., Williams, K. R., Hales, K., Woolley, D. R., ... Linington, C. (2007). Neurofascin as a novel target for autoantibody-mediated axonal injury. *The Journal of Experimental Medicine*, 204(10), 2363–72.
- Matute, C., Alberdi, E., & Domercq, M. (2001). The link between excitotoxic oligodendroglial death and demyelinating diseases. *Trends in Neurosciences*, 24(4), 173–177.
- Matute, C., Torre, I., Pérez-Cerdá, F., Pérez-Samartín, A., Alberdi, E., Etxebarria, E., ... Domercq, M. (2007). P2X(7) receptor blockade prevents ATP excitotoxicity in oligodendrocytes and ameliorates experimental autoimmune encephalomyelitis. *The Journal of Neuroscience*, 27(35), 9525–33.
- Mauri, C., Gray, D., Mushtaq, N., & Londei, M. (2003). Prevention of Arthritis by Interleukin 10-producing B Cells. *Journal of Experimental Medicine*, 197(4), 489–501.
- McKenzie, W. (1840). A practical treatise on Diseases of the Eye. *Ed3 London, Longman*.
- McTigue, D. M., & Tripathi, R. B. (2008). The life, death, and replacement of oligodendrocytes in the adult CNS. *Journal of Neurochemistry*, 107(1), 1–19.

- Mebatsion, T., König, M., & Conzelmann, K. (1996). Budding of rabies virus particles in the absence of the spike glycoprotein. *Cell*, *84*(M), 941–951.
- Meinl, E. (2011). Untapped targets in multiple sclerosis. *Journal of the Neurological Sciences*, *311 Suppl 1*, S12–5.
- Mi, S., Miller, R. H., Lee, X., Scott, M. L., Shulag-Morskaya, S., Shao, Z., ... Pepinsky, R. B. (2005). LINGO-1 negatively regulates myelination by oligodendrocytes. *Nature Neuroscience*, *8*(6), 745–51.
- Mikita, J., Dubourdieu-Cassagno, N., Deloire, M. S., Vekris, A., Biran, M., Raffard, G., ... Petry, K. G. (2011). Altered M1/M2 activation patterns of monocytes in severe relapsing experimental rat model of multiple sclerosis. Amelioration of clinical status by M2 activated monocyte administration. *Multiple Sclerosis*, *17*(1), 2–15.
- Millecamps, S., & Julien, J.-P. (2013). Axonal transport deficits and neurodegenerative diseases. *Nature Reviews. Neuroscience*, *14*(3), 161–76.
- Milo, R., & Miller, A. (2014). Revised diagnostic criteria of multiple sclerosis. *Autoimmunity Reviews*, *13*(4-5), 518–524.
- Miron, V. E., Boyd, A., Zhao, J.-W., Yuen, T. J., Ruckh, J. M., Shadrach, J. L., ... ffrench-Constant, C. (2013). M2 microglia and macrophages drive oligodendrocyte differentiation during CNS remyelination. *Nature Neuroscience*, *16*(9), 1211–8.
- Misgeld, T., & Kerschensteiner, M. (2006). In vivo imaging of the diseased nervous system. *Nature Reviews. Neuroscience*, *7*(6), 449–63.
- Misgeld, T., Kerschensteiner, M., Bareyre, F. M., Burgess, R. W., & Lichtman, J. W. (2007b). Imaging axonal transport of mitochondria in vivo. *Nature Methods*, *4*(7), 559–61.
- Misgeld, T., Nikic, I., & Kerschensteiner, M. (2007a). In vivo imaging of single axons in the mouse spinal cord. *Nature Protocols*, *2*(2), 263–8.
- Mitew, S., Hay, C. M., Peckham, H., Xiao, J., Koenning, M., & Emery, B. (2014). Mechanisms regulating the development of oligodendrocytes and central nervous system myelin. *Neuroscience*, *276*, 29–47.
- Mizutani, M., Pino, P. a, Saederup, N., Charo, I. F., Ransohoff, R. M., & Cardona, A. E. (2012). The fractalkine receptor but not CCR2 is present on microglia from embryonic development throughout adulthood. *Journal of Immunology*, *188*(1), 29–36.
- Monsma, P. C., & Brown, A. (2012). FluoroMyelinTM Red is a bright, photostable and non-toxic fluorescent stain for live imaging of myelin. *Journal of Neuroscience Methods*, *209*(2), 344–50.
- Moreira, T. J. T. P., Pierre, K., Maekawa, F., Repond, C., Cebere, A., Liljequist, S., & Pellerin, L. (2009). Enhanced cerebral expression of MCT1 and MCT2 in a rat ischemia model occurs in activated microglial cells. *Journal of Cerebral Blood Flow and*

Metabolism : Official Journal of the International Society of Cerebral Blood Flow and Metabolism, 29(7), 1273–83.

- Morris-Downes, M., & Smith, P. (2002). Pathological and regulatory effects of anti-myelin antibodies in experimental allergic encephalomyelitis in mice. *Journal of Neuroimmunology*, 125(1-2), 114–124.
- Morrison, B. M., Lee, Y., & Rothstein, J. D. (2013). Oligodendroglia: metabolic supporters of axons. *Trends in Cell Biology*, 23(12), 644–51.
- Mues, M., Bartholomäus, I., Thestrup, T., Griesbeck, O., Wekerle, H., Kawakami, N., & Krishnamoorthy, G. (2013). Real-time in vivo analysis of T cell activation in the central nervous system using a genetically encoded calcium indicator. *Nature Medicine*, 19(6), 778–83.
- Nakanishi, H., & Takai, Y. (2008). Frabin and other related Cdc42-specific guanine nucleotide exchange factors couple the actin cytoskeleton with the plasma membrane. *Journal of Cellular and Molecular Medicine*, 12(4), 1169–1176.
- Nakatani, H., Martin, E., Hassani, H., Clavairoly, A., Maire, C. L., Viadieu, A., ... Parras, C. (2013). *Ascl1/Mash1* promotes brain oligodendrogenesis during myelination and remyelination. *The Journal of Neuroscience*, 33(23), 9752–68.
- Nauta, a. J., Castellano, G., Xu, W., Woltman, a. M., Borrias, M. C., Daha, M. R., ... Roos, a. (2004). Opsonization with C1q and Mannose-Binding Lectin Targets Apoptotic Cells to Dendritic Cells. *The Journal of Immunology*, 173(5), 3044–3050.
- Nave, K.-A. (2010). Myelination and support of axonal integrity by glia. *Nature*, 468(7321), 244–52.
- Nguyen, Q. T., Sanes, J. R., & Lichtman, J. W. (2002). Pre-existing pathways promote precise projection patterns. *Nature Neuroscience*, 5(9), 861–7.
- Niehaus, A., Shi, J., Grzenkowski, M., Diers-Fenger, M., Archelos, J., Hartung, H.-P., ... Trotter, J. (2000). Patients with active relapsing-remitting multiple sclerosis synthesize antibodies recognizing oligodendrocyte progenitor cell surface protein: Implications for remyelination. *Annals of Neurology*, 48(3), 362–371.
- Nikić, I., Merkler, D., Sorbara, C., Brinkoetter, M., Kreutzfeldt, M., Bareyre, F. M., ... Kerschensteiner, M. (2011). A reversible form of axon damage in experimental autoimmune encephalomyelitis and multiple sclerosis. *Nature Medicine*, 17(4), 495–9.
- Nimmerjahn, A., Kirchhoff, F., Kerr, J. N. D., & Helmchen, F. (2004). Sulforhodamine 101 as a specific marker of astroglia in the neocortex in vivo. *Nature Methods*, 1(1), 31–7.
- Nimmerjahn, A., Mukamel, E. a, & Schnitzer, M. J. (2009). Motor behavior activates Bergmann glial networks. *Neuron*, 62(3), 400–12.

- Nishimura, N., Schaffer, C. B., Friedman, B., Tsai, P. S., Lyden, P. D., & Kleinfeld, D. (2006). Targeted insult to subsurface cortical blood vessels using ultrashort laser pulses: three models of stroke. *Nature Methods*, 3(2), 99–108.
- Nunes, M. C., Roy, N. S., Keyoung, H. M., Goodman, R. R., McKhann, G., Jiang, L., ... Goldman, S. a. (2003). Identification and isolation of multipotential neural progenitor cells from the subcortical white matter of the adult human brain. *Nature Medicine*, 9(4), 439–47.
- Oh, J., & O'Connor, P.W. (2013). Teriflunomide. *Neurology. Clinical Practice*, 3(3), 254–260.
- Olitsky, P., & Yager, R. (1949). Experimental disseminated encephalomyelitis in white mice. *The Journal of Experimental Medicine*, 90,(3), 213-224.
- Olsen, J. a, & Akirav, E. M. (2014). Remyelination in multiple sclerosis: Cellular mechanisms and novel therapeutic approaches. *Journal of Neuroscience Research*, 93(5), 687-96.
- Oluich, L.-J., Stratton, J. A. S., Xing, Y. L., Ng, S. W., Cate, H. S., Sah, P., ... Merson, T. D. (2012). Targeted ablation of oligodendrocytes induces axonal pathology independent of overt demyelination. *The Journal of Neuroscience*, 32(24), 8317–30.
- Panitch, H.S., Hirsch, R.L., Schindler, J., Johnson, K.P. (1987). Treatment of multiple sclerosis with gamma interferon: exacerbations associated with activation of the immune system. *Neurology*, 37, 1097–1102.
- Pearce, J. M. S. (2005). Historical descriptions of multiple sclerosis. *European Neurology*, 54(1), 49–53.
- Pedotti, R., DeVoss, J. J., Youssef, S., Mitchell, D., Wedemeyer, J., Madanat, R., ... Steinman, L. (2003). Multiple elements of the allergic arm of the immune response modulate autoimmune demyelination. *Proceedings of the National Academy of Sciences of the United States of America*, 100(4), 1867–72.
- Pedraza, L., Huang, J. K., & Colman, D. (2009). Disposition of axonal caspr with respect to glial cell membranes: Implications for the process of myelination. *Journal of Neuroscience Research*, 87(15), 3480–91.
- Peelen, E., Damoiseaux, J., Smolders, J., Knippenberg, S., Menheere, P., Tervaert, J. W. C., ... Thewissen, M. (2011). Th17 expansion in MS patients is counterbalanced by an expanded CD39+ regulatory T cell population during remission but not during relapse. *Journal of Neuroimmunology*, 240-241, 97–103.
- Peiris, M., Monteith, G. R., Roberts-Thomson, S. J., & Cabot, P. J. (2007). A model of experimental autoimmune encephalomyelitis (EAE) in C57BL/6 mice for the characterisation of intervention therapies. *Journal of Neuroscience Methods*, 163(2), 245–254.

- Pereira, J. a, Lebrun-Julien, F., & Suter, U. (2012). Molecular mechanisms regulating myelination in the peripheral nervous system. *Trends in Neurosciences*, 35(2), 123–34.
- Piddlesden, S., & Lassmann, H. (1993). The demyelinating potential of antibodies to myelin oligodendrocyte glycoprotein is related to their ability to fix complement. *The American Journal of Pathology*, 143(2), 555–564.
- Pistoia, V. (1997). Production of cytokines by human B cells in health and disease. *Immunology Today*, 18(7), 345-350.
- Pitt, D., Werner, P., & Raine, C. (2000). Glutamate excitotoxicity in a model of multiple sclerosis. *Nature Medicine*, 6(1), 67–70.
- Pöllinger, B., Krishnamoorthy, G., Berer, K., Lassmann, H., Bösl, M. R., Dunn, R., ... Wekerle, H. (2009). Spontaneous relapsing-remitting EAE in the SJL/J mouse: MOG-reactive transgenic T cells recruit endogenous MOG-specific B cells. *The Journal of Experimental Medicine*, 206(6), 1303–1316.
- Popescu, B. F. G., Pirko, I., & Lucchinetti, C. F. (2013). Pathology of multiple sclerosis: where do we stand? *Continuum (Minneapolis, Minn.)*, 19(4 Multiple Sclerosis), 901–21.
- Porcheray, F., Viaud, S., Rimaniol, a-C., Léone, C., Samah, B., Dereuddre-Bosquet, N., ... Gras, G. (2005). Macrophage activation switching: an asset for the resolution of inflammation. *Clinical and Experimental Immunology*, 142(3), 481–499.
- Prat, A., & Biernacki, K. (2002). Migration of multiple sclerosis lymphocytes through brain endothelium. *Arch Neurol*, 59(3), 391-7.
- Prinz, M., Tay, T. L., Wolf, Y., & Jung, S. (2014). Microglia: unique and common features with other tissue macrophages. *Acta Neuropathologica*, 128(3), 319–331.
- Privat, A., Jacque, C., & Bourre, J. (1979). Absence of the major dense line in myelin of the mutant mouse “shiverer.” *Neuroscience letters*, 12(1), 107-112.
- Pröbstel, A., Dornmair, K., Bittner, R., & Sperl, P. (2011). Antibodies to MOG are transient in childhood acute disseminated encephalomyelitis. *Neurology*, 77(6), 580-588.
- Quintana, F. J., Farez, M. F., Izquierdo, G., Lucas, M., Cohen, I. R., & Weiner, H. L. (2012). Antigen microarrays identify CNS-produced autoantibodies in RRMS. *Neurology*, 78(8), 532–9.
- Ramaglia, V., & Jackson, S. (2015). Complement activation and expression during chronic relapsing experimental autoimmune encephalomyelitis in the Biozzi ABH mouse. *Clinical & Experimental Immunology* 180(3), 432-41.
- Ramaglia, V., Hughes, T. R., Donev, R. M., Ruseva, M. M., Wu, X., Huitinga, I., ... Morgan, B. P. (2012). C3-dependent mechanism of microglial priming relevant to multiple sclerosis. *Proceedings of the National Academy of Sciences of the United States of America*, 109(3), 965–70.

- Ransohoff, R. M. (2012). Animal models of multiple sclerosis: the good, the bad and the bottom line. *Nature Neuroscience*, 15(8), 1074–1077.
- Ravetch, J., & Clynes, R. (1998). Divergent roles for Fc receptors and complement in vivo. *Annual Review of Immunology*, 16, 421–32.
- Reichert, F., & Rotshenker, S. (2003). Complement-receptor-3 and scavenger-receptor-AI/II mediated myelin phagocytosis in microglia and macrophages. *Neurobiology of Disease*, 12(1), 65–72.
- Reindl, M., Khalil, M., & Berger, T. (2006). Antibodies as biological markers for pathophysiological processes in MS. *Journal of Neuroimmunology*, 180(1-2), 50–62.
- Rivers, T., Sprunt, D., & Berry, G. (1933). Observations on attempts to produce acute disseminated encephalomyelitis in monkeys. *The Journal of Experimental Medicine*, 58(1), 39–53.
- Rodriguez, M. (1985). Virus-induced demyelination in mice: "dying back" of oligodendrocytes. *Mayo Clinic Proceedings*, 60(7), 433–8.
- Romanelli, E., Sorbara, C. D., Nikić, I., Dagkalis, A., Misgeld, T., & Kerschensteiner, M. (2013). Cellular, subcellular and functional in vivo labeling of the spinal cord using vital dyes. *Nature Protocols*, 8(3), 481–90.
- Rosenbluth, J. (1999). A brief history of myelinated nerve fibers: one hundred and fifty years of controversy. *Journal of Neurocytology*, 262(1999), 251–262.
- Rothhammer, V., Muschaweckh, A., Gasteiger, G., Petermann, F., Heink, S., Busch, D. H., ... Korn, T. (2014). α 4-integrins control viral meningoencephalitis through differential recruitment of T helper cell subsets. *Acta Neuropathologica Communications*, 2, 27.
- Rowitch, D. H. (2004). Glial specification in the vertebrate neural tube. *Nature Reviews Neuroscience*, 5(5), 409–19.
- Rubanyi, G.M., 1988. Vascular effects of oxygen-derived free radical. *Free Radic. Biol. Med.* 4, 107–120.
- Sádaba, M. C., Tzartos, J., Paíno, C., García-Villanueva, M., Alvarez-Cermeño, J. C., Villar, L. M., & Esiri, M. M. (2012). Axonal and oligodendrocyte-localized IgM and IgG deposits in MS lesions. *Journal of Neuroimmunology*, 247(1-2), 86–94.
- Saederup, N., Cardona, A. E., Croft, K., Mizutani, M., Cotleur, A. C., Tsou, C.-L., ... Charo, I. F. (2010). Selective chemokine receptor usage by central nervous system myeloid cells in CCR2-red fluorescent protein knock-in mice. *PloS One*, 5(10), e13693.
- Sakadžić, S., Roussakis, E., Yaseen, M. a, Mandeville, E. T., Srinivasan, V. J., Arai, K., ... Boas, D. a. (2010). Two-photon high-resolution measurement of partial pressure of oxygen in cerebral vasculature and tissue. *Nature Methods*, 7(9), 755–9.

- Schmidt, H., Williamson, D., & Ashley-Koch, A. (2007). HLA-DR15 haplotype and multiple sclerosis: a HuGE review. *American Journal of Epidemiology*, *165*(10), 1097–1109.
- Siffrin, V., Brandt, A. U., Radbruch, H., Herz, J., Boldakowa, N., Leuenberger, T., ... Zipp, F. (2009). Differential immune cell dynamics in the CNS cause CD4+ T cell compartmentalization. *Brain : A Journal of Neurology*, *132*(Pt 5), 1247–58.
- Siffrin, V., Radbruch, H., Glumm, R., Niesner, R., Paterka, M., Herz, J., ... Zipp, F. (2010). In vivo imaging of partially reversible th17 cell-induced neuronal dysfunction in the course of encephalomyelitis. *Immunity*, *33*(3), 424–36.
- Silbereis, J. C., Huang, E. J., Back, S. a, & Rowitch, D. H. (2010). Towards improved animal models of neonatal white matter injury associated with cerebral palsy. *Disease Models & Mechanisms*, *3*(11-12), 678–88.
- Simmons, S. B., Pierson, E. R., Lee, S. Y., & Goverman, J. M. (2013a). Modeling the heterogeneity of multiple sclerosis in animals. *Trends in Immunology*, *34*(8), 410–422.
- Simons, M., Misgeld, T., & Kerschensteiner, M. (2014). A unified cell biological perspective on axon-myelin injury. *The Journal of Cell Biology*, *206*(3), 335–45.
- Singbartl, K., Thatte, J., Smith, M. L., Wethmar, K., Day, K., & Ley, K. (2001). A CD2-Green Fluorescence Protein-Transgenic Mouse Reveals Very Late Antigen-4-Dependent CD8+ Lymphocyte Rolling in Inflamed Venules. *The Journal of Immunology*, *166*(12), 7520–7526.
- Skulina, C., & Schmidt, S. (2004). Multiple sclerosis: brain-infiltrating CD8+ T cells persist as clonal expansions in the cerebrospinal fluid and blood. *Proceedings of the National Academy of Sciences of the United States of America*, *101*(8), 2428-2433.
- Skurkovich, S., Boiko, a, Beliaeva, I., Buglak, a, Alekseeva, T., Smirnova, N., ... Gusev, E. (2001). Randomized study of antibodies to IFN-g and TNF-a in secondary progressive multiple sclerosis. *Multiple Sclerosis*, *7*(5), 277–284.
- Smith, K., & Lassmann, H. (2002). The role of nitric oxide in multiple sclerosis. *The Lancet Neurology*, *1*(August), 232–241.
- Smith, K., Blakemore, W., & McDonald, W. (1979). Central remyelination restores secure conduction.
- Smith, M. (2001). Phagocytic properties of microglia in vitro: implications for a role in multiple sclerosis and EAE. *Microscopy Research and Technique*, *94*(November 2000), 81–94.
- Smith, T., Groom, A., Zhu, B., & Turski, L. (2000). Autoimmune encephalomyelitis ameliorated by AMPA antagonists. *Nature Medicine*, *6*(1), 62-6.
- Smith, T., Groom, A., Zhu, B., & Turski, L. (2000). Autoimmune encephalomyelitis ameliorated by AMPA antagonists. *Nature Medicine*, *6*(1), 62-6.

- Snaidero, N., & Simons, M. (2014). Myelination at a glance. *Journal of Cell Science*, 127(Pt 14), 2999–3004.
- Snaidero, N., Möbius, W., Czopka, T., Hekking, L. H. P., Mathisen, C., Verkleij, D., ... Simons, M. (2014). Myelin membrane wrapping of CNS axons by PI(3,4,5)P3-dependent polarized growth at the inner tongue. *Cell*, 156(1-2), 277–90.
- Sobottka, B., Ziegler, U., Kaech, A., Becher, B., & Goebels, N. (2011). CNS live imaging reveals a new mechanism of myelination: the liquid croissant model. *Glia*, 59(12), 1841–9.
- Sorbara, C. D., Wagner, N. E., Ladwig, A., Nikić, I., Merkler, D., Kleele, T., ... Kerschensteiner, M. (2014). Pervasive Axonal Transport Deficits in Multiple Sclerosis Models. *Neuron*, 1183–1190.
- Sorbara, C., Misgeld, T., & Kerschensteiner, M. (2012). In Vivo Imaging of the Diseased Nervous System: An Update. *Current Pharmaceutical Design*, 18(29), 4465–4470.
- Srivastava, R., Aslam, M., Kalluri, S. R., Schirmer, L., Buck, D., Tackenberg, B., ... Hemmer, B. (2012). Potassium channel KIR4.1 as an immune target in multiple sclerosis. *The New England Journal of Medicine*, 367(2), 115–23.
- Steinman, L., & Zamvil, S. S. (2006). How to successfully apply animal studies in experimental allergic encephalomyelitis to research on multiple sclerosis. *Annals of Neurology*, 60(1), 12–21.
- Stendel, C., Roos, A., Deconinck, T., Pereira, J., Castagner, F., Niemann, A., ... Senderek, J. (2007). Peripheral nerve demyelination caused by a mutant Rho GTPase guanine nucleotide exchange factor, frabin/FGD4. *American Journal of Human Genetics*, 81(1), 158–64.
- Storch, M.K., Piddlesden, S., Haltia, M., Iivanainen, M., Morgan, P., Lassmann, H. (1998). Multiple sclerosis: in situ evidence for antibody- and complement-mediated demyelination. *Annals of Neurology*, 43(4), 465–71.
- Stosiek, C., Garaschuk, O., Holthoff, K., & Konnerth, A. (2003). In vivo two-photon calcium imaging of neuronal networks. *Proceedings of the National Academy of Sciences of the United States of America*, 100(12), 7319–24.
- Stromnes, I. M., & Goverman, J. M. (2006a). Active induction of experimental allergic encephalomyelitis. *Nature Protocols*, 1(4), 1810–1819.
- Stromnes, I. M., & Goverman, J. M. (2006b). Passive induction of experimental allergic encephalomyelitis. *Nature Protocols*, 1(4), 1952–1960.
- Stuve, O., Dooley, N.P., Uhm, J.H.,... Yong, V. W. (1996). Interferon beta-1b decreases the migration of T lymphocytes in vitro: effects on matrix metalloproteinase-9. *Annals of Neurology*, 40, 853–863.

- Svoboda, K., Denk, W., Kleinfeld, D., & Tank, D. (1997). In vivo dendritic calcium dynamics in neocortical pyramidal neurons. *Nature*, 385(6612), 161-5.
- Svoboda, K., Tank, D., & Denk, W. (1996). Direct measurement of coupling between dendritic spines and shafts. *Science*, 272(5262), 716-9.
- Tal, C., Laufer, A., & Behar, A. (1958). An experimental demyelinating disease in the Syrian hamster. *British Journal of Experimental Pathology*, 39(2), 158-164.
- The CAMMS223 Trial Investigators. (2008). Alemtuzumab vs. interferon beta-1a in early multiple sclerosis. *The New England Journal of Medicine*, 359(17), 1786-1801.
- The Lenercept Multiple Sclerosis Study Group and The University of British Columbia MS/MRI Analysis Group (1999). TNF neutralization in MS-Results of a randomized, placebo-controlled multicenter study. *Neurology*, 53(3), 457-465.
- Thomas, L., Paterson, P.Y., Smithwick, B. (1950). Acute disseminated encephalomyelitis following immunization with homologous brain extracts; studies on the role of a circulating antibody in the production of the condition in dogs. *Journal of Experimental Medicine*, 92(2), 133-152.
- Todorich, B., Pasquini, J. M., Garcia, C. I., Paez, P. M., & Connor, J. R. (2009). Oligodendrocytes and myelination: the role of iron. *Glia*, 57(5), 467-78.
- Traka, M., Arasi, K., Avila, R. L., Podojil, J. R., Christakos, A., Miller, S. D., ... Popko, B. (2010). A genetic mouse model of adult-onset, pervasive central nervous system demyelination with robust remyelination. *Brain: A Journal of Neurology*, 133(10), 3017-29.
- Urich, E., Gutcher, I., Prinz, M., & Becher, B. (2006). Autoantibody-mediated demyelination depends on complement activation but not activatory Fc-receptors. *Proceedings of the National Academy of Sciences of the United States of America*, 103(49), 18697-702.
- Van der Goes, A., Brouwer, J., Hoekstra, K., Roos, D., van den Berg, T. K., & Dijkstra, C. D. (1998). Reactive oxygen species are required for the phagocytosis of myelin by macrophages. *Journal of Neuroimmunology*, 92(1-2), 67-75.
- Viganò, F., Möbius, W., Götz, M., & Dimou, L. (2013). Transplantation reveals regional differences in oligodendrocyte differentiation in the adult brain. *Nature Neuroscience*, 16(10), 1370-2.
- Vogel, C.-W., & Fritzinger, D. C. (2010). Cobra venom factor: Structure, function, and humanization for therapeutic complement depletion. *Toxicon: Official Journal of the International Society on Toxinology*, 56(7), 1198-222.
- Wang, X., Chen, M., Wandinger, K.P., Williams, G., Dhib-Jalbut, S. (2000). IFN beta-1b inhibits IL-12 production in peripheral blood mononuclear cells in an IL-10-dependent mechanism: relevance to IFN beta-1b therapeutic effects in multiple sclerosis. *Journal of Immunology*, 165, 548-557.

- Warren, K. G., & Catz, I. (1994). Relative frequency of autoantibodies to myelin basic protein and proteolipid protein in optic neuritis and multiple sclerosis cerebrospinal fluid. *Journal of the Neurological Sciences*, *121*(1), 66–73.
- Watkins, T. a, Emery, B., Mulinyawe, S., & Barres, B. a. (2008). Distinct stages of myelination regulated by gamma-secretase and astrocytes in a rapidly myelinating CNS coculture system. *Neuron*, *60*(4), 555–69.
- Weber, M. S., Prod'homme, T., Patarroyo, J. C., Molnarfi, N., Karnezis, T., Lehmann-Horn, K., ... Zamvil, S. S. (2010). B-cell activation influences T-cell polarization and outcome of anti-CD20 B-cell depletion in central nervous system autoimmunity. *Annals of Neurology*, *68*(3), 369–383.
- Wickersham, I. R., Finke, S., Conzelmann, K.-K., & Callaway, E. M. (2007). Retrograde neuronal tracing with a deletion-mutant rabies virus. *Nature Methods*, *4*(1), 47–9.
- Wickersham, I. R., Lyon, D. C., Barnard, R. J. O., Mori, T., Finke, S., Conzelmann, K.-K., ... Callaway, E. M. (2007). Monosynaptic restriction of transsynaptic tracing from single, genetically targeted neurons. *Neuron*, *53*(5), 639–47.
- Wickersham, I. R., Sullivan, H. a, & Seung, H. S. (2010). Production of glycoprotein-deleted rabies viruses for monosynaptic tracing and high-level gene expression in neurons. *Nature Protocols*, *5*(3), 595–606.
- Wingerchuk, D. M., & Carter, J. L. (2014). Multiple sclerosis: current and emerging disease-modifying therapies and treatment strategies. *Mayo Clinic Proceedings*, *89*(2), 225-240.
- Wosik, K., Antel, J., Kuhlmann, T., Brück, W., Massie, B., & Nalbantoglu, J. (2003). Oligodendrocyte injury in multiple sclerosis: a role for p53. *Journal of Neurochemistry*, *85*(3), 635–644.
- Xu, H.-T., Pan, F., Yang, G., & Gan, W.-B. (2007). Choice of cranial window type for in vivo imaging affects dendritic spine turnover in the cortex. *Nature Neuroscience*, *10*(5), 549–51.
- Yamasaki, R., Lu, H., Butovsky, O., Ohno, N., Rietsch, A. M., Cialic, R., ... Ransohoff, R. M. (2014). Differential roles of microglia and monocytes in the inflamed central nervous system. *The Journal of Experimental Medicine*, *211*(8), 1533–1549.
- Yang, G., Pan, F., Parkhurst, C. N., Grutzendler, J., & Gan, W.-B. (2010). Thinned-skull cranial window technique for long-term imaging of the cortex in live mice. *Nature Protocols*, *5*(2), 201–8.
- Yeung, M. S. Y., Zdunek, S., Bergmann, O., Bernard, S., Salehpour, M., Alkass, K., ... Frisén, J. (2014). Dynamics of Oligodendrocyte Generation and Myelination in the Human Brain. *Cell*, *159*(4), 766–774.
- Young, K. M., Psachoulia, K., Tripathi, R. B., Dunn, S.-J., Cossell, L., Attwell, D., ... Richardson, W. D. (2013). Oligodendrocyte dynamics in the healthy adult CNS: evidence for myelin remodeling. *Neuron*, *77*(5), 873–85.

- Zipfel, W. R., Williams, R. M., & Webb, W. W. (2003). Nonlinear magic: multiphoton microscopy in the biosciences. *Nature Biotechnology*, *21*(11), 1369–77.
- Zuo, Y., Lin, A., Chang, P., & Gan, W.-B. (2005). Development of long-term dendritic spine stability in diverse regions of cerebral cortex. *Neuron*, *46*(2), 181–9.

ELSEVIER LICENSE TERMS AND CONDITIONS

Jul 02, 2015

This is an Agreement between Elisa Romanelli ("You") and Elsevier ("Elsevier"). It consists of your order details, the terms and conditions provided by Elsevier, and the payment terms and conditions.

All payments must be made in full to CCC. For payment instructions, please see information listed at the bottom of this form.

Supplier	Elsevier Limited The Boulevard, Langford Lane Kidlington, Oxford, OX5 1GB, UK
Registered Company Number	1982084
Customer name	Elisa Romanelli
Customer address	Marchioninstr. 17 Munich, None 81377
License number	3644230106422
License date	Jun 08, 2015
Licensed content publisher	Elsevier
Licensed content publication	Trends in Molecular Medicine
Licensed content title	Heterogeneity of multiple sclerosis pathogenesis: implications for diagnosis and therapy
Licensed content author	Hans Lassmann, Wolfgang Brück, Claudia Lucchinetti
Licensed content date	1 March 2001
Licensed content volume number	7
Licensed content issue number	3
Number of pages	7
Start Page	115
End Page	121
Type of Use	reuse in a thesis/dissertation
Portion	figures/tables/illustrations
Number of figures/tables/illustrations	1
Format	both print and electronic
Are you the author of this Elsevier article?	No
Will you be translating?	No
Original figure numbers	figure 1
Title of your thesis/dissertation	In vivo pathogenesis of demyelination in multiple sclerosis and its animal model
Expected completion date	Nov 2015
Estimated size (number of pages)	145
Elsevier VAT number	GB 494 6272 12
Price	0.00 EUR
VAT/Local Sales Tax	0.00 EUR / 0.00 GBP

